STUDIES ON CONFORMATIONAL STABILITY OF THE ECTODOMAIN OF INFLUENZA VIRUS HEMAGGLUTININ

DISSERTATION

Zur Erlangung des akademischen Grades
doctor rerum naturalium
(Dr. rer. nat.)
im Fach Biologie

eingereicht an
Mathematisch-Naturwissenschaftlichen Fakultät I
der Humboldt-Universität zu Berlin

von
Herrn. P. Sivaramakrishna Rachakonda
geboren am 15.01.1969 in Machilipatnam, Indien

Präsident der Humboldt-Universität zu Berlin:
Prof. Dr. Jürgen Mlynek

Dekan der Mathematisch-Naturwissenschaftlichen Fakultät I
Prof. Thomas Buckhout, PhD

Gutachter
Prof. Dr. Andreas Herrmann
Prof. Dr. Klaus Arnold
PD. Dr. Michael Veit

Tag der mündlichen Prüfung: 15.02.2005.

CONTENTS

List of Figures

List of Tables

ABBREVIATIONS

Amp	ampicillin
APS	ammonium peroxydisulphate
BHA	bromelain solubilised hemagglutinin ectodomain
BSA	bovine serum albumin
DMEM	Dulbecco modified Eagle medium
DNA	deoxyribonucleic acid
dNTP	deoxy nucleotide triphosphates
EDTA	ethylenediamine tetra acetic acid
E. coli	*Escherichia coli*
Eppendorf tube	1.5 ml reaction tube
ER	endoplasmic reticulum
EtBr	ethidium bromide
FCS	heat inactivated fetal calf serum
GPI-HA	glycosylphosphatidylinositol-anchored BHA
g	gravitational force
HA	influenza virus hemagglutinin
HA-wt	wildtype influenza virus hemagglutinin
kbp	kilo base pairs
kDa	kilodaltons
µg	microgram
µl	microlitre
M	molar
MEM	minimal essential medium
O/N	overnight
O.D.	optical density
PBS(++)	phosphate buffered saline (with 1 mM $CaCl_2$ and 1 mM $MgCl_2$)
PCR	Polymerase chain reaction
PFU	Plaque forming unit
RBC	human red blood cells
R18	octadodecylrhodamine B chloride
RNA	Ribonucleic acid
rpm	rotations per minute
RT	room temperature
SDS	Sodium dodecyl sulphate
SDS-PAGE	SDS polyacrylamide gel electrophoresis
TEMED	N,N,N',N'-tetramethyl ethylene diamine

ABSTRACT

Enveloped viruses enter host cells by a process that involves fusion of the viral envelope with a membrane of the host cell. The process of membrane fusion which is typical for various cellular processes has been best studied in viral infections, especially in influenza virus. Hemagglutinin (HA), a major envelope glycoprotein is responsible for fusing viral and endosomal membranes during influenza virus entry. This membrane fusion is mediated by a conformational change of HA at low pH conditions in the endosome. The analysis of 3D crystal structure of the bromelain cleaved HA ectodomain shows that the stability of protein is maintained by both non-covalent and covalent interactions. The irreversible conformational change of HA at low pH indicates a role for protonation effects of the ionisable amino acids. While many models explain the various intermediates of the membrane fusion process, the early steps leading to conformational changes have not been consider. In addition, the presence of extensive salt networks in the 3D crystal structure of HA has not been contended. The present research work focuses on these queries in order to bring out the importance of electrostatic interactions for the stability of the spike-like ectodomain in its non-fusogenic structure.

Structural investigations were done using "site directed mutagenesis" in order to conceive the importance of charged amino acids and more emphatically the involvement of salt bridges. The mutagenesis was carried out either at the interface of HA1 and HA2 monomers, or between the HA1 or HA2 monomers. Thus, mutations are designed so as to investigate electrostatic interactions both at inter-monomer and intra-monomer interfaces. The approach was to make new salt bridge or break the existing salt bridge, so as to increase or decrease the interactions within or between the monomers.

Fourteen mutants were constructed based on careful analysis of the 3D crystal structure of the X-31 influenza A virus. The selected amino acids were analysed for their evolutionary significance by sequence homology. All the mutant and HA-wt constructs were expressed in CV-1 cells by transient T7-RNA-polymerase vaccinia virus system. The surface expression of the expressed HA proteins were characterised. The effect of mutations on the conformational change and fusion activity was probed by proteinase K assay and fluorescence microscopy respectively. An effort was made to correlate the results from proteinase K assay with those from fusion assays. It was observed that HA-wt and all the mutants except R109E showed comparable surface expression. The difference in pH threshold between the HA-wt and the mutants showed that breakage of salt bridge and

further incorporation of repulsion at the considered interfaces would lower the energy barrier requirements for the conformational change. Interestingly, mutations involving the same amino acid (viz., R269E /R269G or K299E /K299G) showed a difference in the pH threshold for conformational change. The results explain the molecular basis of the higher pH threshold for naturally occurring amantadine resistant mutants. On the other hand, mutants designed to stabilise the HA were resistant to conformational changes at those pH values which typically trigger the conformational change of HA-wt. Coincidentally these mutations were found to be existing in the natural variant of H2 Japan subtype (A/JPN/305/57), which remains stable for longer periods at low pH.

Interestingly, the study shows that a positive charge and, more specifically, an Arg residue at position 109 (numbering based on X-31 strain) is conserved in all of the influenza A and B viruses underlining the relevance of electrostatic interactions for the HA stability. Aptly a complex salt bridge at the interface of HA1 and HA2 is probably conserved evolutionarily in all the members of influenza A virus. Further, the study shows the importance of ring like salt network in the trimer formation and also their role in the conformational change of HA. This is exemplified by HA from H2 Japan subtype. The present research clearly shows the effect of destabilising and stabilising electrostatic interactions during the conformational transition at low pH. This investigation also confirms the protonation hypothesis of Huang *et al.* (2002). According to this hypothesis, an enhanced protonation of the HA1 subunits at low pH alters electrostatic interactions initiating the conformational transition.

Key words

conformational change/ fusion/ ectodomain/ influenza virus hemagglutinin/ salt bridges/

ZUSAMMENFASSUNG

Die Infektion einer Zelle durch Hüllviren schließt den Prozess der Fusion der viralen Membran mit einer (sub)zellulären Membran ein. Der Prozess der Membranfusion, der für verschiedene zelluläre Phänomene typisch ist, ist bisher am intensivsten für Hüllviren, insbesondere für Influenzavirus, untersucht worden. Das Hüllglykoprotein Hämagglutinin (HA) von Influenzavirus ist verantwortlich sowohl für die Bindung als auch für die nachfolgende Fusion der viralen Hülle mit der endosomalen Membran. Die Membranfusion wird durch eine Konformationsumwandlung des HA vermittelt, die wiederum durch einen erniedrigten pH-Wert im endosomalen Lumen ausgelöst wird. Eine Analyse der dreidimensionalen Struktur der Bromelain-gespaltenen HA-Ektodomaine zeigt, dass die Stabilität des Proteins sowohl durch kovalente als auch durch nicht-kovalente Wechselwirkungen bedingt ist. Die irreversible Konformationsänderung von HA bei saurem pH-Wert weißt auf eine mögliche Rolle von Protonierungseffekten auf ionisierbare Aminosäuren hin. Während viele Modelle die Intermediate des Membranfusionsprozesses erklären, werden die frühen Schritte, die zu einer Konformationsumwandlung führen, in diesen Modellen nicht berücksichtigt. Insbesondere finden die aus der 3D-Struktur ersichtlichen umfangreichen Netzwerke von Salzbrücken keine Aufmerksamkeit. Die vorliegende Arbeit untersucht die Relevanz dieser Netzwerke durch Charakterisierung der Rolle elektrostatischer Wechselwirkungen für die Stabilität der spikeartigen HA-Ektodomaine in ihrer nichtfusogenen Struktur.

Untersuchungen zur Bedeutung geladener Aminosäuren und Salzbrücken für die Struktur des HA wurden auf der Grundlage von ‚site directed mutagenesis' durchgeführt. Mutationen wurden entweder an Kontaktflächen von HA1- bzw. HA2-Monomeren oder zwischen HA1- und HA2-Monomeren vorgenommen. Die Mutationen wurden so ausgewählt, um elektrostatische Wechselwirkungen an intermonomeren oder intramonomeren Kontakstellen charakterisieren zu können. Insbesondere sollten dadurch neue Salzbrücken aufgebaut bzw. existierende Salzbrücken aufgebrochen werden.

Vierzehn entsprechende Mutanten wurden auf der Basis der Analyse der 3D-Struktur von Influenzavirus X31 konstruiert. Die ausgewählten Aminosäuren wurden hinsichtlich ihrer evolutionären Bedeutung charakterisiert (Sequenzhomologien). Wildtyp sowie Mutanten des HA wurden in CV-1 Zellen mittels eines transienten T7-RNA-Polymerase-Vacciniavirus-Sytem exprimiert und die Oberflächenexpression analysiert. Der Einfluss der Mutationen auf die Konformationsänderung und die Fusionsaktivität von HA wurden durch einen Proteinase K-Assay bzw. Fluoreszenzmikroskopie erfasst. Die Ergebnisse

beider Methoden wurden miteinander korreliert. Abgesehen von der Mutante R109E zeigten Wildtyp-HA und alle anderen Mutanten eine vergleichbare Oberflächenexpression. Die beobachteten Unterschiede in der pH-Abhängigkeit der Konformationumwandlung zwischen Wildtyp-HA und HA-Mutanten zeigen, daß eine Zerstörung von Salzbrücken und ggf. eine Erhöhung der elektrostatischen Abstoßung an den betrachteten Kontakstellen sehr wahrscheinlich eine Herabsetzung der energetischen Barriere der Konformationsumwandlung verursacht. Zwischen Mutanten, bei denen dieselbe Aminosäure mutiert wurde, aber durch eine andere Aminosäure ersetzt wurde (z.B R269E /R269G or K299E /K299G), ergaben sich ebenfalls Unterschiede hinsichtlich der pH-Abhängigkeit der Konformationsumwandlung. Dieser Ergebnisse erklären die molekularen Grundlagen des erhöhten pH-Schwellwertes der HA-Konformationsumwandlung von Amantadin-resistenten Influenzaviren. Im Gegensatz wurde für Mutanten, die die Stabilität von HA erhöhten, keine Konformationsumwandlung bei einem pH-Wert beobachtet, der typisch für die Konformationumwandlung von Wildtyp-HA war. Aminosäuren, die denen dieser stabiliserenden Mutationen entsprachen, wurden in einer natürlichen Influenzavirusvariante – A/JPN/305/57 – gefunden. HA dieser Virusvariante zeichnet sich durch eine extreme Stabilität bei niedrigem pH-Wet aus. Die Bedeutung von Ladungen für die Stabilität der HA-Ektodomaine wird dadurch unterstrichen, dass eine Konservierung einer positiven Ladung und insbesondere eines Argininrestes in der Position 109 (Nummerierung auf der Basis von HA X31) für alle Influenzaviren A und B gefunden wurde. Die Ergebnisse der Arbeit zeigen, dass sehr wahrscheinlich eine komplexe Salzbrücke an der Kontaktfläche zwischen HA1 und HA2 für alle Influenzaviren A evolutionär konserviert ist. Weiterhin ist ein ringartig angelegtes Salzbrückennetzwerk wichtig für die Trimerisierung des HA und spielt eine hervorgehobene Rolle bei der Konformationsumwandlung. Dieses wird am Beispiel des HA von A/JPN/305/57 illustriert. Diese Arbeit zeigt den Einfluss destabilisierender und stabilisierender elektrostatischer Wechselwirkungen auf die Konformationsumwandlung von HA bei saurem pH-Wert. Die Ergebnisse unterstützen die Protonierungshypothese von Huang et al. (2002), die davon ausgeht, dass eine erhöhte Protonierung die elektrostatischen Wechselwirkungen in der HA-Ektodomaine so verändert, dass eine entsprechende Konformationsumwandlung ausgelöst wird.

Schlagwörtern

Konformationsänderung/ fusion/ Ektodomaine/ influenzavirus Hämagglutinin/ Salzbrücken/

1 INTRODUCTION

The stability of the tertiary structure (3D structure) of a protein is a function of many weak non-covalent interactions. These interactions involve hydrophobic effect, van der Waals interactions, hydrogen bonds, and ionic interactions. The most intriguing question for a structural biologist is which one of these interactions is likely to stabilise the protein. While there is consensus on the contribution of hydrophobic interactions in protein stability, the role of electrostatic interactions remains enigmatic. Viewed from the perspective of electrostatic interactions, the stability of a protein is the result of a delicate balance of both positive and negative charges of the amino acids. In the recent past, researchers have shown that the contribution of salt bridges (ion pairs) to protein stability is highly variable being sometimes favourable and sometimes unfavourable. Generally, salt bridges are dependent on pH and ion concentrations. Further, the pH of the medium also influences many biochemical and biological processes occurring in the system. In addition, changes in pH result in altered conformation of the protein leading to either protein activation or denaturation. One such example of pH dependency for proteins is the endocytic pathway of viral propogation. Some enveloped viruses enter the host cell by a specialised mechanism called receptor mediated endocytosis.

Endocytosis is a specialized process adopted by eukaryotes for the regulation of the entry or exit of the small and large molecules. While small molecules are transported across the permeable plasma membrane, the large molecules such as micro-organisms are endocytosed. In this process, the material to be ingested is progressively enclosed by a small portion of the plasma membrane, which first invaginates and then pinches off to form an endocytic vesicle containing the ingested substance or particle. Viruses on being internalised, fuse with endosomal membrane to release its genomic content into cytoplasm. Membrane fusion occurs when the lipid bilayers of the apposing membranes are within 1.5 nm distance. In this process, water must be displaced from the hydrophilic surface of the membrane – a process that is energetically highly unfavourable. It seems that specialized fusion proteins catalyse all membrane fusion processes in cells. These fusion proteins provide a way to overcome this energy barrier. Thus membrane fusion is a ubiquitous and critical event in biological systems. It is a required step for the infectious cycle of enveloped viruses, zygote formation, endocytosis, exocytosis, intracellular traffic, and many other biological processes. The mechanism of membrane fusion is best understood in the context of enveloped viruses.

The viral fusion mediating glycoproteins from influenza virus (HA), HIV/SIV (gp160), retroviruses (env), paramyxoviruses (F), and filoviruses (GP) are synthesised as trimers and share similar features. Similarity in sequence suggests similar functional activity (Skehel and Wiley, 1998). Moreover, all the known fusion proteins are class I integral membrane glycoproteins, i.e., they have one transmembrane helix, and the majority of their mass resides on the extracellular side of the host cell (Bechor and Ben-Tal, 2001). Class I fusion proteins are composed of three identical monomers, the functional forms of which are generated from a precursor that is cleaved into two subunits. The cleavage is followed by an irreversible conformational change by which they compensate the energy requirements for fusion. All the above-mentioned proteins are synthesised as precursor molecules before being cleaved to become fusion active. The proteolytic cleavage occurs late in the biosynthetic phase and fusion proteins once cleaved will be in a metastable state (section 1.3.1). To mediate fusion, activated proteins undergo a conformational change triggered either by a pH change or interaction with host cell receptors. During the fusion process, usually the proteins tend to refold into a stable conformation with thermodynamically low energy.

The fusion of influenza virus with target membranes is one of the most extensively studied viral fusion processes. Colman and Lawrence (review 2003) attributed the understanding of influenza virus HA largely to the pioneering work done by Wiley and Skehel. Till recently, hemagglutinin (HA) of influenza virus is the only characterised protein structurally in both pre and post fusion states. Hence all the fusion models were based essentially on the HA protein (discussed later). Though, it is widely accepted that fusion mechanism is a multi-step process, still the models fall short of explaining the fundamental questions on early steps leading to destabilisation of HA protein. Since HA protein resembles the prototype of a fusion protein, understanding the structure and dynamics of HA is essential for designing novel antiviral agents that can potentially inhibit binding or fusogenic activities not only for HA, but also for other viral fusion proteins.

1.1 The influenza A virus

Influenza is an orthomyxovirus, a term coined by Andrews *et al.,* in 1955 to denote the affinity of the virus for mucus in the form of mucopolysaccharides and glycoproteins. Influenza viruses are classified into A, B and C types, based on the antigenic differences of the internal proteins (nucleoprotein and matrix). The virus has a wide host range of birds and mammals. The different strains of these viruses are nomenclatured based on the host of

origin, geographic location, strain number, year of isolation and mostly the antigenic classification of hemagglutinin (HA) and neuraminidase (NA) mentioned in the parenthesis, viz., A/Hong Kong/1/68(H3N2). About 15 antigenic subtypes of HA (HA1-HA15) and 9 subtypes of NA (NA1-NA9) have been reported. Though birds are the natural hosts for all the subtypes, only subtypes H1, H2, H3 and N1, N2 have established stable lineages in humans (Nicholson *et al.,* 2003). The type A virus has been isolated from all the hosts, but so far types B and C were reported only in humans. The most studied strains were mostly from type A, associated with pandemic influenza.

The epidemiological behaviour of influenza in human population is related to the two types of antigenic variation of its envelope glycoproteins (HA and NA) namely antigenic drift and antigenic shift (reviewed in Wright and Webster, 2001). Antigenic drift involves point mutations in the surface antigens resulting from an immune selective pressure. The changes in the antigen structure allow the virus to evade the immune system of the host. As a result, new antigenic variants (new subtypes) evolve, but are still related to those circulating during preceding epidemics. On the other hand, the antigenic shift occurs much less frequently but leads to a major antigenic change. This change results from a replacement of the genomic RNA segment encoding surface antigens resulting in emergence of a "new" potentially pandemic, influenza A virus. The new virus would be antigenically distinct from earlier human viruses and could not have arisen from them by mutation.

The wide host range coupled by a high mutation rate and cross species interactions generally results in the development of new virus strains, which would naturally be the major obstacle in controlling the disease by vaccination.

1.1.1 Structure of influenza virus

Influenza A viruses are pleiomorphic, but those adapted to cell culture occur as spherical particles of 100 nm in diameter. These viruses are enveloped i.e., have a lipid membrane surrounding the nucleocapsid. The viral genome is negative single stranded RNA (reviewed in Lamb and Krug, 2001) and non-infectious. The mRNAs will be transcribed from the virion RNA (vRNA) by the virion associated RNA dependent RNA transcriptase. Thus as a convention mRNA is plus-stranded.

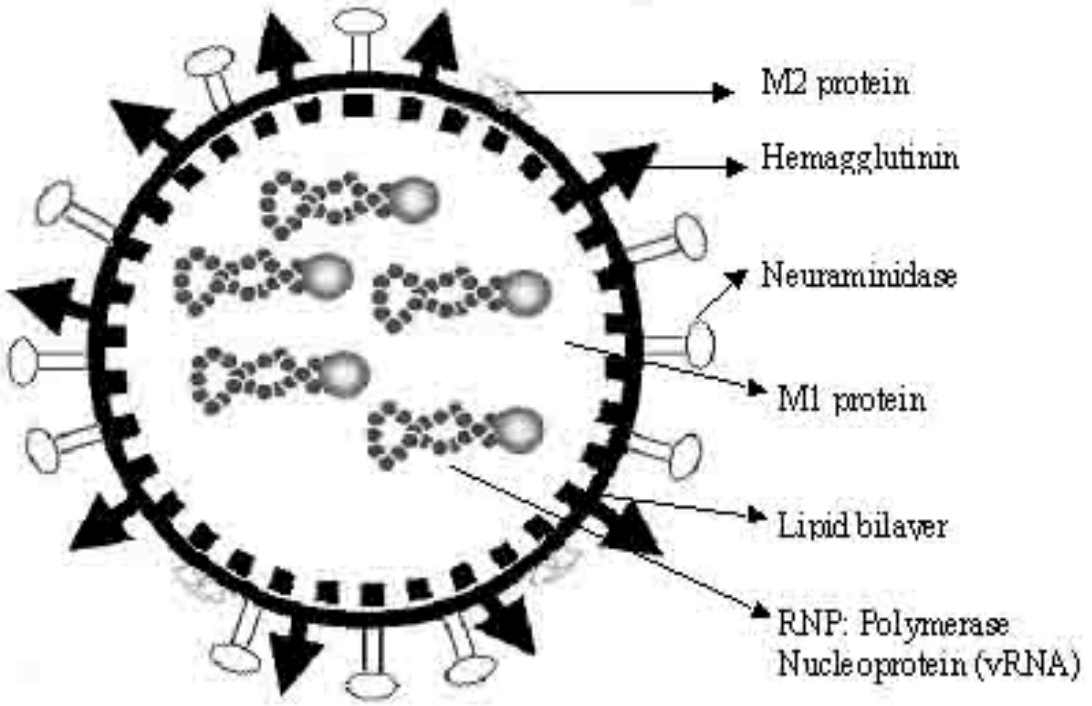

Figure 1.1.1 : Schematic diagram of structure of the influenza A virus with viral proteins

The viral genome consists of eight separate RNA segments and the segments 1, 2 and 3 code for viral polymerase i.e., PB2, PB1, and PA respectively, segment 4 for hemagglutinin (HA), segment 5 for Nucleoprotein (NP), segment 6 for neuraminidase (NA), segment 7 for matrix protein (M1), and membrane channel proteins (M2), segment 8 for non-structural proteins (NS1 and NS2).

1.1.2 Viral proteins

The viral genome encodes 10 different viral proteins. These proteins can be separated into three major subviral components:

The viral envelope containing hemagglutinin (HA), neuraminidase (NA), and M2 proteins;

Matrix protein (M1);

Viral nucleocapsid (viral ribonucleoprotein, vRNP).

Considering A/Puerto Rico/8/34 virus (PR8) as an example, the influenza viral gene segments range from 890 to 2341 nucleotides in length containing approximately 20-45 non-coding nucleotides at the 3' end and 23-61 at the 5' end, depending on the segment (Steinhauer and Skehel 2002). Usually the terminal 13 and 12 nucleotides of the 5' and 3' ends respectively are conserved in all eight vRNA gene segments and form the vRNA promoter. This base pairing for vRNA promoter was found to be critical for efficient virus replication in MDBK cells (Fodor *et al.*, 1998).

Membrane proteins

The viral membrane constitutes three distinct proteins i.e., spike like hemagglutinin (HA), neuraminidase (NA) and a membrane channel protein (M2).

The 3D structure of HA, and NA have been determined (mentioned below). HA exists as homotrimer and NA as a homotetramer. These proteins are critically involved in viral pathogencity, its virulence, and host and tissue tropism. When examined by negative staining, the virus particles show the presence of "spikes" representing the two glycoproteins namely HA and NA. Overall, HA represents about 25% of viral protein and NA represents about 5%. The M2 ion channel protein however, is present in low quantities, at only a few copies per particle.

Hemagglutinin: HA primarily serves for the attachment of virus to cells and subsequently for the penetration of viral components into the cells. The HA serves as a major antigen and elicits a strong immune response. The antibodies associated with this protein neutralise viral infectivity. In X-31 virus strain, HA is synthesised as a single polypeptide chain of 550 amino acids with a molecular weight of 77 kD. Each monomer of the activated HA harbours two chains – HA1 and HA2 linked by a disulphide bond. Depending on the virus strain, host cell type and growth conditions, the precursor protein HA0 can be proteolytically cleaved into HA1 and HA2. This cleavage was reported to be essential for virus infectivity (Klenk *et al.,* 1994; Zhirnov *et al.,* 2002). The infectivity of poorly infectious virus could be increased by trypsin treatment. The sensitivity of HA to host proteases is determined by the composition of the proteolytic site in the external loop of the HA0 molecule which links HA1 and HA2 (Chen *et al.,* 1998). This loop typically contains either a single Arg/Lys residue (monobasic cleavage site) or several Lys and/or Arg residues, with an R-X-K/R-R motif, forming a multibasic cleavage site. Influenza A viruses with multibasic cleavage sites (only H5, H7 subtypes) could be more virulent and induce systemic infection in hosts than these viruses (all other influenza A viruses) with monobasic cleavage site (Klenk *et al.,* 1994). The crystal structure of the HA ectodomain was determined with a resolution of 3 Å (Wilson *et al.*, 1981). The ectodomain of HA was obtained by bromelain cleavage (BHA). The bromelain cleaves the HA2 chain just beyond the N-terminal end of the trans-membrane sequence. The HA2 portion of HA is essentially hydrophobic and highly conserved in all types of influenza virus strains. It has been implicated that HA2 participates in fusion activity (see below).

Neuraminidase: The NA is encoded by the sixth gene segment and is the second major surface antigen. The neuraminidase (NA) protein plays a crucial role late in the infection by removing sialic acid from sialyloligosaccharides, releasing newly assembled virions from the cell surface and preventing the self-aggregation of virus particles. The neuraminidase protein was found to be an identical tetramer, linked by disulphide bonds. The 3-D structure of pronase-isolated NA heads was determined by X-ray crystallography at 2.2Å resolution (Varghese *et al.,* 1991). The NA protein has long been considered a valid target for antiviral therapy (Oxford *et al.,* 1998). The amino acid residues in the active site of the enzyme are highly conserved between different NA subtypes. The inhibitors against NA were shown to have antiviral activities against a broad range of influenza viruses (Varghese *et al.,* 1995). Several potent and selective medically used inhibitors, for instance, oseltamivir carboxylate (Tamiflu, Ro64-0802, and GS4071) and zanamivir (Relenza, GG167) have been discovered through structure-based rational drug design (Jackson *et al.,* 2000).

M2 protein: It forms a proton-specific transmembrane (TM) ion channel, and is activated at acidic pH (reviewed by Kelly *et al.,* 2003). The M2 protein plays significant role in both early and late stages of virus infection. During early stages, the M2 ion channel functions between the steps of virus penetration and uncoating (reviewed by Lamb *et al.,* 1994).

Matrix protein (M1): The M1 matrix protein is the major structural component inside the virion and forms a shell around the viral ribonucleoproteins (vRNPs). In addition, M1 protein is considered to be the driving force behind the budding of the virus (Gomez-Puertas *et a*l., 2000).

Viral ribonucleoproteins (vRNP): The vRNPs are comprised of 4 proteins - the nucleoprotein (NP), and the three subunits of the polymerase (proteins PB1, PB2, and PA), and are associated with each of the viral genomic RNA, forming ribonucleoprotein (RNP) complexes.

The last two proteins are encoded by the eighth gene segment and designated as non-structural proteins (NS1 and NS2). The NS1 was found to be responsible for optimal replication of the virus in the host cell. Importantly, the NS1 protein represses the host cell antiviral response by multiple mechanisms (Geiss *et al.,* 2002). The NS2 is also referred to

as nuclear export protein (NEP) and was found to be essential for export of progeny vRNPs (Neumann *et al.,* 2000) by acting as an adapter protein between the nuclear export machinery and the M1-vRNP complex. In addition, the C terminus of NS2 has been shown to interact with M1 both *in vivo* and *in vitro* (Ward *et al.,* 1995).

1.1.3 Viral propagation

Influenza virus has affinity primarily for cells in the epithelial lining of the respiratory mucosa. The virus needs to infect these cells in order to propagate itself. Virus spreads by aerosol route. As it is typical for enveloped viruses, influenza virus also initiates infection by binding to host cell surface followed by the fusion of viral and cell membranes.

Infection by influenza virus can be categorised into

A) Early stages

Attachment; binding; and fusion.

B) Late stages

Primary transcription of vRNA;
Replication of vRNA and secondary transcription;
Translation of viral mRNAs to produce viral proteins;
Post-translational modification of viral proteins;
Assembly of viral structural components and release of progeny virus.

The early steps are mediated by the surface glycoprotein hemagglutinin (HA). The proteolytic cleavage of HA0 generates HA1 and HA2 and is mostly mediated extracellularly, possibly by proteases such as those secreted by Clara cells in the lung or by co-infecting bacteria such as *Staphylococcus aureus*, *Haemophilus influenzae* , *Streptococcus pneumoniae* etc. (Whittaker, 2001). The HA mediates binding of virus to cell surface receptors containing sialic acid and subsequently mediates the fusion of viral and host cell membranes. The cell receptor contains sialic acid and the viral acceptor (anti-receptor) is at the distal end of the HA molecule. Binding to sialic acid occurs via a shallow cavity near the membrane-distal tip of the HA glycoprotein. Subsequently, influenza virus enters the cell by receptor-mediated endocytosis.

The low pH of the endosomes triggers a dramatic conformational change in HA protein, exposing the otherwise deeply embedded fusion peptide (mentioned below). Alterations of HA pull the membranes of the virus and of the endosome together. Eventually both the

membranes merge, creating a fusion pore through which the viral content is delivered into the cytoplasm. Simultaneously, acidification also activates the M2 proton channel mediating the transfer of protons into virus particles. This is assumed to be a pre-requisite for uncoating of nucleocapsid and further for releasing the RNPs and M1 protein complex into the cytoplasm of host cell. During early viral infection, dissociation of M1 from RNP is required for entry of viral RNP into the cytoplasm of the host cell (Bui *et al.,* 1996). The M1 protein was shown to inhibit viral transcription and might contribute to the shift of viral RNA synthesis towards replication in the late phase of infection (Watanabe *et al.,* 1996). In addition, antiviral compounds like amantadine and rimantadine (Monto, 2003) were shown to inhibit the M2 proton channel activity and thus the replication of the virus.

As influenza virus life cycle does not involve any DNA coding stage, the transcription occurs in the nucleus. Accordingly, after release of the RNPs into the cytoplasm, they migrate into the nucleus, by an active process and are mediated by the cellular importin a/b pathway (O'Neill *et al.,* 1995). Upon RNPs migrating into nucleus, the viral polymerase directs transcription of the negative sense RNA into a positive sense RNA that forms the template for either viral messenger RNAs (vmRNA) or for self-replication. The vmRNAs move into cytoplasm through the nuclear pores. The vmRNA directs synthesis of nucleoproteins, matrix proteins, and transmembrane proteins (HA and NA). The matrix protein and NPs synthesised are redirected to nucleus.

The production of HA and NA starts in the rough endoplasmic reticulum and progresses through the Golgi apparatus before being released onto the cell surface. As a result, these membrane glycoproteins undergo posttranslational modifications such as disulphide bond formations, glycosylation and protein folding. The oligomer formation occurs in pre-Golgi (Tatu *et al.,* 1997) and the protein undergoes trimming of carbohydrate chains in Golgi.

The vmRNAs coding for internal proteins (other than membrane associated proteins) are synthesised earlier than vmRNA coding for glycoproteins, implying some transcriptional regulation. In the nucleus, the positive sense RNA replicates to create further copies of the viral genome. These new negative sense viral genomic RNAs become associated with nucleoproteins and some matrix proteins that have migrated into the nucleus. The whole complex leaves the nucleus via nuclear pore.

The last step in the viral morphogenesis involves budding and release of the virus into extra-cellular medium. Budding takes place at the apical plasma membrane and is heavily dependent on the presence of lipid microdomains, or "rafts," which are enriched in cholesterol and sphingomyelin. Both the HA and NA, are transported from the trans-Golgi

network (TGN) and associate with lipid microdomains (Suomalainen, 2002). As a result, a complete virion is formed only at the point of budding. The viral components (HA, NA, M2 forming viral envelope; matrix protein M1; and vRNP) upon transportation to assembly site on plasma membrane interact with one another in an orderly manner (Avalos *et al.,* 1997). The viral membrane anchored proteins (HA, NA and M2) co-localize in the membrane by a selective process excluding cell proteins and come in contact with the viral nucleocapsid (the RNPs coated by M1 proteins) at the cytoplasmic leaflet of the plasma membrane. The M1 binds to the cytoplasmic tail and transmembrane protein domain of HA and NA (Ali *et al.,* 2000) on the outer side and vRNP on the inner side at the budding site. Finally, the plasma membrane at the assembly site bends, causing an outward membrane curvature, and pinches off, releasing the enveloped progeny virus particle into the extracellular medium.

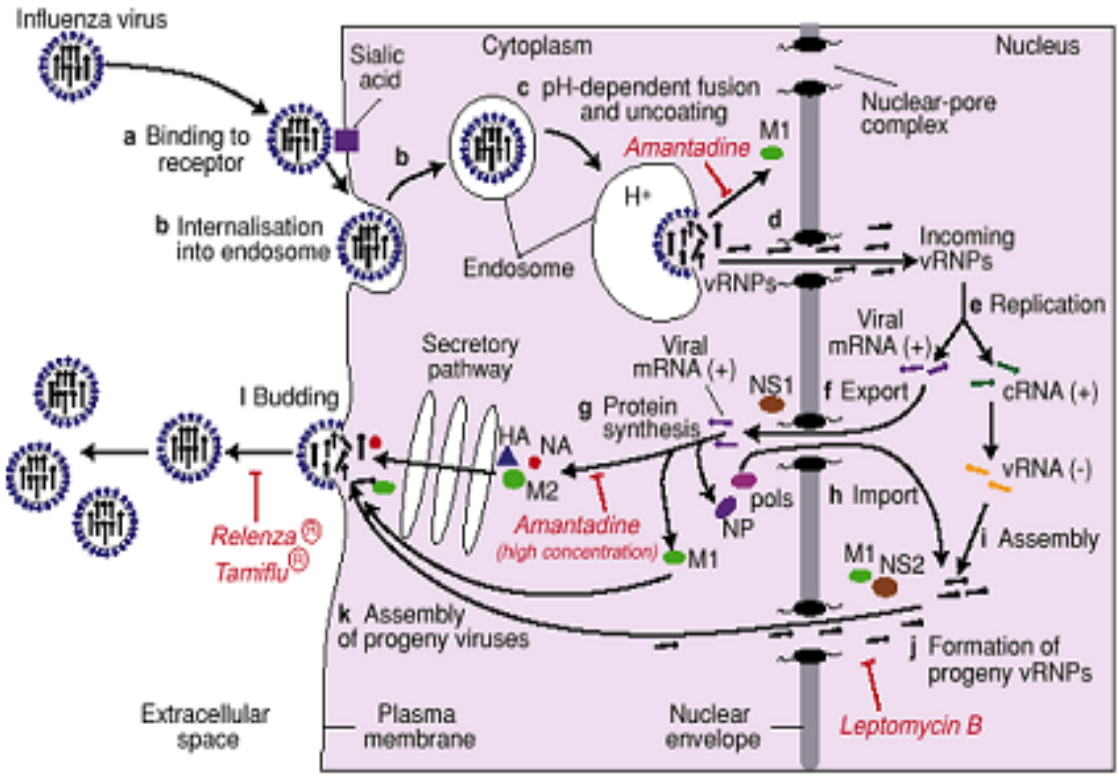

Replication cycle of an influenza virus

Expert Reviews in Molecular Medicine ©2001 Cambridge University Press

Fig 1.1.3: Replication cycle of an influenza virus (*picture along with the legend from Whittaker, 2001)*

(a) The virus binds to receptors on the surface of the host cell and (b) is internalised into endosomes. (c) Fusion and uncoating events, which are pH dependent, result in (d) the release of the viral genome (in the form of viral ribonucleoproteins; vRNPs) into the cytoplasm. The vRNPs are then imported into the nucleus for (e) replication. (f) Positive-sense viral messenger RNAs (mRNAs) are exported out of the nucleus into the cytoplasm for (g) protein synthesis. (h) Some of the proteins are imported into the nucleus to assist in viral RNA replication and (i) vRNP assembly, which also occur in the nucleus. (j) Late in infection, the vRNPs form and leave the nucleus, and (k) progeny viruses assemble and (l) bud from the plasma membrane. The sites of action of anti-viral drugs are shown in red, italic text.

Abbreviations used: cRNA(+), positive-sense complementary RNA; HA, hemagglutinin; M1, matrix protein; M2, tetrameric ion channel; mRNA (+), positive-sense messenger RNA; NA, neuraminidase; NP, nucleoprotein; NS1, a non-structural protein, NS2, a viral protein; pols, polymerases; vRNA (-), negative-sense genomic RNA.

1.2 The influenza virus hemagglutinin – its role in fusion mechanism

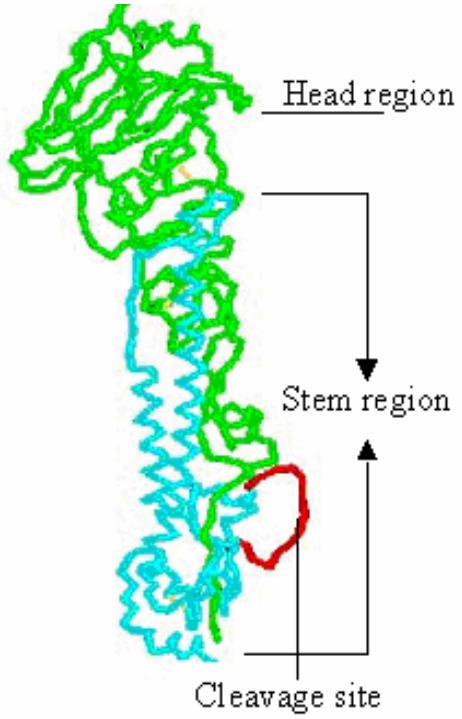

Fig.1.2: 3D structure (PDB:1QU1) of the ectodomain of the HA monomer at neutral pH
Green coloured portion is the HA1, HA2 is cyan coloured, and the cleavage site is red coloured.

The spike protein HA of influenza virus is the most and best-studied viral membrane glycoprotein. The HA0 is synthesised as a precursor that trimerises in ER and is transported to cell surface through Golgi apparatus. In X-31 strain, the cleavage of HA0 occurs at residue 328, and is absolutely required for infectivity and further for acid-induced fusion mechanism of the virus. Cleavage occurs either at the cell surface or on the released viruses. In H7 subtype, the cleavage occurs in the trans-Golgi network by furin proteases. The structure (Fig 1.2) is divided into two distinct regions: 1) a long fibrous stem region, containing residues from both HA2 and HA1; 2) a globular head region containing residues entirely from HA1. A hinge region connects these two regions. The head is composed of three independently folded globular domains made up of entirely HA1. The sialic acid binding site as well as the major antibody sites – loop, hinge, and tip/interface are located in this region. The interesting feature of the stem domain is the triple stranded coiled coil, formed by a complex of three long α-helices (from each HA2 subunit) stabilised by electrostatic, hydrophobic and other non-covalent interactions (Wilson *et al.*, 1981). The presence of cleaved HA is sufficient for fusion. This significance is confirmed by the expression of HA protein alone in tissue culture. HA expressed in mature cleaved form is capable of promoting fusion when exposed to low pH (White *et al.,* 1982) . Fusion

studies with reconstituted vesicles containing isolated HA has further confirmed the role of HA in the fusion process (Stegmann *et al.,* 1987). Thus, HA in the absence of other viral proteins can catalyse the fusion reaction, provided it is anchored in one of the fusing membranes (White *et al.,* 1982).

1.2.1 Conformational changes due to cleavage

The crystal structure of uncleaved HA0 of A/Hong Kong/68 virus was determined using a mutant R329Q, to prevent its cleavage into HA1 and HA2 (Chen *et al.*, 1998). Only 19 residues are positioned differently in the uncleaved as compared to the cleaved HA form. These residues are HA1 323- 328, R329Q and 1-12 of HA2. All of these 19 residues formed a loop at the cleavage site projecting 8 residues (HA1 327 to HA2 5) away from the molecular surface (Skehel and Wiley 2000).

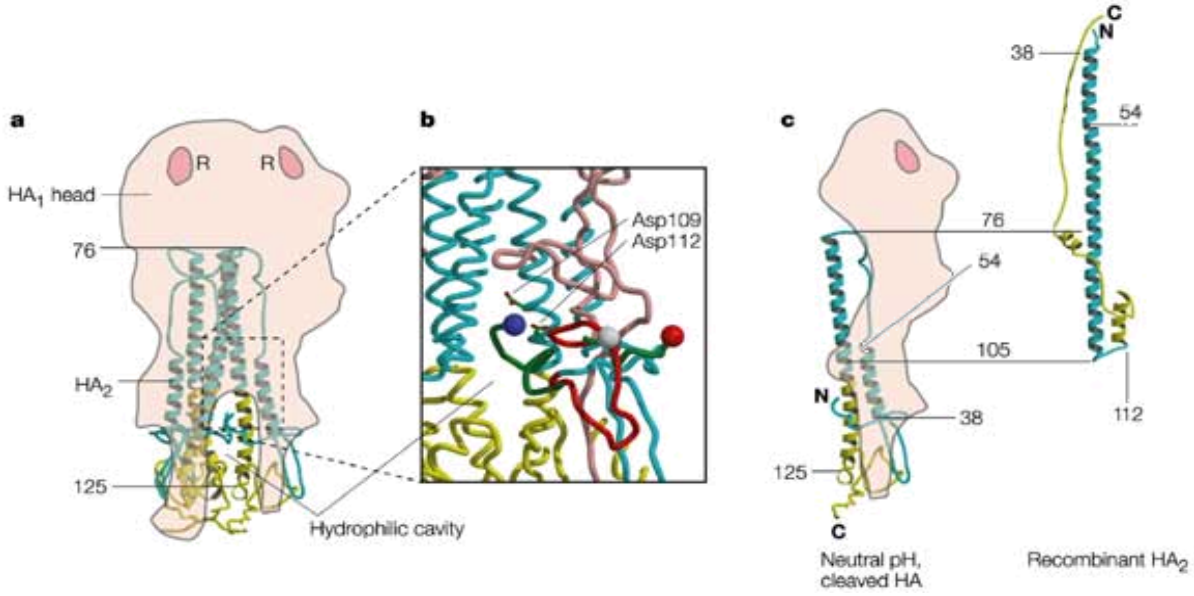

Fig 1.2.1: Three structures of the influenza virus HA. (from Colman and Lawrence 2003).
a) The extracellular domain of the neutral pH, cleaved HA trimer. The HA1 polypeptide is shown as a pink-shaded surface, and two of the three receptor-binding sites are labelled by 'R'. HA2 is represented by its backbone, which is coloured blue and yellow according to the positions of the helical regions that are shown in the structure in panel c.
b) An expanded view of the cleavage site (white sphere), which was determined from the structure of a mutant, uncleavable form of HA0. The uncleaved loop in HA0 is shown in red, and its post-cleavage conformation is shown in green. The blue and red spheres mark the amino terminus of HA2 (which is the end of the fusion peptide) and the carboxyl terminus of HA1, respectively, and the pink, blue and yellow shading are as in panel a. Two aspartic acid residues in HA2 — Asp109 and Asp112 — contribute to the hydrophilic cavity into which the fusion peptide folds on cleavage.
c) A comparison of the structure of the HA2 polypeptide in neutral pH, cleaved HA (left; taken from part a) and in recombinant, bacterially-expressed HA2 (right). The latter structure corresponds to the low pH form of HA2. In both cases, only one monomer of the trimer is shown for clarity.

The fusion peptide formed by 1-10 residues after cleavage inserts itself into a negatively charged cavity adjacent to the loop. This insertion is probably guided by an electrostatic interaction between the positively charged amino terminus of HA2 and the negatively charged cavity (Skehel and Wiley, 2000). The cavity contains Asp of HA2 109 and112 and His 17 of HA1, which upon cleavage are buried without pairing to other ionisable residues. Two HA1 C-terminal residues, Glu 325 and Arg 321, move out of the cavity on cleavage.

1.2.2 Conformational changes at low pH

The hydrophobic fusion peptide of HA2, that is originally buried in the interior of HA trimer becomes exposed at a pH of 5.0 – 6.0 depending on the strain of the virus. This conformational change presented a difficulty for crystal structure determination of low pH HA2. The exposure of hydrophobic fusion peptide leads to protein aggregation and thus prevents crystal formation. Nevertheless, the X-ray crystal structure of the HA2 at low pH (TBHA2) was determined (Bullough *et al.,* 1994; Chen *et al.,* 1999) after solubilising the low pH treated BHA with either protease Lys C or trypsin into HA1 monomers. The left over aggregates from such a solubilised BHA were further proteolysed by thermolysin, which removed the fusion peptide region from HA2 domain. The crystal structure of the remaining fragment (TBHA2) containing HA2 residues 38-175 disulphide linked to HA1 residues 1-27 in the low pH conformation was identified.

The X-ray crystal structure of TBHA2 revealed that the residues from 76-105 remain unchanged with respect to BHA at the neutral pH. However, this structure reveals three major changes in BHA at low pH. First, the residues 54 to 76 of HA2 (HA2 54–76) which were unstructured in neutral-pH BHA are helical in TBHA2. Second, residues 106 to 112 of HA2 (HA2 106–112 region) have undergone a helix-to-loop transition at low pH. Third, the helix C-terminal of the new loop has flipped to lie antiparallel to the coiled coil. Chen *et al,* (1999) from their *E. coli* expressed TBHA2, reported that the monomer structure is 110 Å long. The overall conformational change brings the fusion peptide in proximity to the target membrane and also bends the molecule in such a way that the fusion peptide and viral membrane anchor are towards the same end. Upon acidification, the conformational change described above is rapid compared to the fusion process (Godley *et al.,* 1992).

1.2.3 Structure of the fusion peptide

The fusion peptide constitutes of the first 20-25 amino acids of the N-terminus of HA2 chain formed by cleavage (Epand, 2003). These residues are essentially hydrophobic. They are highly conserved among different strains of the influenza virus. Even very conservative single point mutations have been shown to effect fusion. The fusion peptide is rich in Gly providing it greater flexibility of the peptide. The fusion peptide is followed by nine polar residues, which though form a part of the low pH crystallised structure, do not form any ordered structure in these crystals. For this reason, it is likely that the fusion peptide constitutes an independently folded domain when it is inserted into target membrane. Although there is convincing evidence that the fusion peptide inserts into the hydrophobic phase of the membrane, it is still unclear whether it solely inserts into the target membrane (Shangguan *et al.,* 1998) or whether it inserts at an early stage into the viral membrane before relocation to the target membrane (Kozlov and Chernomordik 1998). Kozlov and Chernomordik (1998), and Bentz (2000) reason that HAs with the fusion peptide embedded initially into the viral membrane are along the fusion pathway. Though the structure of HA fusion peptide has been observed in random coil, α-helical and β-sheet based on environment, there is strong evidence that it is the helical form which promotes fusion. The mutants inhibiting fusion are less helical and have a tendency to self-associate into β-sheets (Li *et al.* 2003).

1.2.4 Role of the ectodomains in membrane fusion

The role of structural changes of the HA ectodomain in membrane fusion was highlighted from polarised Fourier transform infrared (FTIR) studies of full-length HA and some of its fragments (Tatulian and Tamm, 2000; Gray and Tamm, 1998). These experiments provided some information about the possibility of the low pH structure of HA or of its intermediates to fit in between the two membranes that are to be fused. Gray and Tamm (1998) reported that helical coiled coils were tilted by a large angle at pH 5. The tilting might occur before or after insertion of fusion peptide providing a mechanism to pull the target and viral membranes into close proximity. The distance between the two membranes is reduced from 13 nm to approximately 4 nm if the ectodomains tilt by an angle of 70°. Further, Tatulian *et al.* (1996) reported that tilting was a reversible process in the absence of the target membrane. Gray and Tamm (1997) confirmed that tilting occurred in X-31 HA and that the hinge region was at the base of the HA near the transmembrane (TM)

domain. Tamm (2003) hypothesised that the process was more a membrane-driven rather than a protein-driven process. It is attributed to a protein clamp, which could hold the structure at neutral pH and release at low pH. The clamp may be reattached in the absence of target membranes, but removed from interaction with the core protein in the presence of target membranes, if the clamp interacts with these membranes. The possible candidates for this protein clamp could be parts of the HA1 domain shown to be interacting with bilayer model membranes (Bui *et al.,* 1996). A second hinge domain was also identified by the same research group between the fusion peptide and the ectodomain. It is hypothesised that several trimers tilt simultaneously towards each other, pull the membranes that are to be fused into close proximity, and thereby establish a precursor of the fusion pore.

1.3 Models for membrane fusion

The rate of fusion is influenced both by the HA surface density and the target lipid composition (Clague *et al.,* 1991). The number of trimers required for initiating fusion pore formation is not clear and the number varied from three to eight trimers. Daniele *et al. (*1996) reported the number as either three or four; Blumenthal *et al.* (1996) suggested six trimers and Bentz *et al.* (2000) proposed that at least eight trimers have to be at the fusion site, of which only two or three trimers might be needed to enable the fusion competent conformational changes.

All the models proposed for the mechanism of HA mediated fusion were based on the low pH conformational changes of the HA protein, but differ in that the formation of the initial fusion pore to be either lipidic or proteinaceous. Bentz and Mittal (2000) took into account various fusion models and suggested four distinct intermediates, subsequent to close apposition of the membranes and low pH induced conformational changes of HA. These are

1) Fusion proceeds from an aggregation of HA, formed either before or after acidification.
2) The sign of a fusion pore is defined by the first measurable conductivity (2-5 nS) across the membranes. Additional flickering of the pore may follow which eventually may lead to the formation of an irreversible opening of the pore.
3) Formation of a lipidic channel, monitored by lipid dye transfer between membranes.
4) The fusion site monitored by the mixing of aqueous contents (e.g., fluorophors) and the stable merging of the two membranes and complete-mixing of aqueous

contents.

The mechanisms of fusion mediated by HA were investigated by monitoring fusion of erythrocytes (RBCs) stained with fluorescent lipids and solutes with cells expressing HA (Blumenthal *et al.,* 1996). A delay in lipid redistribution following the low pH treatment implies that fusion could be a multistep process (Clague *et al.,* 1991). The kinetic studies of fusion cascade have revealed a number of intermediates, which include formation of a hemi-fusion diaphragm which allows lipid redistribution, transient fusion pore, and a large pore which allows transfer of solutes (Blumenthal *et al.,* 1996). Hemifusion (Chernomordik *et al.,* 1999) was referred to as a stage of the stalk wherein the contacting monolayers are in contact while the distal (*trans)* monolayers are apart giving the appearance of an "hour-glass".

In the proteinaceous model (Lindau and Almers, 1995; Tse *et al.,* 1993) the fusion pore is an oligomeric ring structure formed by aggregates of HA trimers. Thus, the aqueous fusion pore would be initially lined by proteins and subsequently lipids would be directed to the fusion site. On the other hand, the lipid theory (Hernandez et al., 1996; Jahn and Sudhof, 1999) assigns a greater role for lipids in the formation of the fusion intermediate. This method advocates a hemifusion intermediate, which further continues to expand resulting in the formation of a lipid lined fusion pore.

However the model of stalk-lipidic pore was strongly supported by Chernomordik *et al,* (1998) showing lipids which do not favour the formation of stalk inhibits fusion while lipids which support stalk formation promote fusion. The concept of hemifusion was supported by glycosylphosphatidylinositol-linked ectodomain of HA (GPI-HA) lacking the transmembrane domain and cytoplasmic tail (Kemble *et al.,* 1994) which showed lipid mixing with similar time course and efficiency as wt-HA, but did not mediate transfer of soluble contents. The hemifusion under these sub optimal conditions could not make progress to complete fusion even after reversal to optimal conditions suggested it to be a branch of the regular HA mediated fusion pathway. Chernomordik *et al.* (1998) described another fusion intermediate – FIF (frozen intermediate of fusion). The low temperature (4° C) arrested-intermediate, (after low pH conformational change) has not shown either lipid mixing or aqueous pore formation. Furthermore, it was revealed to be a part of the pathway leading to hemifusion.

1.3.1 HA – a metastable conformation

The fusogenic state of HA molecule is more stable than the cleaved, non-fusogenic HA molecule at neutral pH (Carr and Kim 1993). In addition, the ectodomain is kinetically trapped behind an energy barrier because of extensive non-covalent interactions. It has been experimentally deduced (Carr *et al.,* 1997) that the HA molecule at non-fusogenic state was metastable and that the conformational change could be triggered even at neutral pH either by heat or by urea-mediated denaturation leading to membrane fusion activity. Chen et al. (1995) reported that the bacterial expressed ectodomain of HA2 (comprising amino acids 23-185) at neutral pH, folds spontaneously into a fusion-pH-induced conformation. This observation supports the metastable nature of HA.

To elucidate whether the HA conformational transition is associated with exothermic reaction; Differential scanning calorimetry (DSC) is the method of choice (Huang *et al.,* 2003). There is difference in opinion about the energetics of conformational change of HA ectodomain.

Investigating the energetics, Remeta *et al.* (2002), and Epand and Epand (2002) found endotherm DSC peaks during the unfolding process of HA ectodomain. In addition, they report that neutral pH; non-fusogenic HA is very stable and is not metastable.

Contradicting the above statement, Huang *et al.* (2003) opined that the formation of extended coiled coil involves exothermic reaction and the experiments from Remeta *et al.* (2002) and Epand and Epand, (2002) did not cover the temperature region at which the exothermic peak occurs. Further, it may be envisaged that both the DSC studies may have failed to detect an exothermic peak. Probably, the extended coiled-coil could have formed already prior to DSC measurement as already acknowledged by Epand and Epand (2002).

1.3.2 Opening of the HA1 distal domain – an essential step for the conformational change

Extensive studies have been performed on the acid-triggered conformational changes that are related to the fusogenic activity of influenza HA (Skehel and Wiley, 2000). White and Wilson (1987) using a panel of anti-HA antibodies concluded that acid triggered conformational change of isolated HA occurs in two steps:

Changes occur in the stem region of the trimer resulting in the release of the fusion peptides from the trimer interface.

The globular heads dissociate substantially from one another apparently by bending around the hinge region.

The characterisation of HA of X-31 at 0°C and the HA from the Japan strain of influenza virus at 37°C supported this two stage conformational change (Puri *et al.,* 1990; Stegmann *et al.,* 1987 and 1990). HA after conformational change is found to be extremely susceptible to proteolysis at specific residues. Studies using circular dichroism and monoclonal antibodies indicated that the molecule has not just denatured, but low pH-induced changes involved movement of molecular domains relative to each other (Skehel *et al.,* 1982; Daniels *et al.,* 1985). Furthermore, Wiley and Skehel (1987) suggested that interactions between the membrane distal globular domains containing the receptor binding sites and the epitopes for infectivity-neutralising monoclonal antibodies were perturbed specifically at fusion pH. Studies from electron microscopy, chemical cross-linking (Ruigrok *et al.,* 1986) and size estimates of HA fragment in solution (Bizebard *et al.,* 1995) clearly indicated that the dissociation of HA membrane-distal domains occur at low pH. The locking of the HA1 subunits by intermolecular di-sulphide bonds in the distal part (Thr 212 and Asp 216 residues of HA1) prevented the conformational change of HA and abolished the fusion activity (Godley *et al.,* 1992; Kemble *et al.,* 1992). In a comparable approach, Barbey-Martin *et al.,* 2002 cross-linked HA monomers using an antibody whose epitope comprised residues from two HA monomers (complex consisted of HA monomer and Fab in 2:1 ratio). This complex was resistant to any conformational change even at low pH demonstrating the need for a partial dissociation and reorientation of HA membrane distal domains for fusion activity. Though it is clear from the above experiments that dissociation of globular domains forms the initial step towards successful fusion activity, the mechanism of dissociation and the forces involved remain still unsolved.

1.4 Protonation effects – possible role in dissociation of HA1 domains

An attractive model for the stability of the non-fusogenic state of HA protein is provided by Huang *et al.* (2002). The model posits that the stability of HA is contributed by the net charges of the HA1 and HA2. At neutral pH, the charges are balanced viz., zero. This stability is disturbed only due to enhanced protonation at low pH (discussed below).

This model takes into consideration, the crystal structure of HA (X31 strain) at neutral pH (PDB: 1HGF). The theory is based on molecular modelling techniques (Beroza *et al.,* 1991; Ullmann and Knapp 1999). The protonation calculations were performed on HA at neutral pH with respect to dependence on pH and temperature. Based on the calculations, the model proposes that the net charge of HA1 domain is positive and the HA2 domain, in particular the distal part, is locally enriched with negative charges. The HA1 domains by

themselves would not be able to form a stable trimer. This indicates that, in the HA ectodomain at neutral pH, the electrostatic force between either three subunits of HA1 or of HA2 is repulsive, however that between HA1 and HA2 domains is attractive. The work also involves comparing the protonation patterns with that of the HA ectodomain stability assessed by proteolysis (proteinase K assay).

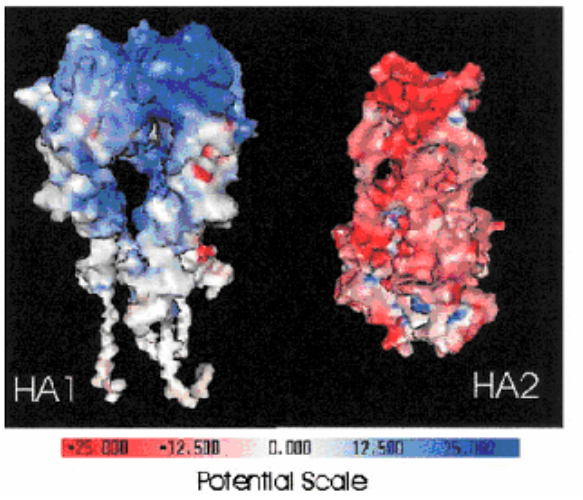

Fig 1.4: Surface electrostatic potential of HA1 domain and HA2 domain with GRASP.
(Figure courtesy (Huang et al., 2002 Biophysical Journal 82; 1050–1058))
Electrostatic potential is color-coded using a sliding scale indicated in the lower part of the figure (unit in k B T/e). Red represents negative electrostatic potential; blue represents positive electrostatic potential, and white is neutral.

According to this model, the HA1 domains exposed to solvent show enhanced protonation at low pH and further, the enhanced protonation gives rise to electrostatic repulsion resulting in destabilisation of the head domains of HA1. Indeed the largest contribution to the electrostatic potential within a protein may arise from protonable amino acids that can carry a net charge. The model argues that the solvent components (water, proton, other ions etc.) interact directly with the surface of HA1 domain. The HA2 domain being buried under the HA1 domain is shielded from the interaction with the solvent. Thus the authors surmise that initially, the protonation state of HA1 domain could be influenced by a pH decrease, whereas the protonation of the HA2 subunits only after an initial destabilisation and re-arrangement of the HA1 domains of a trimer. The hypothesis points out that at low pH, the enhanced protonation of HA1 affects the non-covalent interactions (van der Waals and electrostatic forces) between the HA1 subunits, in particular the electrostatic forces. As the three subunits of a trimer are identical and symmetrical (Wilson *et al.,* 1981), the protonation state and respective changes at low pH should be similar for each subunit.
To describe the destabilisation process, the essential features are summarised in the figure.

At neutral pH, ignoring the local thermal vibrations of the atoms, the HA ectodomain can be viewed as a stationary, force-balanced-structure implying the overall forces between the monomers as zero (all attractive and repulsive contributions cancel each other taking also into account the solvent interactions).

When decreasing the pH, the electrostatic repulsive force between the HA1 monomers becomes enhanced by protonation. As the original attractive forces cannot cancel the increased repulsion, the neutral pH, non-fusion active structure becomes force unbalanced.

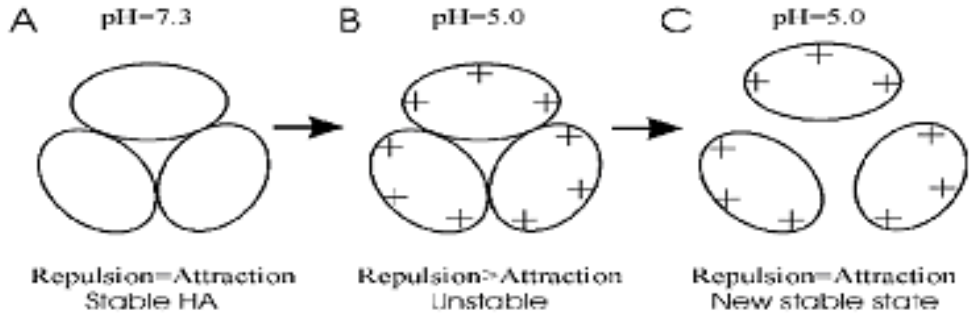

Fig 1.4.1: Protonation model for HA stability *(Huang et al., 2002 Biophysical Journal 82; 1050–1058)*

a) Top view of the HA1 domain of the stable trimeric HA ectodomain at neutral pH; b) Enhanced protonation of the solvent-exposed HA1 domain weakens the attraction between three HA1 subunits at low pH; c) The new stable state of HA1 domain after its partial dissociation at low pH is determined by a balance between attractive and repulsive forces.

Thus the three HA1 monomers will move apart and a new balance between the attractive and repulsive forces depending on the atomic coordinates will determine their new positions i.e., the extent of the dissociation depends on the changes of attractive and repulsive forces with respect to the dissociation state itself. The calculations and related experiments by the authors supported that the protonation of HA1 was enhanced at fusion pH conditions.

This modelling approach provides a basis and explanation to the puzzling observations on conformational changes of HA occurring at higher temperatures and neutral pH as reported by Carr *et al.* (1997). It may be deduced that protonation becomes enhanced by increasing the temperature and results in a conformational change. Furthermore, a weakened attraction between the HA subunits may facilitate not only a relocation of the HA1 subunits, but also enable the subsequent steps of the conformational change of the HA into a fusogenic state by the spring-loaded mechanism. Thus it is quiet evident from the above observation and by disulfide linking experiments from Godley *et al.* (1992) and Kemble *et al.* (1992) that the HA1 domains act as “clamp” enclosing the HA2 domains and shielding them from solvent exposure.

This attractive model emphasises the role of electrostatic interactions in maintaining the stability of HA protein at neutral pH. Also taking into account that the HA protein crystal structure indicates a high number of salt bridges (discussed below), this model needs an experimental approach by selectively targeting ion-pair interactions specifically in the interface region of HA1 and HA2.

1.5 Role of salt-bridges (ion pairs) in protein conformation

When amino acid side chains of opposite charge are in close proximity, they can form an ion pair (also called a salt bridge). They are also capable of hydrogen bonding and hence, are usually found on the surface of the protein. If they can form a salt bridge, they will usually be buried. The maintenance of the tertiary (3D) structure of the protein depends essentially on the non-covalent forces and more so on the salt bridges, as these are the most important interactions involved in the oligomerization of proteins. An ion pair is defined as a salt bridge if the centroids of the side-chain charged group atoms in the residues lie within 4.0 Å each other and at least one pair of Asp or Glu side chain carbonyl oxygen and side chain nitrogen atoms of Arg, Lys, or His are also within this distance (Kumar *et al.,* 1999). As a salt bridge is basically made of charged residues and that charge is affected by pH, salt bridges can be broken by either low or high pH conditions or by high concentrations of salts like Na^+, K^+, etc. Since the present work is aimed at the effects of protonation on early conformational changes in HA protein, salt bridges obviously would be the focus of the present study. Salt bridges could be broadly categorised as “simple” or “complex” depending upon the number of residues involved (Musafia *et al.,* 1995). A simple salt bridge involves a non-bonded or hydrogen-bonded ion paired interaction that joins a single pair of charged amino acid residues, where as a complex salt bridge joins more than two residues (such as the triad Asp-Arg-Asp) in single or adjacent protein chains. It was reported that complex salt bridges probably serve a more significant role because of the co-operativity involved (Marqusee and Sauer, 1994). In recent past, salt bridges were among the more thoroughly investigated functional groups with respect to homo and hetero protein complexes (mostly dimers), but the research related to higher multimeric states like trimers and tetramers and especially those of viral coat proteins has still not been addressed (Jones and Thorton, 1996). Musafia *et al.* (1995) worked on the statistical analysis of complex salt bridges from 94 proteins found in PDB database and reported that 60 % of the proteins contained complex salt bridges, more so triad salt bridges (involving 3 charged residues) were abundant. Further, the report quoted that

influenza virus hemagglutinin-3 (PDB ID: 3hmg) contained the largest complex salt bridge involving 15 charged amino acids interacting among themselves to connect the three subunits. Indeed, a look into the 3 D structure of HA protein (1hge or 1hgf) shows that the protein has an extensive network of salt bridges involving 97 cationic residues forming salt bridges with an equal number of anionic residues. The focus of the present investigation is on the interface region between HA1 and HA2 chains of monomer, which is strongly engaged in the conformational change (described above). Xu *et al.* (1997) reports that interface regions are similar to the protein surfaces and more hydrophilic than the protein interiors. In addition, the interface regions tend to form more hydrogen bonds and salt bridges than protein interiors. This argument gains credence as the interface region between HA1 and HA2 containing the sequences Lys 58 till Arg 76 of HA2 region forms nearly seven salt bridges (protein explorer view) within the same monomer and also with the adjacent monomers.

2 AIM

It is very evident that salt bridges are sensitive to pH changes and the low pH causes breakage of salt bridges. This results in interaction of negatively charged Asp or Glu amino acids with the solvent. This interaction would in turn leads to an enhanced net positive charge in the region, resulting in repulsion and partial dissociation of HA1 and HA2 domains. Taking this assumption as a cue, the present work aims

1. Make and break the salt linkages in the HA molecule from X-31 strain.
2. To either destabilize or stabilize the HA protein with respect to salt bridges, and thereby determine the contribution of electrostatic interactions towards HA protein stability.
3. Investigate to determine the important amino acids that are responsible for the stability of the non-fusogenic HA at neutral pH.
4. Experimentally prove the protonation model and there by the metastability of HA protein at low pH.
5. To correlate the mutants with naturally existing variants and based on the results derive a model for early steps of conformational changes leading to successful fusion.

3 MATERIALS

3.1 Biological Material

3.1.1 Host Strains (Escherichia coli & Genotype)

XL1-Blue from Stratagene
*recA1 endA1 gyrA*96 *thi*-1 *hsdR*17 *supE*44 *relA*1 *lac F' proAB lacI*^{q}*ZΔM15* Tn*10*

XL1-Blue Supercompetent cells
recA1 endA1 gyrA96 thi-1 hsdR17 supE44 relA1 lac [F' proAB lacI^{q}*ZΔM15 Tn10 (Tet*^{r}*)]*^{c}

3.1.2 Cell lines

CV-1 cell line
COS-7 cell line

3.1.3 Vaccinia virus

Vaccinia virus strain vTF7-3

3.1.4 Vector DNA

pTM1 vector DNA **(**Amp^{r}) containing Hemagglutinin (HA) gene (pTM1-HA)– as a gift from Dr. Judith White (Department of Cell Biology, University of Virginia Health System, Charlottesville, VA, USA)

3.1.5 Antibodies

N2 antibody – as a generous gift from Dr. Judith White

C-HA1 antibody - as a generous gift from Dr. Judith White

FHA2 antibody - as a generous gift from Dr. Leonid Chernomordik (Unit of Lipid Inermediates in Fusion. National Institutes of Health, LCMB, NICHD, Bethesda, MD. USA).

3.2 Oligonucleotides

The following were the oligonucleotides synthesized for mutations and further cloning of the synthesised mutants into pTM1-HA vector DNA. All were synthesised by Invitek GmbH, Berlin, Germany.

R109G1 (32mer) (BamHI site generated)
5'ATTATGCCTCCCTTGGATCCCTAGTTGCCTCG 3'
R109G2 (33mer)
5'ACGAGGCAACTAGGGATCCAAGGGAGGCATAAT 3'

R109E1 (30 mer) (xhoI site generated)
5'ATTATGCCTCCCTCGAGTCACTAGTTGCCT 3'
R109E2 (32 mer)
5'GCAACTAGTGACTCGAGGGAGGCATAATCTGG 3'

R269G1 (29 mer) (BamHI site generated)
5‘ AGCTCAATAATGGGATCCGATGCACCTAT 3‘
R269G2 (30 mer)
5‘ ATAGGTGCATCGGATCCCATTATTGAGCTT 3‘

R269E1 (28 mer)
5‘ AGCTCAATAATGGAATCAGATGCACCTA 3‘
R269E2 (28 mer)
5‘ AGGTGCATCTGATTCCATTATTGAGCTT 3‘

K299G1 (34 mer) (alwI site generated)
5‘ CAAAACGTAAACGGGATCACTTATGGAGCATGCC 3‘
K299G2 (35 mer)
5‘ GCATGCTCCATAAGTGATCCCGTTTACGTTTTGAA 3‘

K299E1 (34 mer) (Nde I site abolished)
5‘ CAAAACGTAAACGAGATCACTTATGGAGCATGCC 3‘
K299E2 (35 mer)
5‘ GCATGCTCCATAAGTGATCTCGTTTACGTTTTGAA 3’

S110D1 (27 mer) (Bgl II site generated)
5'GCCTCCCTTAGAGATCTAGTTGCCTCG 3'
S110D2 (27 mer)
5'CGAGGCAACTAGATCTCTAAGGGAGGC 3'

I89E1 (24 mer)
5'AGACACTAAAGAAGATCTCTGGTC 3'
I89E2 (24 mer)
5'GACCAGAGATCTTCTTTAGTGTCT 3'

I89R1 (26 mer)
5'GAAGACACTAAAAGAGATCTCTGGTC 3'
I89R2 (26mer)
5'GACCAGAGATCTCTTTTAGTGTCTTC 3'

Y308R1 (27 mer)
5'GCATGCCCCAAGAGAGTTAAGCAAAAC 3'
Y308R2 (27mer)
5'GTTTTGCTTAACTCTCTTGGGGCATGC 3'

T212E-N216R1 (40mer) (Avr II site generated)
5’AGAAGCCAGCAAGAAATAATCCCTAGGATCGGGTCCAGAC 3’
T212E-N216R2 (40mer)
5’GTCTGGACCCGATCCTAGGGATTATTTCTTGCTGGCTTCT 3’

N216E1 (26mer)
5’AGAAGCCAGCAAGAAATAATCCCTGAAATAGGGTCCAGAC 3’
N216E2 (26mer)
5’GTCTGGACCCTATTTCAGGGATTATT 3’

3.3 Chemicals and Film material

Acrylamide, bis-acrylamide, sucrose, Tris, HCl, sodium chloride, sodium hydroxide, cetyltrimethylammonium bromide (CTAB), glycerol, parafilm, powder-free gloves, potassium chloride, ethylenediaminetetraaceticacid (EDTA) **(Carl Roth GmbH, Karlsruhe, Germany).**

Agarose **(Hybaid GmbH, Heidelberg, Germany).**

Calcein-AM (acetoxymethylester of calcein, used 50 mM in DMSO); R18 (octadecylrhodamin B chloride, used 2 mM in ethanol;

calcein(MW 623, excitation at 495 nm, emission at 520 nm), excitation at 560 nm, emission at 590 nm), dextran-conjugated tetramethylrhodamine, neutral (TMR-D, MW 10,000; excitation at 555 nm, emission at 580 nm) **(Molecular Probes, Göttingen, Germany)**.

Cell culture flasks, cell culture dishes **(Greiner Bio-one GmbH, Frickenhausen, Germany)**.

Dimethylsulphoxide (DMSO), isopropanol, bovine serum albumin (BSA), ammonim per sulphate (APS), ammonium chloride, Tween 20, citric acid, salicylic acid, TPCK trypsin (type XIII from bovine pancreas, TPCK treated), trypsin inhibitor, fixer and developer for X-ray film development, N,N,N',N'-tetramethylethylenediamine (TEMED), 3-3'-dithiobissuccinymidylpropionate (DSP; cross-linking reagent), phenyl-methylsulonylflouride (PMSF; protease inhibitor) **(Sigma Chemicals).**

DMEM (with L-methionine, L-Glutamine and Glucose), Lipofectin reagent, bacto-agar, peptone, 2YT medium **(Invitrogen GmbH, Karlsruhe, Germany)**.

DMEM (with L-methionine, L-Glutamine and Glucose), Trypsin-EDTA solution (0.05%/0.02% in PBS) **(Cambrex Bio Science Verviers, Belgium)**.

Ethanol, acetic acid **(Merck, Darmstadt, Germany)**.

Ethidium bromide, Triton X-100 **(Boehringer Mannheim, Mannheim, Germany).**

Foetal bovine serum (FBS), PBS^{++} (PBS with Ca^{++} and Mg^{++}). **(Biochrom KG, Berlin, Germany).**

Hepes, L-glutamine, bromophenol blue **(Serva, Heidelberg, Germany)**.

Oligonucleotides **(Invitek GmbH, Berlin, Germany)**.

Pre stained protein standard markers for SDS-gel electrophoresis **(Peqlab)**.

Qiagen plasmid maxi-kit along with buffers for plasmid DNA extraction **(Qiagen GmbH, Hilden, Germany)**.

QuikChange site-directed mutagenesis kit **(Stratagene, La Jolla, CA, USA)**.
Restriction enzymes and buffers, Rnase A1, lysozyme, lambda maker for DNA analysis on ge electrophoresis **(New England Biolabs, Schwalbach/Taunus, Germany)**.
Sodiumdodecylsulphate (SDS) **(Biomol Feinchemikalien GmbH, Hamburg, Germany).**
X-ray films **(Kodak, England).**

3.4 Equipments

Avanti J25 High performance centrifuge (rotors: JA-25.50, JLA-16.250), Ultra centrifuge L7 65 (rotor Ti 45), FACS machine **(Beckmann Coulter)**.
Vertical gel electrophoresis tank and power pack, ScanPack 2.0 software for densitometry **(Biometra GmbH, Göttingen, Germany)**.
Agarose mini-gel electrophoresis tank **(Blomed Analytik GmbH, Göttingen, Germany).**
Thermomixer, pipette tips, pipette man **(Eppendorf).**
CO_2 incubator **(Forma Scientific, Life sciences GmbH, Frankfurt a.M, Germany).**
Gilson micro-pipettes **(Gilson medical electronics, France).**
Inverted microscope **(Helmut hund GmbH, Wetzlar, Germany)**.
Lamin Air **(Heraeus Industries GmbH, Berlin, Germany).**
Wterbath **(Lauda DR. R. Wobser GmbH & Co, Lauda-koenigshofen, Germany).**
PCR thermalcycler **(Perkin Elmer, Vaterstetten, Germany).**
Mcro pipettes **(SC-pette Nichiryo, Sued-Labordedarf GmbH, Gauting, Germany).**
Vortexer **(Scientific Industries, NY, USA).**
Toshiba Microwave **(TÜV Rheinland Koeln, Germany).**
Gel dryer **(UniEquip Laborgeraetebau + vertriebs GmbH, Martinsried, Germany).**

3.5 Glass and Plastic ware

Micropipettes, Eppendorf tubes, Glass flasks, Glass pipettes, Glass spreader, Petriplates, Tubes.

3.6 Solutions and Media

2YT medium: Bacto Trypton 16 g, Yeast extract 5 g, NaCl 5 g, distilled water made upto 1000 ml. The solution pH is adjusted to 7.2 with 1N NaOH. The solution is sterilized by autoclaving.
Ampicillin: solution of 50 mg/ml in dist.water and filter sterilized.
Fusion buffer: 10 mM MES, 100 mM NaCl, 10 mM HEPES, 2 mg/ml glucose. The fusion

buffer is adjusted to desired pH with 2 M NaOH.

Lysis buffer (for trimer assay with DSP): 50 mM NaOH, 150 mM NaCl, 1 % NP 40, 5 mM Iodoacetamide, 1 mM PMSF.

Lysis buffer: 100 mM Tris pH 7.4, 1 % NP-40.

RIPA buffer: 1 % Triton X-100, 1 % deoxycholate, 0.1 % SDS, 0.15 M NaCl, 20 mM Tris, 10 mM EDTA, 10 mM iodoacetamide, 1 mM PMSF.

SDS-PAGE reagents

10X PAGE buffer : 30 g Tris-base, 110 g Glycin, 10 g SDS in 1 liter dist.water.

Tris pH 8.8 (1.5 M): 181.71 g of Tris-base in 1 liter of dist.water and pH is adjusted to 8.8 with 2M NaOH and stored at –4°c.

Tris pH 6.8 (0.5 M) : 60.57 g of Tris-base in 1 liter of dist.water and pH adjusted to 6.8 stored at – 4°c.

6 X SDS-PAGE loading buffer: 15 % DTT, 15 % SDS, 1.5 % Bromophenol blue, 50 % glycerol.

Fixing solution for PAGE gels: 10 % acetic acid, 40 % methanol.

Solutions for DNA extraction

Resuspension buffer: 50 mM Tris-Cl, pH 8.0; 10 mM EDTA; 100 µg/ml RNase A.

Lysis buffer: 200 mM NaOH; 1 % SDS.

Neutralisation buffer: 3.0 M potassium acetate, pH 5.5.

Equilibration buffer: 750 mM NaCl; 50 mM MOPS, pH 7.0; 15 % isoproponal; 0.15 % Triton X-100.

Wash buffer: 1 M NaCl; 50 mM MOPS, pH 7.0; 15 % isoproponal.

TE: 10 mM Tris-Cl, pH 8.0; 1 mM EDTA.

STET buffer: 8 % sucrose, 0.1 % Triton X-100, 50 mM EDTA, 50 mM Tris/HCl pH8.0.

TAE buffer: 1 mM EDTA, 200 mM acetic acid, 40 mM Tris.

4 METHODS

4.1 Site Directed Mutagenesis

In vitro site-directed mutagenesis was performed using QuikChange™ site-directed mutagenesis kit from Stratagene. The reaction was based on PCR performed according to the manufacturer's instructions.

A typical PCR contained approximately 50 ng of dsDNA, 125 ng each of the two oligonucleotide primers, 1 µl of dNTP mix, 1 µl (2.5 U) of polymerase and 5 µl of 10X reaction buffer in a reaction volume of 50 µl. All the components except the oligonucleotide primers were provided in the kit. The reaction was performed using *PfuTurbo* DNA polymerase and two synthetic oligonucleotide primers comprising the desired mutation. Oligonucleotide primers (oligos) were designed to incorporate the desired mutation, and the *PfuTurbo* DNA polymerase replicates both the plasmid strands with high fidelity without displacing the mutant oligos. The thermal cycles consisted of an initial denaturation cycle of 95°C for 30 seconds, followed by 16 cycles of denaturation for 30 sec, annealing at 55°C for 1 minute and extension at 68°C for 15 min (2 min/kb of plasmid length). The oligos complementing the opposite strand of the plasmid DNA are extended during thermal cycling thus generating the entire copy of the mutant plasmid containing staggered nicks. Following the thermal cycling, the product was treated with *Dpn* I enzyme (target sequence 5'-Gm^{6}ATC-3'). The nicked vector DNA containing the mutation was then transformed into XL1-Blue supercompetent cells. A volume of 1 µl of the product was used for transformation and the transformation mix was plated on an YT-ampicillin agar plates, incubated at 37°C for approximately 16 hrs. The recombinant colonies were screened by mini-prep, followed by RE analysis and further confirmed in some cases by sequencing.

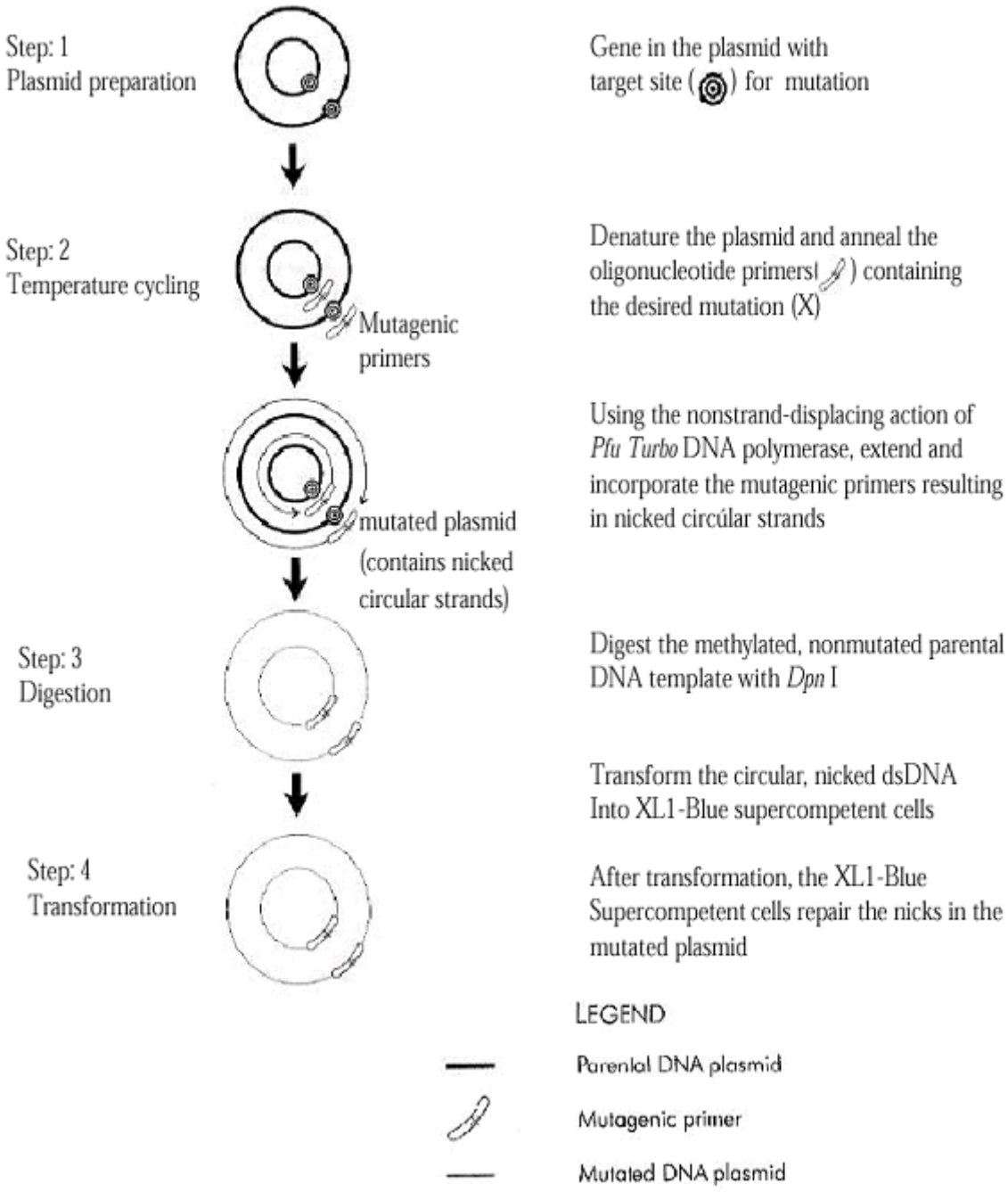

Figure 4.1: Overview of the Quik-change Site-directed Mutagenesis experiment.

4.2 Oligonucleotide primer designing

Guidelines mentioned in the product manual of the QuikChange^{TM} site-directed mutagenesis kit from Stratagene were followed for designing of primers. In most cases, the primers were designed in such a manner so as to facilitate either incorporation of a new RE site or remove the existing RE site. This was achieved by creating silent mutations in or around the desired mutation region. Both the forward and reverse primers contained the

desired mutant. The primers anneal to the same sequence on opposite strands of the plasmid (schematically shown in figure). The length of the primers was set to approximately 25 – 30 bases. Care was taken to have a minimum of 10 bases flanking the mutant site. GC content was maintained between 40 – 60 %. The melting temperature (T_m) of the primers was calculated using the following formula

T_m = 81.5 +0.41(%GC) – 675/N- (% mismatch), where N is the primer length in bases, values of % GC and % mismatch are in whole numbers.

The oligonucleotide sequence was further analysed for any hairpin formation or dimmer formations using online software from "Net Primer" of Premierbiosoft or by using Jellyfish 1.5 from Biowire.

4.3 Extraction of plasmid DNA

4.3.1 Mini-Preparation

Mini-preparation was usually performed to screen the recombinants following the PCR based site-directed mutagenesis experiment.

The plasmid extraction was done according to Sambrook *et al.* (1989). A single colony was grown overnight in 3 ml of YT medium containing ampicillin to a final concentration of 50 µg/ml. The culture was incubated overnight at 37°C with vigorous shaking at approximately 200 cycles/min.

An aliquot (1.5 ml) of the overnight culture was transferred into an Eppendorf tube, and centrifuged for 5 min at 21,000 x *g*. The pellet was resuspended in 200 µl of STET buffer containing 1 mg/ml lysozyme and incubated for 5 min at RT. The lysate was boiled for 45 sec in a water bath. The sample was centrifuged for 10 min at 21,000 x *g*, and the viscous pellet was removed with a tooth-pick. Eight microlitres of 5 % CTAB solution (prewarmed to 37°C) was added to the lysate followed by vortexing and centrifugation at 21,000 x *g* for 5 min. The supernatant was discarded, and the pellet was resuspended in 300 µl of 1.2 M sodium chloride. The DNA was precipitated using 2.5 volumes of ice-cold absolute alcohol (750 µl). The sample was centrifuged at 21,000 x *g* for 10 min, and supernatant was discarded. The pellet was washed for 10 min with 70 % ice-cold alcohol and air-dried. Finally, the pellet was resuspended in 20 µl of TE-buffer containing RNase A1 (20 µg/ml). The extracted plasmid DNA was further used for restriction analysis. The remaining bacterial suspension was either stored as glycerol stock (15 %) or used for Maxi-prep.

4.3.2 Maxi-preparation (Qiagen kit)

Maxi-prep was typically done according to the protocol of the manufacturer. One hundred millilitres of YT medium containing 50 µg/ml ampicillin was inoculated with either the bacterial glycerol stock or rest of the bacterial culture from the mini-prep. The culture was incubated over night at 37°C with vigorous shaking at approximately 200 cycles/min.

The entire suspension was centrifuged at 6000 x *g*, 4°C for 10 min in a Beckmann JLA 16.250 rotor. The pellet was resuspended in 10 ml of resuspension buffer containing 100 µg/ml of RNase A. Further a volume of 10 ml of lysis buffer was added. The sample was gently mixed and left for 5 min at RT to allow bacterial cell lysis. A volume of 10 ml of ice-cold neutralisation buffer was added and kept on ice for another 20 min. The suspension was centrifuged at 20,000 x *g*, 4°C for 30 min. The resultant supernatant was passed through a previously equilibrated Qiagen Tip 500 column. Once the solution was filtered, the column was washed twice with 30 ml of wash buffer. Finally the DNA was eluted with 15 ml of elution buffer into a centrifuge tube. An additional 10.5 ml of isoproponal was added slowly to elute along the walls of the centrifuge tube. Immediately, the DNA precipitate could be visualised forming a white ring at the interface of the two solutions. The DNA was pelleted by ultra centrifugation for 30 min at 20,000 x *g*, and 4°C. The pellet was subsequently washed with 5 ml of 70 % ice-cold ethanol. Finally the pellet was air dried, and resuspended in appropriate amount of TE-buffer (pH 7.6). The purified DNA was stored at –20°C for further use.

4.4 Transformation

An aliquot (50µl) of frozen XL-1 Blue supercompetent cells (provided by manufacturer) were thawed on ice. The cells were mixed with 1 µl of PCR product and kept on ice for 30 min. The cells were then subjected to a heat shock at 42°C for 45 sec, and chilled on ice for 2 min. The cells were diluted 10 fold with prewarmed YT medium. The diluted suspension was incubated at 37°C for 1 hr to allow the expression of antibiotic resistance. Samples were pelleted and resuspended in 100 µl of fresh YT medium. The product was plated on an agar plate containing 50 µg/ml of sodium salt of ampicillin. The plates were incubated at 37°C for nearly 16 hrs for the appearance of colonies. The colonies were further screened for the presence of recombinant plasmid DNA with desired mutation.

4.4.1 Growth and Purification of vaccinia virus stocks

CV-1 cells were grown to nearly full confluence in two 15 cm petri dishes with 10 % FCS in DMEM. The cells were infected with a purified recombinant vaccinia virus (vTF7-3) at 0.05 – 0.1 pfu/cell in nearly 5 ml of serum-free DMEM per dish. The plates were incubated in an incubator at 37°C for 1 hr. At the end of infection time, the virus was removed from the plates and 20 ml of DMEM/5 % FCS was added to each dish. The cells were further incubated for another 2- 3 days at 37°C, by which time most or all the cells appear rounded, but remain attached to the dish. The purification of the virus was performed by scraping the cells into their medium with a rubber policeman. The medium from both petri dishes was transferred into a single 50 ml disposable sterile tube and centrifuged for 5 min at 200 g and at 4°C. The pellet was resuspended in 4 ml of 10 mM Tris Hcl, pH 9.0. The product was homogenized on ice in a 7 ml dounce using a tight pestle, and centrifuged for 5 min at 200 *g* at 4°C to remove nuclei. The supernatant was transferred into a fresh tube. The pellet was again resuspended with another 4 ml of 10 mM Tris-HCl (pH 9.0), and centrifuged for another 5 min at 200 *g* at 4°C. The supernatants from both centrifugations were mixed and recentrifuged at 650 *g* for 10 min at 4°C to remove any remaining debris. The supernatants were sonicated in a water bath for 5 min and centrifuged at 13,500 rpm (33,000 *g*) for 80 min in an ultra centrifuge. At the end of centrifugation, the pellet was resuspended in 2 ml of 1 mM Tris-Hcl, pH 9.0, aliquoted into 100 µl fractions and stored at –80°C. All the glassware and discarded solutions were treated with sodium hypo chlorite. The solutions were then discarded and glassware was further autoclaved.

4.5 Expression of HA mutants in CV-1 /COS-7 cells

4.5.1 Transient T7-RNA-polymerase vaccinia expression system

CV-1 cells were grown as monolayers in DMEM supplemented with 5 % heat-inactivated FCS in an incubator at 37°C and 5 % CO_2. Medium also contained 1 % penicillin and streptomycin. Usually FCS is contained in the medium only for the growth purpose and plain DMEM (without FCS and antibiotics) was used for the transfection experiments.

For expression purposes, CV-1 cells were grown near to confluence in 3.5 cm dishes. Cells were washed twice with 1 ml DMEM and infected with vTF7-3 virus at 10 pfu/cell in 500 µl of DMEM. The cells were incubated for 1 hr at 37°C with 5 % CO_2. After optimising different plasmid DNA concentrations, finally 6 µg of plasmid DNA per 3.5 cm dish was

used as standard for all the transfections. Transfections were performed using lipofectin (a cationic lipid liposome formulation used for transfection of DNA into tissue culture cells). Ten micro litres of lipofectin was diluted in 100 µl of DMEM medium and incubated at RT for 30 min along with 6 µg of plasmid DNA in 100 µl of DMEM medium. At the end of 30 min, the DNA was added drop-by-drop to the lipofectin and incubated for another 15 min. The virus inoculum was removed after 1 hr. The cells were washed twice with DMEM. A volume of 800 µl of DMEM was added to the cells and the DNA-lipofectin mix (200 µl /dish) was added to the medium. The cells were further incubated for another 4 hrs at 37°C with 5 % CO_2. The DNA containing medium was replaced with plain DMEM and cells were incubated at 31°C with 5 % CO_2 for 14 – 16 hrs.

4.5.2 Metabolic labelling with Trans ^{35}S (cysteine & methionine)

CV-1 cells were grown nearer to confluence in 3.5 cm dishes. The cells were infected with vTF7-3 virus as mentioned before. The protocol was identical as mentioned earlier with the exception that lipofectin and DNA were diluted in MEM (deficient in methionine, cysteine and L-glutamine) instead of DMEM. The virus inoculum was removed, and the cells were washed twice with MEM. The cells were incubated for 4 hrs at 37°C with 5 % CO_2 with MEM upon addition of lipofectin:DNA mixture. At the end of the transfection time, the DNA-lipofectin mixture was removed and substituted with MEM by the addition 3 µl of Trans [^{35}S]-label (1000 Ci/mmol). In addition, L-Glutamine was added externally. Incubation was continued at 31°C with 5 % CO_2 for 14-16 hrs.

4.5.3 Processing of surface expressed HA

The cells were washed with pre-warmed (37°C) PBS and treated with TPCK-trypsin at 8 µg in 1 ml of PBS for 10 min at RT to cleave surface expressed HA0 to HA1 and HA2. Trypsin activity was inhibited by the addition of soyabean trypsin inhibitor (STI) to a final conc., of 50 µg /ml and incubated at RT of another 10 min. Finally, the cells were lysed in a cell lysis buffer of 800 µl containing 1 % NP-40 and protease inhibitors. The cell debris was removed by centrifugation at 12,000 rpm for 15 min.

4.6 Immunoprecipitation

An appropriate anti-HA antibody (mostly N2 antibody) was added to the clear lysate. The antigen- antibody complex was incubated at 4°C for either 1 hr or overnight on a shaker

platform. At the end of the incubation, 35 µl of protein-A sepharose was added. The solution was further incubated for another 1 hr to allow the protein-A to bind the Fc portion of the antibodies. The immune complex (antigen:antibody: protein-A sepharose) was centrifuged at 12,000 rpm for 5 min. The immune complex was washed 3 times with 800 µl of RIPA buffer to remove unbound proteins. Sample buffer (reducing or non-reducing) was added to the pellet and boiled at 95°C for 5 min. The sample was centrifuged for 5 min and the supernatant was loaded onto a 12 % SDS-PAGE gel along with a pre-stained standard protein molecular weight marker.

4.7 Fluorography of the gels

The SDS-PAGE gel was treated with fixer solution for 30 min on a rotating platform. The gel was then washed twice with distilled water for 30 min each. Finally, the gel was treated with 1 M sodium salicylate for 30 min before it was dried on a gel-dryer for 90 min at 85°C. The dried gel was exposed to a X-ray film in a cassette. The fluorogram was developed after over-night incubation of the cassette at –80°C. Quantification of fluorogram was carried out with an Epson GT-9000 scanner and ScanPack software.

4.8 Glycosidase assay

The glycosylation pattern was determined by using endoglycosidases - Endoglycosidase H (Endo H) and peptide-N-glycosidsae F (PNGase F). The HA protein for this assay was expressed as previously mentioned by using ^{35}S metabolic labelling. The cells expressing HA protein were trypsin processed if needed. The processed cells were lysed, and digested with either Endo H or PNGase F following the manufacturers instructions. The digested product was routinely processed for immunoprecipitation and visualised by fluorography after SDS-PAGE in a 12 % polyacrylamide gel.

4.9 Cross-Linking Experiment

CV-1 cells were routinely infected, transfected and metabolically labelled, lysed and centrifuged as described earlier. The surface expressed HA was not trypsin processed. The cells were lysed in a lysis buffer without amines in a volume of 500 µl. The lysate was aliquoted into two Eppendorf tubes with 200 µl each. To one aliquot, 4 µl of DMSO was

added which served as a control. To the other aliquot, 4 µl of cross-linking reagent DSP (40 mM in DMSO) to a final conc., of 0.3 mM was added. Both the samples were incubated at 15°C for 15 min. The reaction was stopped by addition of 4 µl of 1 M ammonium chloride and immunoprecipitation was carried out using N2 antibody. The samples were analysed on a 6 % SDS-PAGE gel using non-reducing sample buffer. The gel was further processed for visible bands on a fluorogram.

4.10 Conformational change assay (Proteinase-K assay)

The wild type and mutant forms of HA were analysed for variation in their conformations at a gradient of reducing pH conditions. HA expressed in CV-1 cells were metabolically labelled as mentioned above. After treatment with TPCK-trypsin and trypsin inhibitor, cells were incubated at 37°C for 6 min in fusion buffer adjusted to desired pH (7.0, 6.0, 5.8, 5.6, 5.4, 5.2 and 5.0). The cells were then re-neutralised with pH 7.0 fusion buffer and lysed with 800 µl of lysis buffer. The lysate from centrifugation was digested with 0.2 mg/ml of Proteinase-K and 2 mM $CaCl_2$ at 37°C for 30- 45 min. The digestion was stopped by addition of 1 mM PMSF and a protease inhibitor cocktail. The samples were immunoprecipitated with N2 antibody, and subsequently the protein bands were analysed using fluorography.

4.11 Densitometric analysis

The fluorograms were scanned using Epson scanner (GT-9000) attached to a Personal Computer. The scanned pictures were analysed using ScanPack version 2.0 software. The quantity of protein seen on the fluorogram was expressed as a percentage taking the sample treated with pH 7.0 buffer as 100 % for that particular mutant. The graphs were plotted using MS-Office Excel software using standard error as statistical tool to know the sampling fluctuations.

4.12 Fusion assays

4.12.1 Preparation of HA-expressing cells for fusion assay

CV-1 cells were grown on sterile glass sildes of 20 x 20 mm placed inside 3.5 cm dishes using DMEM with 10 % FCS. HA protein was expressed in CV-1 cells for nearly 14-16 hrs as mentioned earlier with out any metabolic labelling. The cells were processed with

TPCK-trypsin and additionally with neuraminidase (0.2 mg/ml), followed by trypsin inhibitor. Further the cells were treated with pre-adjusted low pH fusion buffer and re-neutralised. As a control, CV-1 cells infected with vaccinia virus and treated according to the transfection protocol, but without DNA, were used.

4.12.2 Preparation, labelling of RBC for fusion assay

Human RBC were prepared and labelled as described by Kozerski *et al.* (2000). Human RBC was washed for three times with PBS (centrifuged at 2,000 x *g* for 10 min), and RBC was resuspended in PBS (50 % hematocrit). Twenty microliters R18-solution (octadecylrhodamine B chloride; 2 mM in ethanol) was added to 5 ml RBC suspension in PBS (heamtocrit 4 %) under gentle vortexing. After addition of 10 ml of PBS and incubation of the suspension for 30 min at RT in the dark, 25 ml of DMEM with 5 % FCS were added to the suspension to absorb unbound label. After further incubation for 20 min at RT in the dark, the RBC suspension was washed in 40 ml PBS. The RBC pellet was resuspended in 2 ml PBS, after addition of the calcein-AM solution (50 µg freshly dissolved in 50 µl DMSO), cells were incubated for 45 min at 37°C in the dark. Calcein-AM is known to enter the cell cytoplasm where it is cleaved by unspecific esterases of the RBC. The resulting fluorescent calcein becomes trapped in the cytoplasm because it cannot permeate the membrane. Subsequently, the suspension was centrifuged and washed in 20 ml PBS. After resuspension of the pellet in 10 ml PBS, cells were incubated for another 20 min at 37°C in the dark to allow cleavage of intracellular calcein-AM. The suspension of R18 and calcein-AM labelled RBCs was washed five times in 30 ml PBS, rsuspended in 5 ml PBS++, was kept at 4°C until binding to the HA expressing CV-1 cells.

4.12.3 Fusion assay and fluorescence microscopy

For binding, 1 ml of labelled RBC with a hematocrit of 0.4 % was added to the monolayer of HA expressing cells and incubated for 15 min at RT in the dark with occassinal gentle shaking. Unbound RBCs were removed by 4-5 washes with PBS++. The medium was replaced by MES-saline adjusted to indicated pH and incubated at 37°C for 5 min, followed by neutral pH buffer for a brief 2 min at 37°C. Finally the slide is carefully lifted from the dish and placed inverted on a 24 x 60 mm cover slip with a drop of PBS++. The corners of the slide were fixed with a clear transparent nail polish. The slides were observed for fusion under a fluorescence microscope. Fusion was monitored at RT by transfer of fluorescent dyes from labelled RBCs to HA expressing cells. Label

redistribution was observed under the fluorescence microscope (Axiovert 100 with a 40x Achroplan objective [Zeiss]). R18 fluoroscence was visualised using a green filter (excitation: 510-560 nm and emission: 590 nm). Similarly calcein fluorescence was observed with a blue filter (excitation: 450-490 nm & emission: 520 nm). Images were acquired with a CCD camera Coolsnap *fx* (Photometrics, AZ, USA) and analysed using Metamorph 6.1 software (Universal Imaging, PA, USA).

5 RESULTS

5.1 Aim of performing mutations

The mutations were designed to characterize the role of electrostatic interactions for the stability of the ectodomain of the HA protein in its native conformation. The mutations were categorised as stabilising or destabilising. An effort was made to identify amino acids specifically responsible for inter-monomer and intra-monomer stability.

5.1.1 Intra-monomer destabilisation

The tetrad salt bridge involving Glu 89, Arg 109, Arg 269 of HA1 with Glu 67 of HA2 (Fig.5.1.1.A) and that of Lys 299 of HA1 with Glu 69 of HA2 (Fig.5.1.1B) were the target regions to destabilise the HA protein. In each of the instances, positively charged Arg or Lys residues were substituted either by the negative Glu or by the neutral Gly amino acid. The mutations were designed to mimic the possible protonation effects of the negatively charged Glu residues. Thus, the intended destabilisation mutations were R109G, R109E, R269G, R269E, K299G, and K299E.

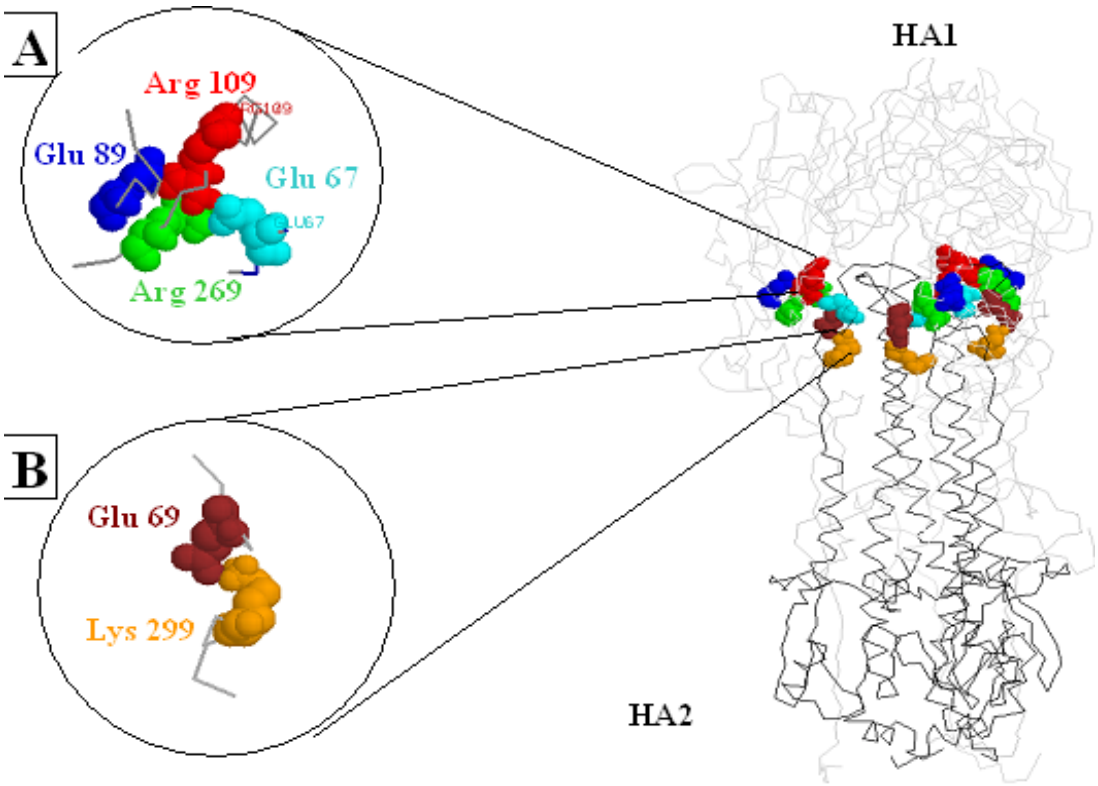

Fig.5.1.1: HA crystal structure in backbone formation (mutants R109 and K299).
The crystal structure of trimeric HA (right hand side) is shown with respective HA1 and HA2 monomers. The amino acids in the hinge region forming salt bridges are shown as spacefilled molecules. All the three monomers are shown with the respective residues.. The insets highlight the respective amino acids of only one monomer. The inset "A" shows Arg 109 of the HA1 chain forming a complex salt bridge with Glu 89 of HA1 and with Glu 67 of HA2. Arg 269 of the HA1 chain is also involved in the salt bridge formation with Glu 67 of the HA2 chain. The inset "B" shows Glu 69 of the HA2 chain forming a simple (single) salt bridge with Lys 299 of the HA1 chain.

5.1.2 Inter-monomer detsabilisation

A destabilising mutation was introduced at the distal tip of the HA protein, at the interface of the three HA1 monomers (Fig.5.1.2). The mutant was created by substitution of Thr 212 and Asn 216 to Glu. The mutant was designated as T212E-N216E. Selection of the site for mutation was based on the disulphide linking experiment of Godley *et al.* (1992).

5.1.3 Inter-monomer stabilisation

A stabilising mutant was created at the same site as mentioned earlier, but with an attempt to create a salt bridge (Fig.5.1.2). To this end, the Thr 212 to Glu mutation was retained, and Asn in position 216 was changed to Arg. The resultant mutant was designated as T212E-N216R.

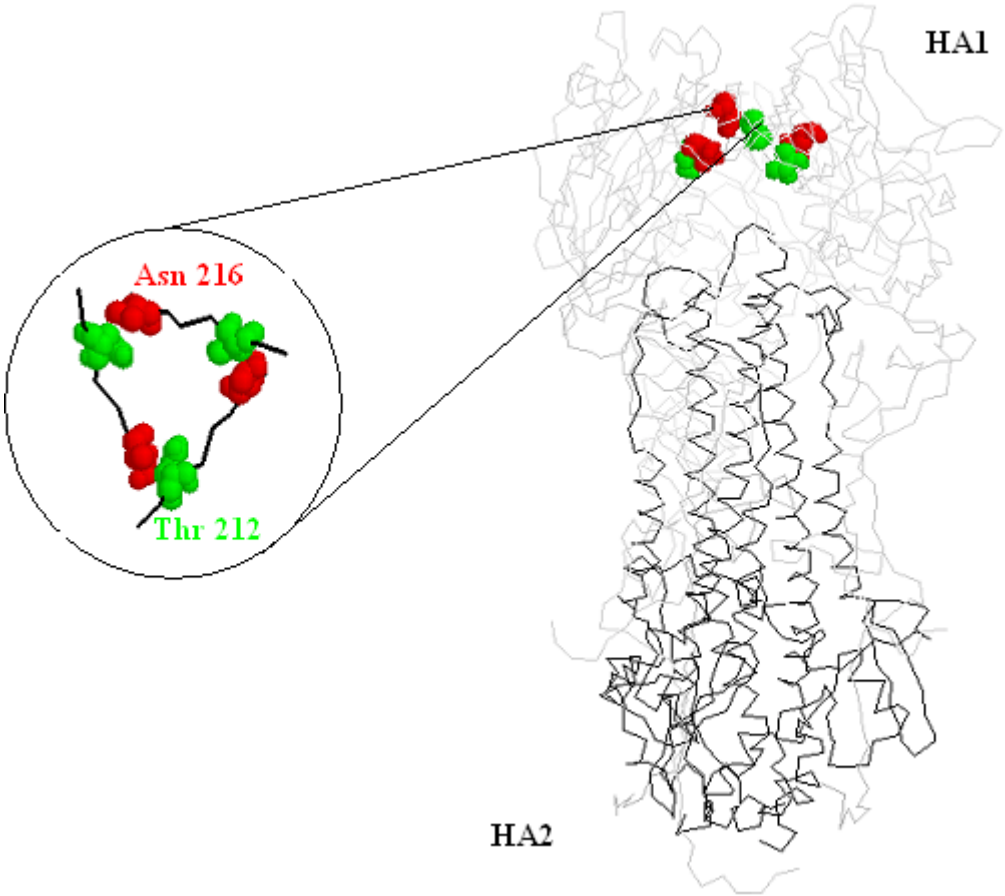

Fig.5.1.2: HA crystal structure in backbone formation (mutant T212-N216).
The crystal structure of trimeric HA (right hand side) is shown with respective HA1 and HA2 chains. Mutated amino acids in the three monomers are highlighted. The spacefilled molecules are located at the interface region of the HA1 monomers. The inset shows Asn at 216 of one monomer in close contact with Thr at 212 position of neighbouring monomers. These amino acids were mutated for either stabilising or destabilising the HA molecule (for details refer text).

5.1.4 Intra-monomer stabilisation

An effort was made to enhance the stability of HA protein with the introduction of a salt bridge in the stem region near the interface region of HA1 and HA2. The target site was Ile 89 of HA2 in contact with Tyr 308 of HA1 (Fig.5.1.4B). In one mutation, Ile 89 was changed to Arg to form an ionic link with the OH group of Tyr 308. In another mutation, a double mutant was created with Tyr 308 being changed to Arg and Ile 89 to Glu. The resulting mutants were designated as I89R and I89E-Y308R. In addition, Ser 110 was substituted to Asp (Fig.5.1.4A) to build up ionic interaction with His 64 in its close neighbourhood.

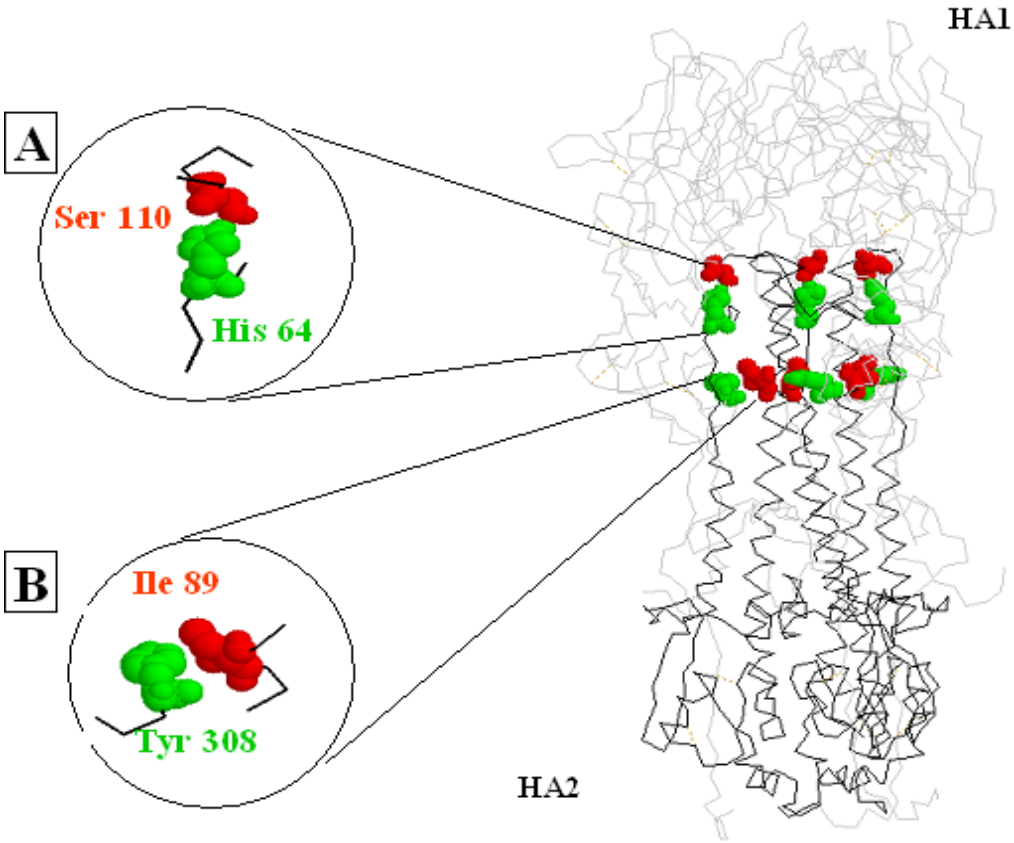

Fig.5.1.4: HA crystal structure in the backbone formation (mutants S110 and I89-Y308).
The crystal structure of trimeric HA (right hand side) is shown with respective HA1 and HA2 chains. The amino acids near the hinge region at the interface of HA1 and HA2 chains are shown as spacefilled molecules. Selected amino acids in HA1 and HA2 are in close apposition within a monomer. Thus specific mutation of those residues could lead to the formation of a salt bridge. The insets highlight the respective amino acids of only one monomer.
The inset "A" shows Ser 110 of the HA1 chain in close contact with His 64 of the HA2 chain. Ser 110 is mutated to Asp to explore the possibility of a salt bridge formation.
The inset "B" shows Ile 89 of the HA2 chain in close contact with Tyr 308 of the HA1 chain. In one case, Ile 89 is mutated to Arg to stabilise the HA molecule with a cation-Pi interaction with Tyr 308. In another instance, a double mutant was generated with Ile 89 mutated to Glu and Tyr 308 mutated to Arg for establishing a new salt bridge formation.

5.1.5 Stabilisation of HA by disulfide mutations

Furthermore, the study also aimed to stabilise the HA by disulfide bonds. An attempt was made to determine the role of HA2 monomers in the low pH induced conformational changes. In particular, the amino acids were selected so as to give also insight into conformational changes relevant for triggering fusion. Therefore, non-covalent interactions (salt bridges) were chosen and substituted with covalent forces (disulfide linkages). In two instances, salt bridges [Glu 74 - Arg 76 (fig.5.1.5 B); and Arg 109 - Glu 67] were substituted with disulfide linkages in an effort to stabilise the HA protein. These mutations were E74C-R76C, and R109C-E67C. Cysteine mutations were also made at two additional sites as Ile 77 (fig.5.1.5 A), and at Thr 111 being in contact with Ala 44 (fig.5.1.5 C). These mutations were designated as I77C and T111C-A44C, respectively.

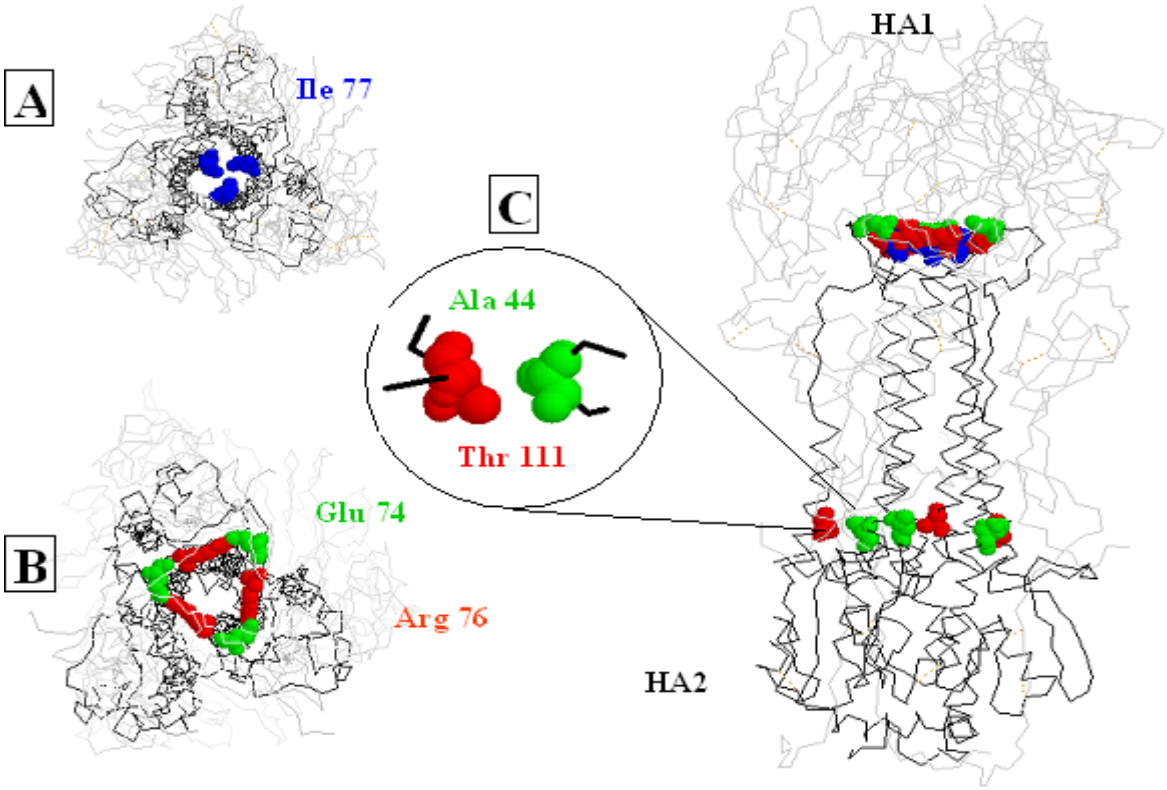

Fig.5.1.5: HA crystal structure in the backbone formation (mutants I77, E74-R76, A44-T111). The crystal structure of trimeric HA (right hand side) is shown with respective HA1 and HA2 chains. The highlighted (spacefilled) amino acids are from three monomers. The spacefilled residues (in the top region of HA2 chains) are located at the interface region of HA2 monomers forming a complex salt bridge. The inset "A" shows (top view) Ile 77 of HA2 chain of all the three monomers. Ile 77 was mutated to cys to explore the possibility of a disulfide bond between the three HA2 monomers. The inset "B" shows (top view) Glu 74 of HA2 chain in close contact with Arg 76 of neighbouring monomer of HA2 chains. The Arg 74 and Glu 76 were mutated to cys amino acids to covalently link the HA2 monomers by disulfide bond. The inset "C" shows Ala 44 and Thr 111 from the same HA2 chain. These amino acids were mutated to Cys residues to cross link the two helices of HA2 chain within a monomer.

5.2 Conservation of the selected amino acids

The selected amino acids for mutations were searched for their conservation among all the entire influenza virus group. The consurf 3D tool from http://consurf.tau.ac.il was used to align all the available HA sequences in PDB database onto the 3D crystal structure of H3 subtype (PBD id: 1Hgd). The results were summarized in the fig.5.2 along with visual colour key for reference. It may be observed that majority of the amino acids selected for mutagenesis were highly conserved.

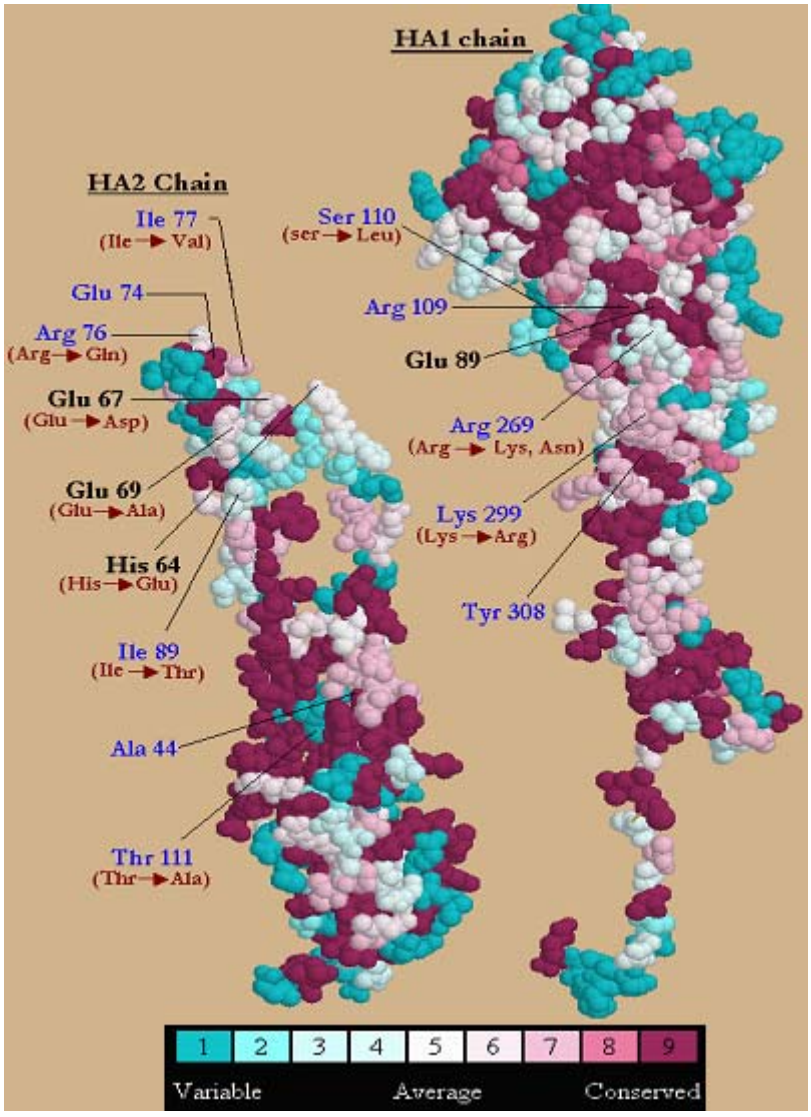

Fig.5.2: Consurf 3D: the amino acid sequence of known infuenza A viruses
Unique amino acid sequences from H1-H13 were aligned using consurf web based tool. The sequences were aligned to the 3D crystal structure of H3 subtype (PBD id: 1HGD) and visualised using protein explorer. The colour key indicating the degree of conservation is given on the bottom. Only the amino acids selected for mutagenesis (labelled in blue) and those involved in the interaction (labelled in black) with the mutants are shown. Those of the amino acids, which are not conserved, are shown with their substituted amino acids (occurring as natural variants) in parenthesis.

5.3 Construction of mutants

The gene of the wild type HA protein (HA-wt) was a generous gift from Dr. Judith White (Department of Cell Biology, University of Virginia Health System, USA). The gene contained the entire HA1 and HA2 sequence cloned behind the T7 promoter in pTM1 plasmid vector. The gene sequence in the plasmid was sequenced and found to be 100 % homologous with that of the published literature. All the mutants were generated using this gene sequence as the source material. Special care was taken to design oligos for easy screening of mutants as described in the section 4.2. The list of the primers with their restriction sites was given in the section 4.2. The PCR technique (as schematically outlined in fig 4.1) synthesises the gene sequence of the whole plasmid (7026 bp) while incorporating the mutant in the desired position. The PCR product was treated with *Dpn* I. The *Dpn* I endonuclease is specific for methylated and hemimethylated DNA and was used to digest parental DNA (DNA from most of the *E.coli* strains is dam methylated). Only the parental DNA is susceptible to *Dpn* I treatment. The resultant gene sequence was subsequently transformed, where in the nicked DNA was repaired and ligated into a circular plasmid by *E.coli* DNA polymerase. The recombinant colonies picked from the YT-ampicillin agar plates were extracted for DNA by mini prep method (section 4.3.1). The resultant DNA was analysed by RE analysis for the incorporation of the new restriction enzyme site. The oligos besides containing desired mutation also had a new RE site as a silent mutation. Hence, the DNA that is proven positive for a new RE site also contained the desired mutant sequence. Finally, the desired sequence of the mutant gene was also confirmed by gene sequencing. Sequencing was commercially done at Invitek GmbH, Berlin.

5.4 Transient expression of the HA proteins

The HA-wt and the associated mutant proteins were expressed in either CV-1 or COS-7 cells (both derivatives of African green monkey kidney; fibroblast-like; monolayers) using T7 RNA polymerase vaccinia system (section 4.5.1). The expression was carried using lipofectin and cells were analysed on incubation for 12-14 hrs with or without metabolic labelling. The HA-wt and its mutants were analysed for surface expression, trimer formation, and conformational changes and further for fusion efficiency with fluorescent labelled RBC's.

5.5 Characterisation of expression by metabolically labelling

HA-wt and its associated mutant proteins (R109E, R109G, R269E, R269G, K299E, K299G, S110D, T212E-N216R, T212E-N216E, I89R, I89E-Y308R) were expressed in CV-1 or COS-7 cells using T7 RNA polymerase vaccinia virus system. The cells after being metabolically labelled with [^{35}S]cysteine /methionine and incubated for 12-14 hrs, were then processed for cleavability of HA0 to HA1 and HA2 (section 4.5.3). The protein was further immunoprecipitated using N2 antibody (conformation-specific mAb, which specifically recognizes HA trimers at neutral pH) as described in section 4.6 and analysed on SDS-PAGE under reducing conditions. The epitope recognized by this antibody is located close to the interface between the HA1 top domains of the native HA trimer (Copeland *et al.*, 1986). The fluorogram of a typically expressed wt-HA in CV-1 cells is shown in Fig.5.5a. It shows the HA protein before and after TPCK treatment. In addition, it is seen that after TPCK treatment not all the HA0 is cleaved into HA1 and HA2. The uncleaved HA0 in lane 2, Fig. 5.5a, indicates that the protein was still under processing and remained within the cell at the point of TPCK treatment. A similar pattern was observed for all the mutants (Fig 5.5b and 5.5c) except that of R109E (lane: 2; Fig 5.5c), which was not expressed on cell surface by immunoprecipitation assays. The DNA concentration used in immunoprecipitation was 6 µg for HA-wt and all mutants except for R109E for which the DNA concentration was increased up to 10 µg. The expression level and its pattern of all mutants except of R109E were found to be comparable to that of HA-wt. Figure 5.5 only shows HA-wt and destabilising mutants. The surface expression of the other mutants will be shown along with the conformational assay.

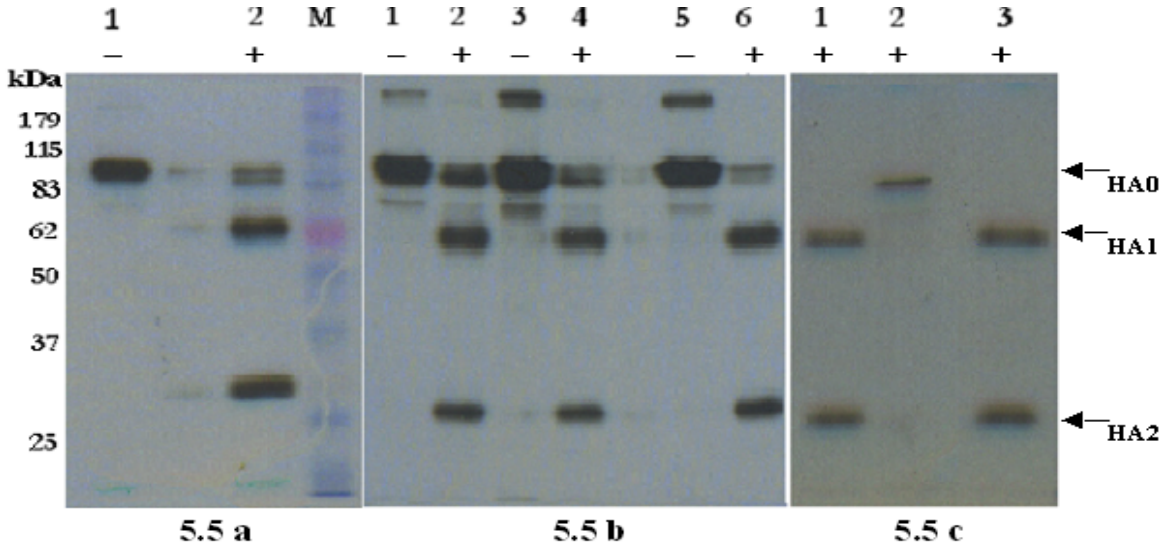

Fig 5.5: Surface expression of HA-wt and destabilising mutants.

" +" *denotes* ***TPCK treatment*** *and* ***"-"*** *denotes* ***without TPCK treatment***
Fig 5.5 a: shows the HA-wt without (lane 1) or with TPCK trypsin treatment (lane 2).
Fig 5.5 b: shows R269G (lane 1and 2), K299G (lane 3 and 4) and K299E (lane 5 and 6). Lanes 1, 3 and 5 show the respective mutant HA protein without TPCK trypsin treatment. Lanes 2, 4 and 6 show the mutant HA protein after TPCK trypsin treatment.
Fig 5.5 c: shows R269E, R109E and R109G mutant HA proteins after TPCK trypsin treatment. Lane 2 shows R109E mutant being resistant to TPCK trypsin treatment indicating the lack of surface expression.

5.6 Glycosylation analysis of R109G, R109E and HA-wt

Secreted glycoproteins are synthesized on endoplasmic reticulum (ER) associated ribosomes and core oligosaccharide chains are attached co-translationally. HA is trimerised, and glycosylated in ER and transported to the Golgi complex on its route to cell surface, as described in section 1.2.3. During passage of the HA through ER and Golgi complex, trimming of oligosaccharides is done. Therefore, the glycosylation pattern of R109E on comparison with that of R109G and HA-wt would give more insight into the location (stacking) of the mutant protein in the cell. The glycosylation of HA protein was assessed using endoglycosidases (Endo H and PNGase F) as described in 4.8. Endo H removes simple, high-mannose N-linked oligosaccharides characteristic of ER localization but cannot remove N-linked glycans typical for processing in the Golgi (Maley et al., 1989). PNGase F digests all N-linked oligosaccharides regardless of their state of processing (Maley et al., 1989).

The fluorograph (Fig.5.6) shows glycosylation patterns for HA-wt (Fig.5.6, lanes 4-6) and R109G (Fig.5.6, lanes 7-9). It may be noticed that, both HA-wt and R109G have similar profile. In contrast, a significant difference was observed for the glycosylation pattern for R109E. The fig. 5.6 shows that HA-wt protein without trypsin treatment (precursor protein: HA0) was Endo H resistance due to loss of high mannose residues in the processed glycosyl chains on its transport to Golgi complex. The Endo-H resistance is a characteristic of proteins that have passed through medial Golgi compartment. A rather similar profile was observed for both HA-wt and R109G proteins even after trypsin treatment (HA0 cleaved into HA1 and HA2). The mutant protein from R109E on the other hand shows sensitivity to Endo H (Fig 5.6; lanes 11 & 14). The PNGase F treatment also showed similar profile (Fig.5.6; lanes 12 & 15) indicating similar activity for both the enzymes. The pattern of R109E was found to be similar irrespective of trypsin treatment in contrast to those for R109G and HA-wt. This shows that the R109E mutant protein was held up either in the ER or in *cis*-Golgi compartment and therefore not transported to the surface.

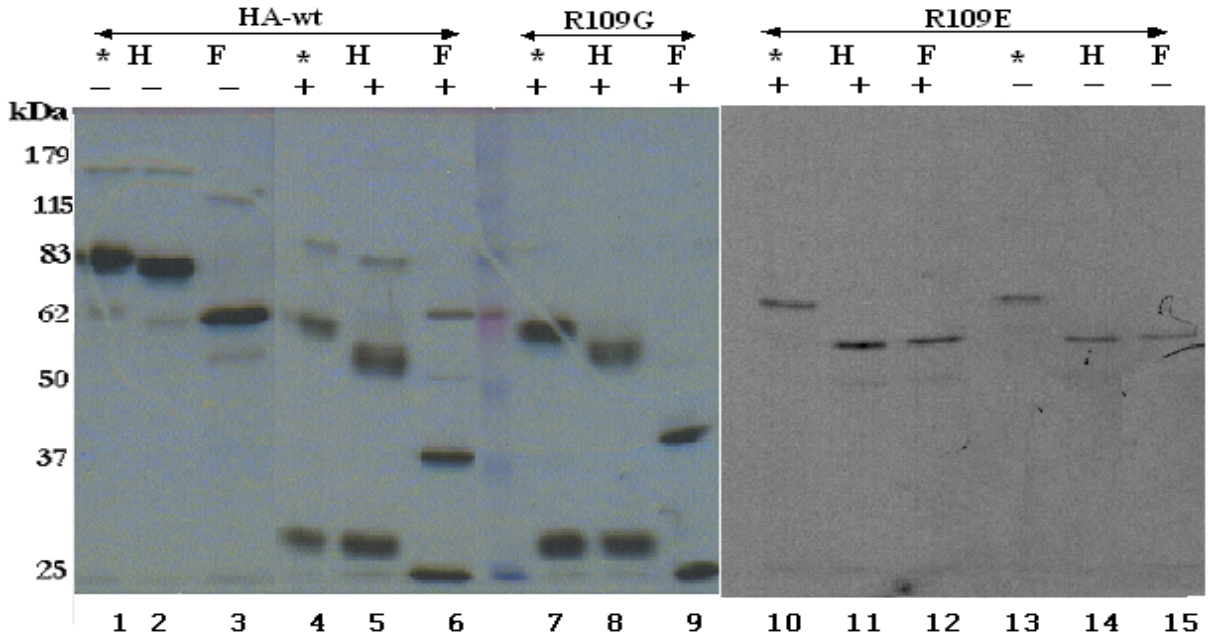

Fig 5.6: Glycosylation assay for HA-wt, R109G and R109E.
" +" *denotes* ***TPCK treatment*** *and* ***"-"*** *denotes* ***without TPCK treatment.***
"H" *stands for* ***Endo H*** *enzyme and* ***"F"*** *stands for* ***PNGase F***
Lanes 1-3 and 4-6 show HA-wt. Lanes 7-9 show R109G. Lanes 10-12 and lanes 13-15 show R109E.
With Endo H*:*lanes 2, 5, 8, 11, and 14. Lane 2 shows HA-wt not treated with TPCK trypsin. Lanes 5, 8 show HA-wt and R109G cleaved by TPCK, treated with Endo H. Lanes 11 & 14 show R109E with or without TPCK treatment respectively, and treated with Endo H.
With PNGase F*:* lanes 3, 6, 9, 12, and 15. Lane 3 shows HA-wt without being treated by TPCK trypsin. Lanes 5, 8 show HA-wt and R109G cleaved by TPCK, treated with PNGase F. Lanes 12 & 15 show R109E with or without TPCK treatment, respectively, and treated with PNGase F.
With no enzyme treatment*:* lanes 1, 4, 7, 10 and 13.

5.7 Trimer formation assay (cross linking with DSP)

Trimerisation of HA molecules is an important step occurring in the ER. A homobifunctional cross-linker DSP was used to assess the trimer formation ability of all the mutants. The lysates as described in 4.9 were incubated with or without DSP reagent for 15 min at 15°C to covalently link the three monomers within each HA trimer. Samples without DSP reagent were taken as controls for the respective protein. The samples were immunoprecipitated and analysed by SDS-PAGE followed by fluorography. Fig. 5.7 reveals that the samples treated with DSP contained a higher molecular weight band when compared to their respective controls. Fig 5.7 shows that almost all mutants form a trimer similar to HA-wt (analysed on a 6% SDS-PAGE gel). The other mutants T212E-N216R, T212E-N216E, and R109E also showed trimer formation with DSP reagent, but the figures are not enclosed.

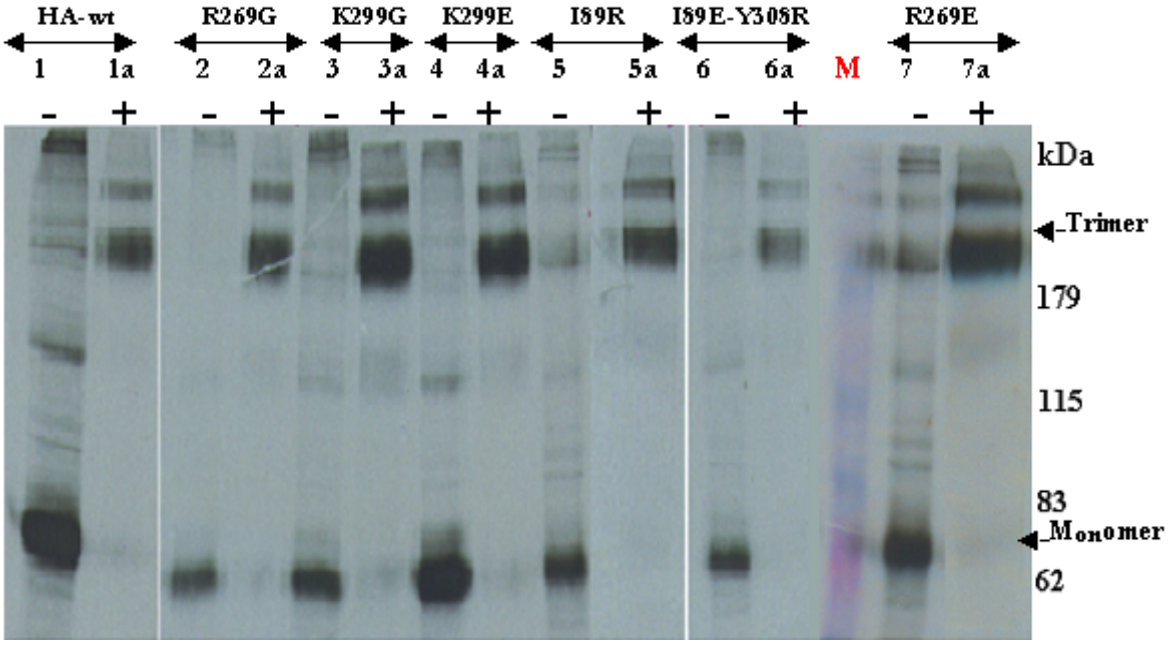

Fig 5.7 : Trimer formation with DSP on a 6 % SDS-PAGE gel with non-reducing dye.
" +" *denotes* ***TPCK treatment*** *and* ***"-"*** *denotes* ***without TPCK treatment***
The figure shows HA-wt (lanes 1, 1a); R269G (lanes 2, 2a); K299G (lanes 3, 3a); K299E (lanes 4, 4a); I89R (lanes 5, 5a); I89E-Y308R (lanes 6, 6a); and R269E (lanes 7, 7a).
Lanes 1, 2, 3, 4, 5, and 6 show the respective HA protein band without DSP treatment. Lanes 1a, 2a, 3a, 4a, 5a, and 6a show the respective HA protein bands after treating with DSP. The difference in molecular weights between HA proteins with and without DSP show that trimer is formed.

5.8 Conformational assay with proteinase K

Lowering the pH triggers the conformational change of the native state HA into its fusogenic state as described in section 1.3.2. It is known that the ectodomain of HA upon triggering the conformational change becomes sensitive to proteinase K (Godley *et al.*, 1992). Thus, resistance of the HA protein to proteinase K treatment reflects its stability. The assay was performed as outlined in section 4.10, and the stability was probed stepwise decreasing the pH using the fusion buffer. The assay was done for HA-wt and for all mutants. The assay confirmed that HA-wt was sensitive to conformational changes at pH of ≤5.4 (Fig.5.8).

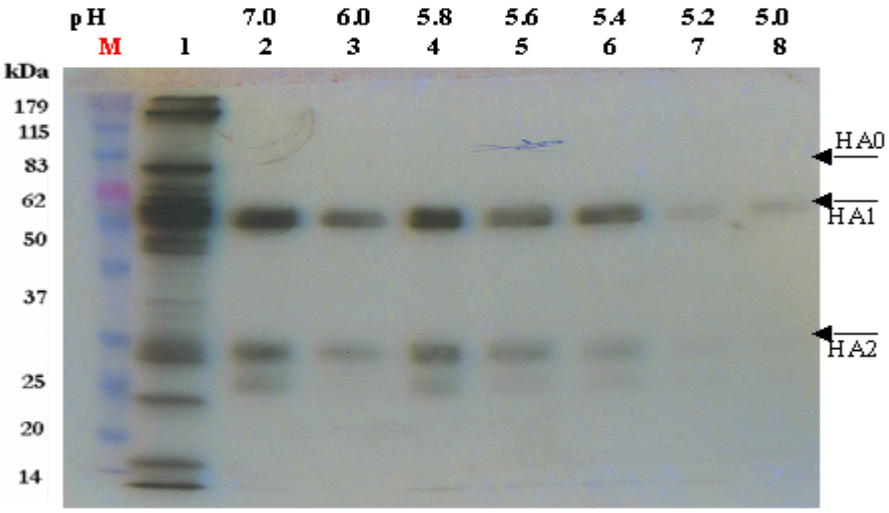

Fig. 5.8: pH triggered conformational change of HA-wt.
Upon incubation at the desired pH HA-wt protein was subjected to proteinase K conformational assay. Proteins were analysed on a 12 % SDS-PAGE gel under reducing conditions. The HA1 domain becomes sensitive to proteinase K upon a conformational change of the HA ectodomain (Section 4.10). Lane 1 shows the protein at neutral pH without proteinase K treatment (control). Lanes from 2 till 8 corresponds to preincubation at pH 7, 6, 5.8, 5.6, 5.4, 5.2, and 5.0, respectively. HA1 becomes sensitive below pH 5.4 (lane 6). HA2 protein band also diminished at pH ≤ 5.4.

5.8.1 Destabilisation of intra-monomer interactions

The destabilising mutants (Fig 5.8.1a – 5.8.1f) were found to be sensitive to proteinase K enzyme at a higher pH (ranging from pH 5.6 till pH 7.0) as compared to HA-wt (Fig 5.8). The pH threshold for proteinase K sensitivity was always at higher pH for mutants carrying "Glu" (R109E; R269E; R299E) with respect to mutants carrying "Gly" (R109G; R269G; K299G) at the same position.

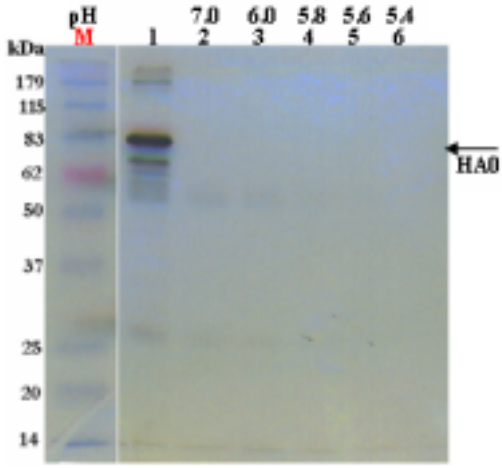

Fig 5.8.1a: pH triggered conformational change of R109E.
Upon incubation at the desired pH, R109E was subjected to proteinase K conformational assay. Proteins were analysed on a 12 % SDS-PAGE gel under reducing conditions. The plasmid DNA of R109E used for transfection was 10 µg as against regular 6 µg for all other mutants.
Lane 1 shows the protein at neutral pH without proteinase K enzyme treatment (control). It may be observed that the HA0 was not cleaved completely (faint bands of HA1 and HA2 could be seen). Lanes from 2 till 6 corresponds to preincubation at pH 7, 6, 5.8, 5.6, and 5.4 respectively. Very faint bands could be seen at pH 7.0 and pH 6.0 (lanes 2 and 3 respectively).

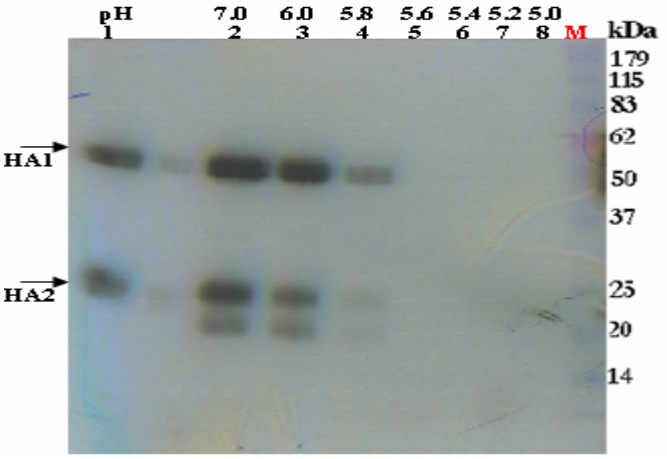

Fig 5.8.1b: pH triggered conformational change of R109G.
Upon incubation at the desired pH, R109G was subjected to proteinase K conformational assay. Proteins were analysed on a 12 % SDS-PAGE gel under reducing conditions. The HA1 domain becomes sensitive to proteinase K upon a conformational change of the HA ectodomain (Section 4.10).
Lane 1 shows the protein at neutral pH without proteinase K treatment (control). Lanes from 2 till 7 corresponds to preincubation at pH 7, 6, 5.8, 5.6, 5.4, and 5.2 respectively. HA1 becomes sensitive below pH 5.8 (lane 4).

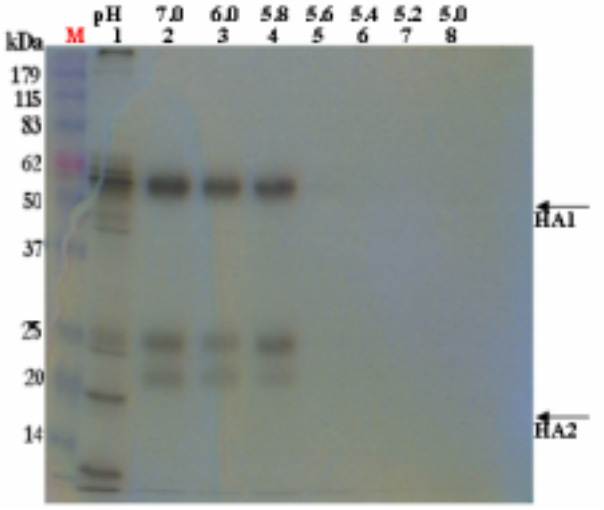

Fig 5.8.1c: pH triggered conformational change of R269E.
Upon incubation at the desired pH, R269E was subjected to proteinase K conformational assay. Proteins were analysed on a 12 % SDS-PAGE gel under reducing conditions.
Lane 1 shows the protein at neutral pH without proteinase K treatment (control). Lanes from 2 till 8 corresponds to preincubation at pH 7, 6, 5.8, 5.6, 5.4, 5.2, and 5.0 respectively. HA1 becomes sensitive below pH 5.8 (lane 4).

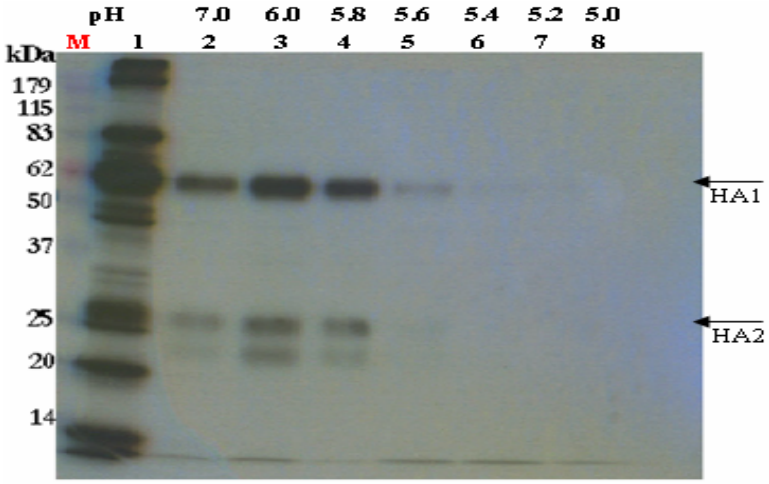

Fig 5.8.1d: pH triggered conformational change of R269G.
Upon incubation at the desired pH, R269G was subjected to proteinase K conformational assay. Proteins were analysed on a 12 % SDS-PAGE gel under reducing conditions.
Lane 1 shows the protein at neutral pH without proteinase K treatment (control). Lanes from 2 till 8 corresponds to preincubation at pH 7, 6, 5.8, 5.6, 5.4, 5.2, and 5.0 respectively. HA1 becomes sensitive below pH 5.8 (lane 4).

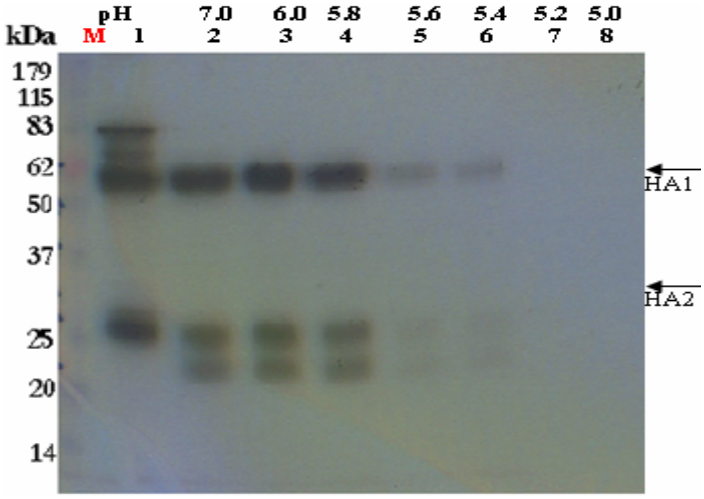

Fig 5.8.1e: pH triggered conformational change of K299E.
Upon incubation at the desired pH, K299E was subjected to proteinase K conformational assay. Proteins were analysed on a 12 % SDS-PAGE gel under reducing conditions.
Lane 1 shows the protein at neutral pH without proteinase K treatment (control). Lanes from 2 till 8 corresponds to preincubation at pH 7, 6, 5.8, 5.6, 5.4, 5.2, and 5.0 respectively. HA1 becomes sensitive below pH 5.8 (lane 4). But still the protein bands were visible till pH 5.4 (lane 6).

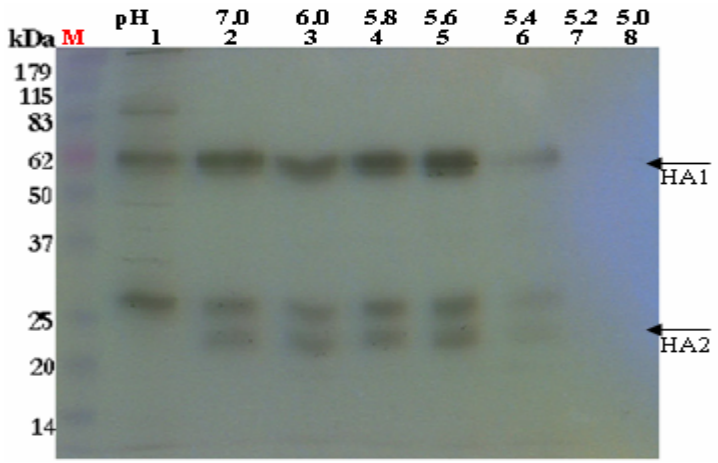

Fig 5.8.1f: pH triggered conformational change of K299G.
Upon incubation at the desired pH, K299G was subjected to proteinase K conformational assay. Proteins were analysed on a 12 % SDS-PAGE gel under reducing conditions.
Lane 1 shows the protein at neutral pH without proteinase K treatment (control). Lanes from 2 till 7 corresponds to preincubation at pH 7, 6, 5.8, 5.6, 5.4, and 5.2 respectively. HA1 becomes sensitive below pH 5.6 (lane 5). Still the protein band was visible till pH 5.4 (lane 6).

5.8.2 Stabilisation of intra-monomer interactions

The stabilising mutants (Fig.5.8.2a – 5.8.2c) were found to be resistant to proteinase K enzyme at all pH (from pH 5.0 –7.0) in contrast to HA-wt (Fig 5.8) and to destabilised mutants (Fig 5.8.1a- 5.8.1f). The mutants studied were I89R, I89E-Y308R, and S110D. The only exception among the stabilising mutants was S110D. The Ser 110 being in close proximity to His 64 of the HA2 chain was mutated to Asp in order to introduce a salt bridge. However, as revealed by proteinase K this mutation lead to a destabilisation of the HA ectodomain as indicated by Fig 5.8.2c.

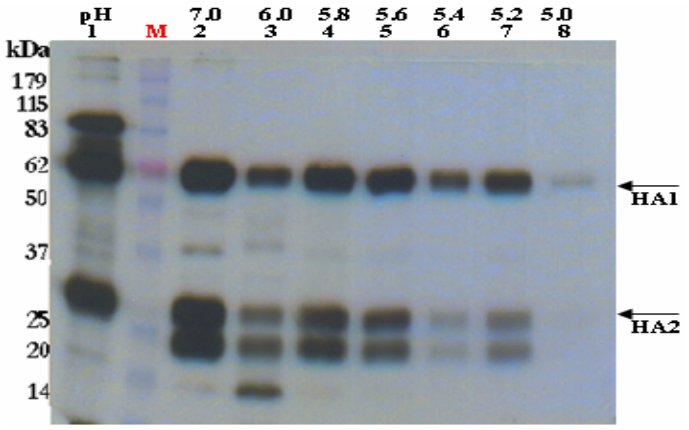

Fig 5.8.2a pH triggered conformational change of I89R.
Upon incubation at the desired pH, I89R was subjected to proteinase K conformational assay. Proteins were analysed on a 12 % SDS-PAGE gel under reducing conditions. The HA1 domain becomes sensitive to proteinase K upon a conformational change of the HA ectodomain (Section 4.10).

Lane 1 shows the protein at neutral pH without proteinase K treatment (control). Lanes from 2 till 8 corresponds to preincubation pH 7, 6, 5.8, 5.6, 5.4, 5.2, and 5.0 respectively. HA1 becomes sensitive at 5.0 (lane 8).

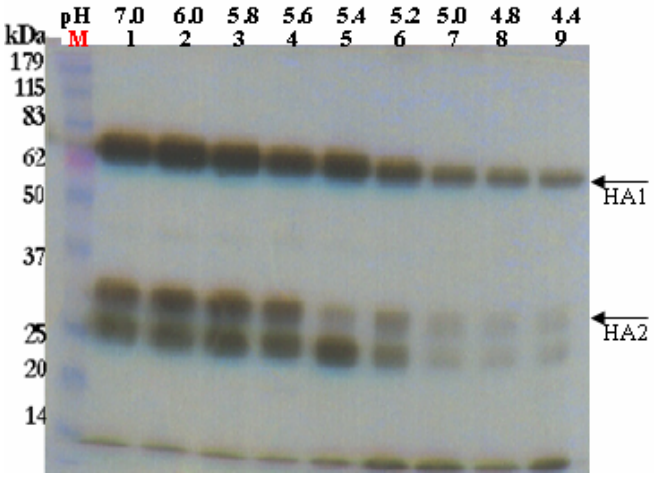

Fig 5.8.2b: pH triggered conformational change of I89E-Y308R.
Upon incubation at the desired pH, I89E-Y308R was subjected to proteinase K conformational assay. Proteins were analysed on a 12 % SDS-PAGE gel under reducing conditions.
Lanes 1 till 8 shows the expressed protein (TPCK trypsin treated) corresponds to preincubation pH 7, 6, 5.8, 5.6, 5.4, 5.2, 5.0, 4.8, and 4.4 respectively. It may be observed that HA1 protein is resistant at the entire range of pH.

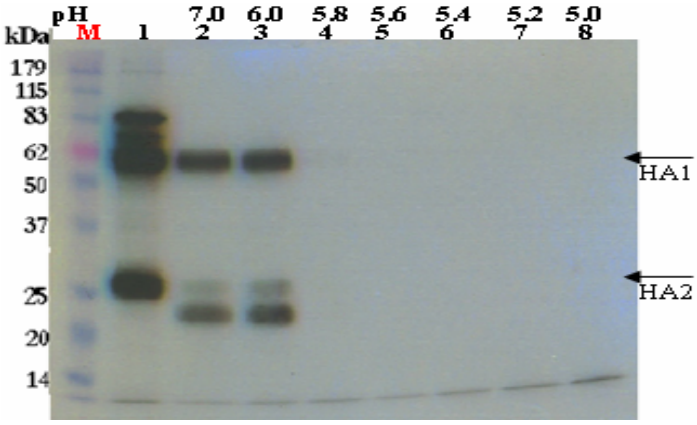

Fig 5.8.2c: pH triggered conformational change of S110D.
Upon incubation at the desired pH, S110D was subjected to proteinase K conformational assay. Proteins were analysed on a 12 % SDS-PAGE gel under reducing conditions.
Lane 1 shows the protein at neutral pH without proteinase K treatment (control). Lanes from 2 till 8 corresponds to preincubation pH 7, 6, 5.8, 5.6, 5.4, 5.2, and 5.0 respectively. HA1 becomes sensitive below pH 6.0 (lane 3) on contrary to other stabilising mutants

5.8.3 Destabilisation of inter-monomer interactions

A destabilising mutant was created to study the inter-monomer interactions in the distal region. The mutant T212E-N216E (Fig.5.8.3) was found to be similar to HA-wt in its sensitivity to proteinase K.

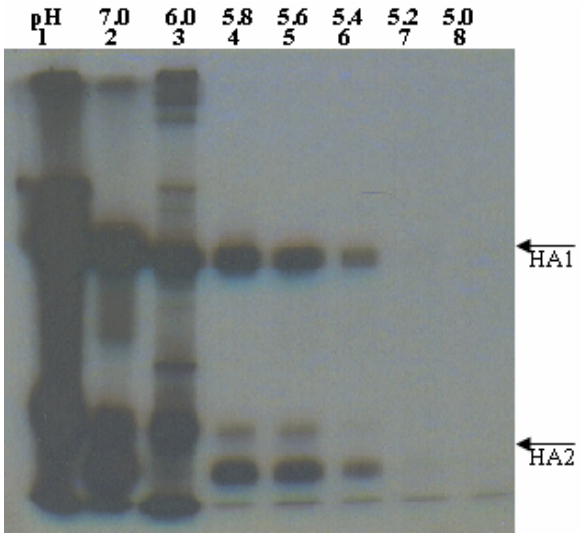

Fig 5.8.3: pH triggered conformational change of T212E-N216E.
Upon incubation at the desired pH, T212E-N216E was subjected to proteinase K conformational assay. Proteins were analysed on a 12 % SDS-PAGE gel under reducing conditions. The HA1 domain becomes sensitive to proteinase K upon a conformational change of the HA ectodomain (Section 4.10).
Lane 1 shows the protein at neutral pH without proteinase K treatment. Lanes from 2 till 8 corresponds to preincubation pH 7, 6, 5.8, 5.6, 5.4, 5.2, and 5.0 respectively. HA1 becomes sensitive below pH 5.4 (lane 3) similar to HA-wt.

5.8.4 Stabilisation of inter-monomer interactions

A destabilising mutant was created to study the inter-monomer interactions in the distal region. The mutant T212E-216R (Fig.5.8.4) was found to be similar to other stabilizing mutants in its resistance to proteinase K. The mutant was resistant to conformational change at the entire range of pH studied.

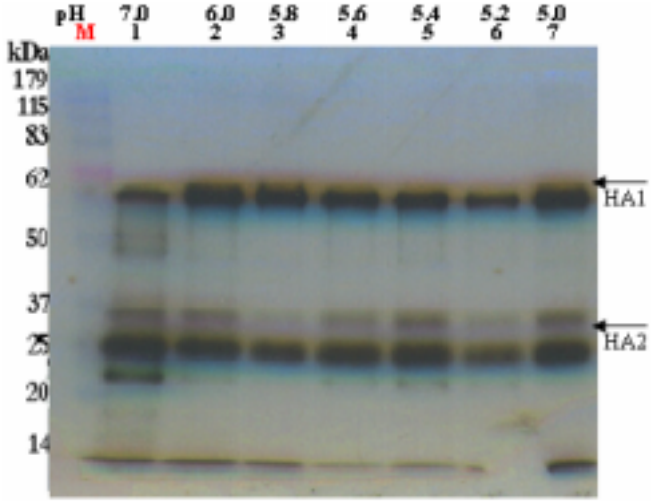

Fig 5.8.4: pH triggered conformational change of T212E-N216R.
Upon incubation at the desired pH, T212E-N216R was subjected to proteinase K conformational assay. Proteins were analysed on a 12 % SDS-PAGE gel under reducing conditions..
Lanes 1 till 7 corresponds to preincubation pH 7, 6, 5.8, 5.6, 5.4, 5.2, and 5.0 respectively. HA1 becomes resistant at the entire range of pH.

5.8.5 Mutations for potential disulfide linkages

Two Cytseine mutants (E74C-R76C and I77C) were studied with respect to the low pH triggered conformational change. The proteianse K sensitivity of mutant I77C (Fig 5.8.5b) was very similar to that of HA-wt (Fig 5.8). The other mutant E74C-R76C (Fig 5.8.5a) shows only low surface expression and its pattern of proteinase K digestion was very indistinct (not clearly visible).

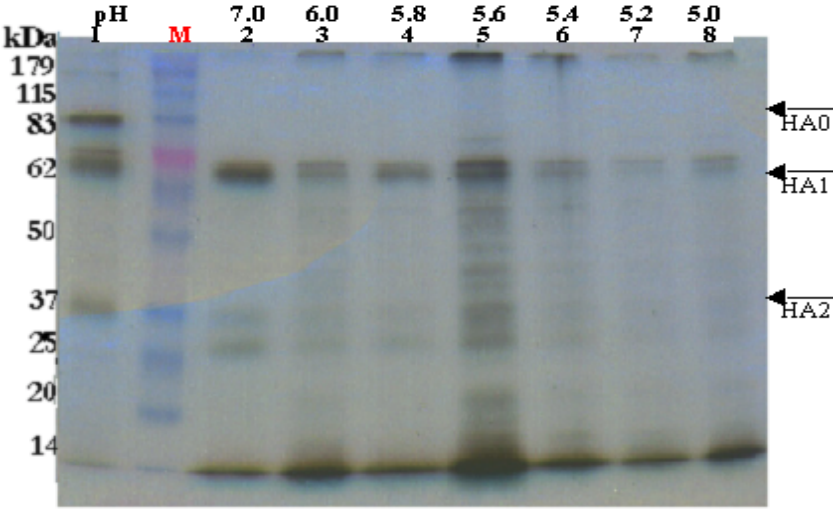

Fig 5.8.5a: pH triggered conformational change of E74C-R76C.
Upon incubation at the desired pH, E74C-R76C was subjected to proteinase K conformational assay. Proteins were analysed on a 12 % SDS-PAGE gel under reducing conditions.
Lane 1 shows the protein at neutral pH without proteinase K treatment. Lanes from 2 till 8 corresponds to preincubation pH 7, 6, 5.8, 5.6, 5.4, 5.2, and 5.0 respectively. HA1 becomes resistant at all the pH. A clear distinct HA2 was not observed at any of the pH.

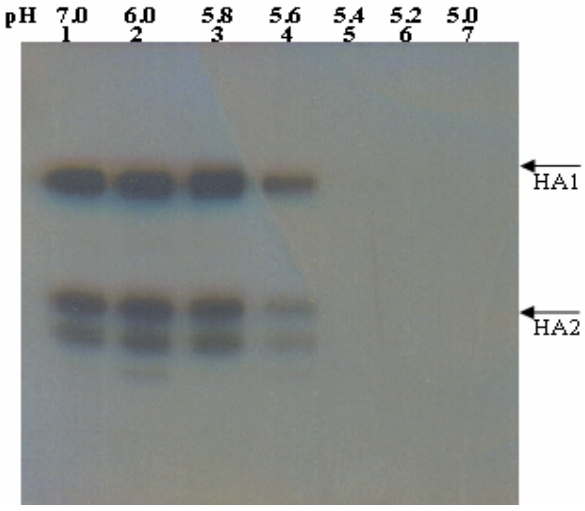

Fig 5.8.5b: pH triggered conformational change of I77C.
Upon incubation at the desired pH, I77C was subjected to proteinase K conformational assay. Proteins were analysed on a 12 % SDS-PAGE gel under reducing conditions.
Lanes 1 till 7 corresponds to preincubation pH 7, 6, 5.8, 5.6, 5.4, 5.2, and 5.0 respectively. HA1 becomes sensitive below pH 5.6, similar to HA-wt.

5.9 Disulfide bond formation for mutants involving cysteine mutants

The formation of disulfide bond among the three HA2 monomers in the mutants E74C-R76C and I77C was explored. The respective mutants were expressed in CV-1 cells, and metabolically labelled as per the standard procedure. The cells were then lysed, and the lysate without being treated with TPCK trypsin was immunoprecipitated. The protein samples were analysed on SDS-PAGE using both reducing and non-reducing loading dyes. The disulfide linkage if formed should be intact in the samples treated with non-reducing dye, due to absence of β-mercaptoethanol in the loading buffer. Those samples treated with reducing buffer were considered as controls for the respective mutant. The Cys mutants were expected to harbour newly formed inter-monomer disulfide linkages in addition to the regular intra-monomer disulfide bonds in the HA-wt. The HA-wt does not have any inter-monomer disulfide linkages. Hence, a typical disulfide linkage in E74C-R76C would show a profile similar to that of DSP cross-linked HA-wt (Fig 5.7).

As may be seen from Fig.5.9, lane 2 the E74C-R76C formed a perfect disulfide bond between all the three monomers, while the I77C (Fig 5.9, lane 4) does not seem to have formed a disulfide bond.

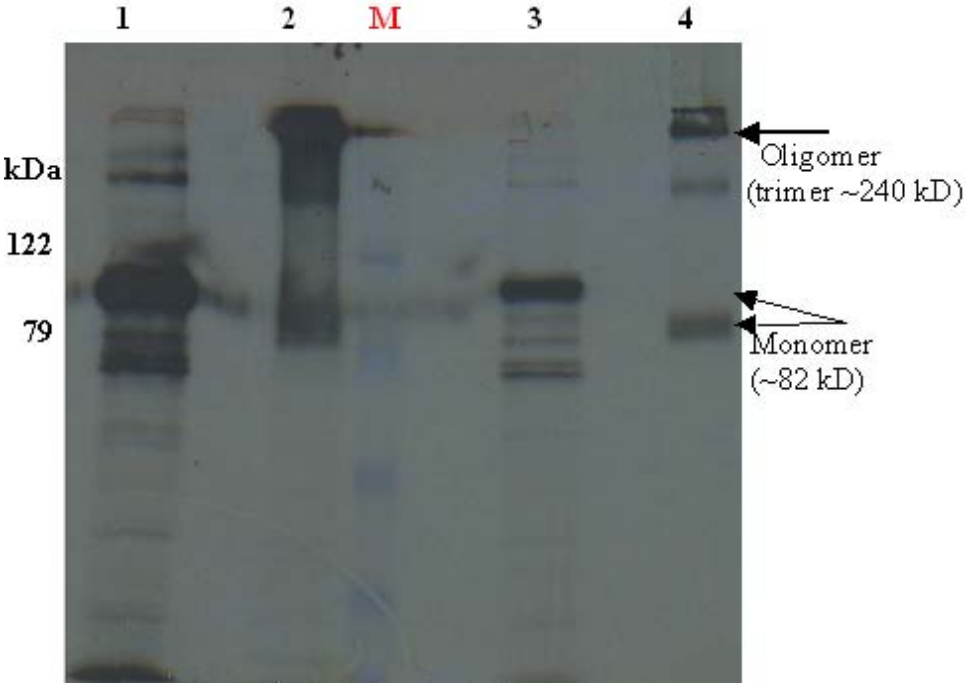

Fig 5.9: Cysteine bond formation for E74C-R76C and I77C.
HA protein samples of E74C-R76C and I77C were analysed on a 9 % SDS-PAGE gel under reducing or non-reducing dye. Lanes 1 and 2 represent E74C-R76C and lanes 3 and 4 represent I77C. Lanes 1 and 3 correspond to reducing conditions while lanes 2 and 4 to non-reducing conditions.

5.10 Fusion assays

The mutants were tested for their ability to promote fusion between CV1 cells and bound human RBCs. The RBCs were labelled using fluorescent-labelled dyes; the membrane bound red fluorescent R18 and the green fluorescent cytoplasmic marker calcein-AM. The fusion activity was monitored under fluorescence microscope by the transfer of lipid dyes from labelled RBC to HA expressing CV-1 cells.

To this end, HA-wt and all mutants were expressed in CV-1 cells (section 4.12.1). HA expressing cells were processed with trypsin and additionally with neuraminidase. The cells were bound to labelled RBC. The fusion was triggered at desired pH by incubating the cells in fusion buffer at 37°C with 5 % CO_2 for 5 min. Subsequently, cell media were re-neutralised with PBS. Fusion activity was monitored at neutral pH (7.4), at pH 5.0, and furthermore, at intermediate pH (5.4 and 5.6). Monitoring the behaviour of R18 alone would not allow differentiating between hemifusion and full membrane fusion and pore formation. To probe for the latter, the redistribution of the cytoplasmic label calcein to was followed. As a control, CV-1 cells transfected with vTF7-3 virus, but without any other DNA, was used.

Visually, binding of RBCs to all mutants was comparable to that of HA-wt at all the pH's, but fusion efficiency varied among mutants (except S110D which was not taken for fusion studies). At pH 5.0, all destabilising mutants showed transfer of R18 and calcein dyes to the CV-1 cells. Although pH dependence of fusion paralleled the pH dependence of proteinase K sensitivity, a difference of ±0.2 pH units was observed between proteinase K assay and fusion experiments (in all destabiliing mutants, other than R269G). The other exception being T212E-N216E, which did not show any fusion activity, while its profile in proteinase K assay was similar to that of HA-wt, i.e., sensitivity below pH 5.4. The results from proteinase K and fusion experiments were summarised in Table .5.10.

None of the stabilising mutants showed any fusion activity at any of the pH, with the only exception being I89R, which showed, only transfer of R18 dye at pH 5.0, indicative ofhemifusion. The cysteine mutants (E74C-R76C, I77C, R109C-E67C, T111C-A44C) were not tested for their fusion efficiency.

As revealed by at least four to five independent experiments, the results from all the mutants were consistent and reproducible. Notably, leakage of calcein was observed to be very low.

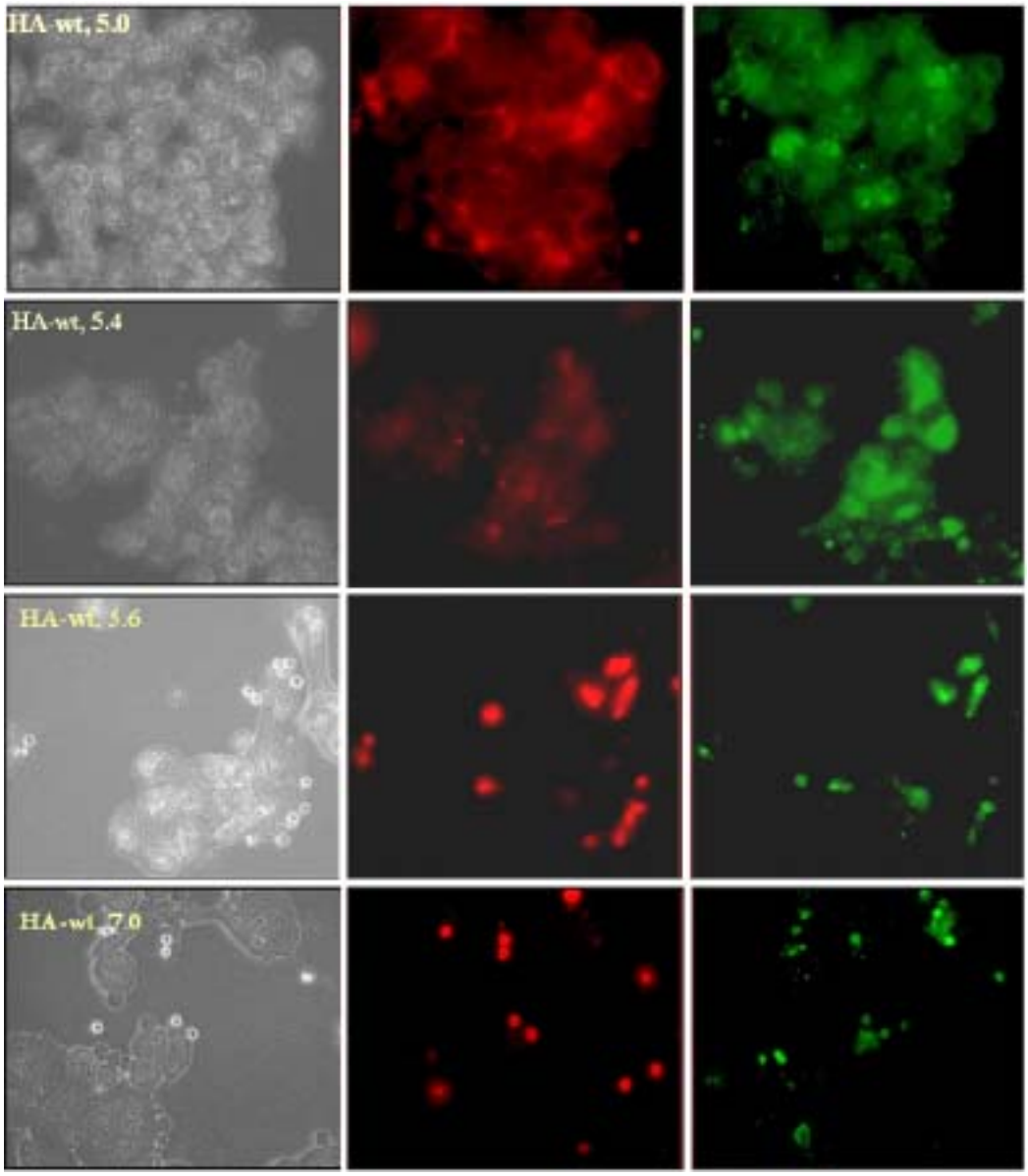

Fig 5.10a: Fusion assay for HA-wt.
Fusion assay was done at 37°C, for 5 min. Transfer of fluorescent lipid dyes (R18 and Calcein) was observed only at preincubated pH 5.0 and 5.4. In comparison, Protinase K conformation assay showed that HA-wt is sensitive below pH 5.2.

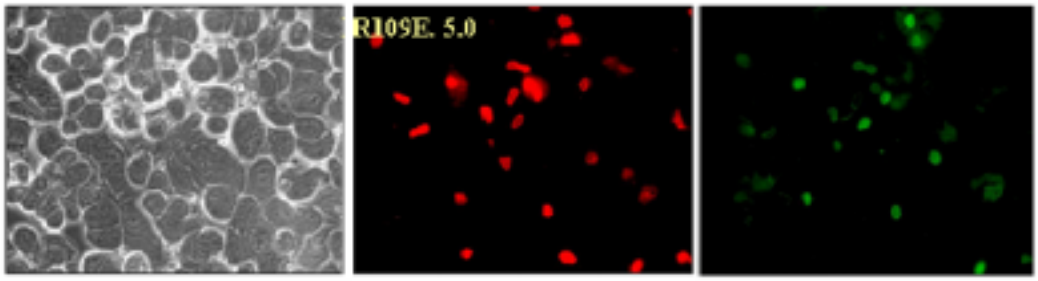

Fig 5.10b: Fusion assay for R109E.
This mutant protein could not be expressed on surface and hence the failure of the fusion with labelled RBC was justified. Fusion was not observed at any of the preincubated pH.

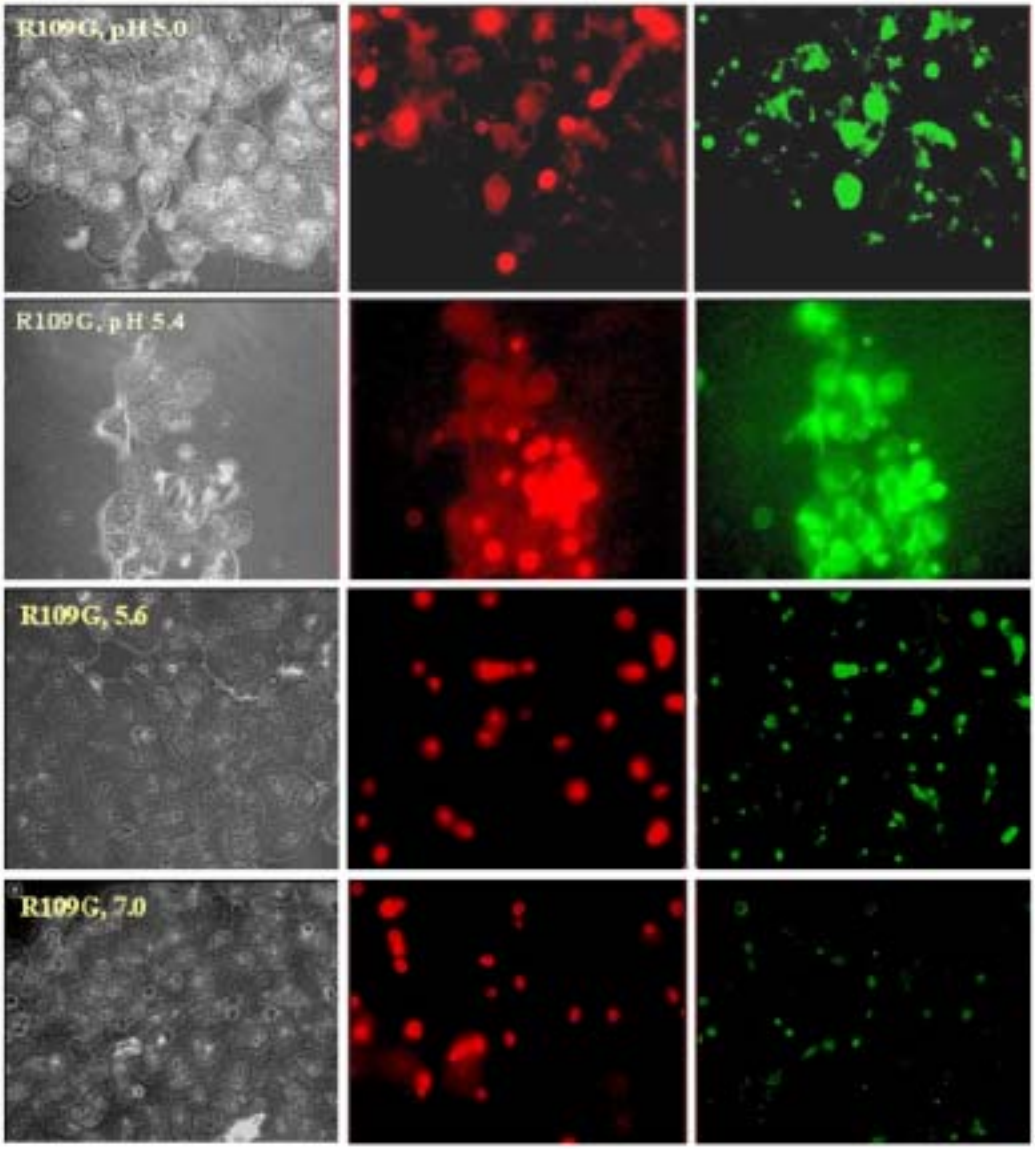

Fig 5.10c: Fusion assay for R109G.
Fusion assay was done at 37°C, for 5 min. Transfer of fluorescent lipid dyes (R18 and Calcein) was observed at pH 5.0 and 5.4. No fusion activity was noticed at pH 5.6 and 7.0. In comparison, Protinase K conformation assay showed that HA-wt is sensitive below pH 5.8.

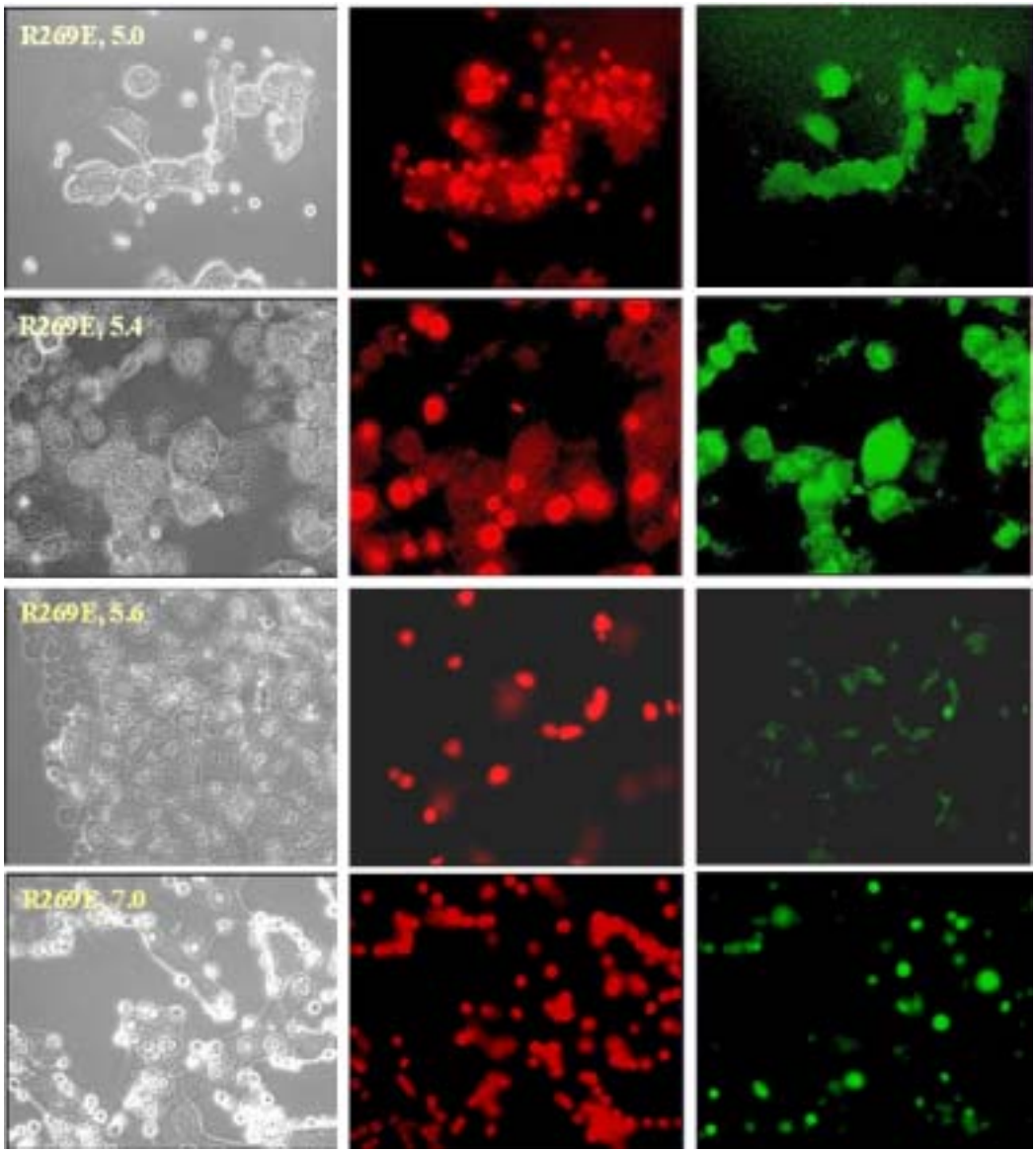

Fig 5.10d: Fusion assay for R269E.
Fusion assay was done at 37°C, for 5 min. Transfer of R18 and Calcein fluorescent lipid dyes was observed at pH 5.0 and 5.4. In comparison, Protinase K conformation assay showed that HA-wt is sensitive below pH 5.8, but no fusion activity was noticed at pre-incubated pH of 5.6 and 7.0.

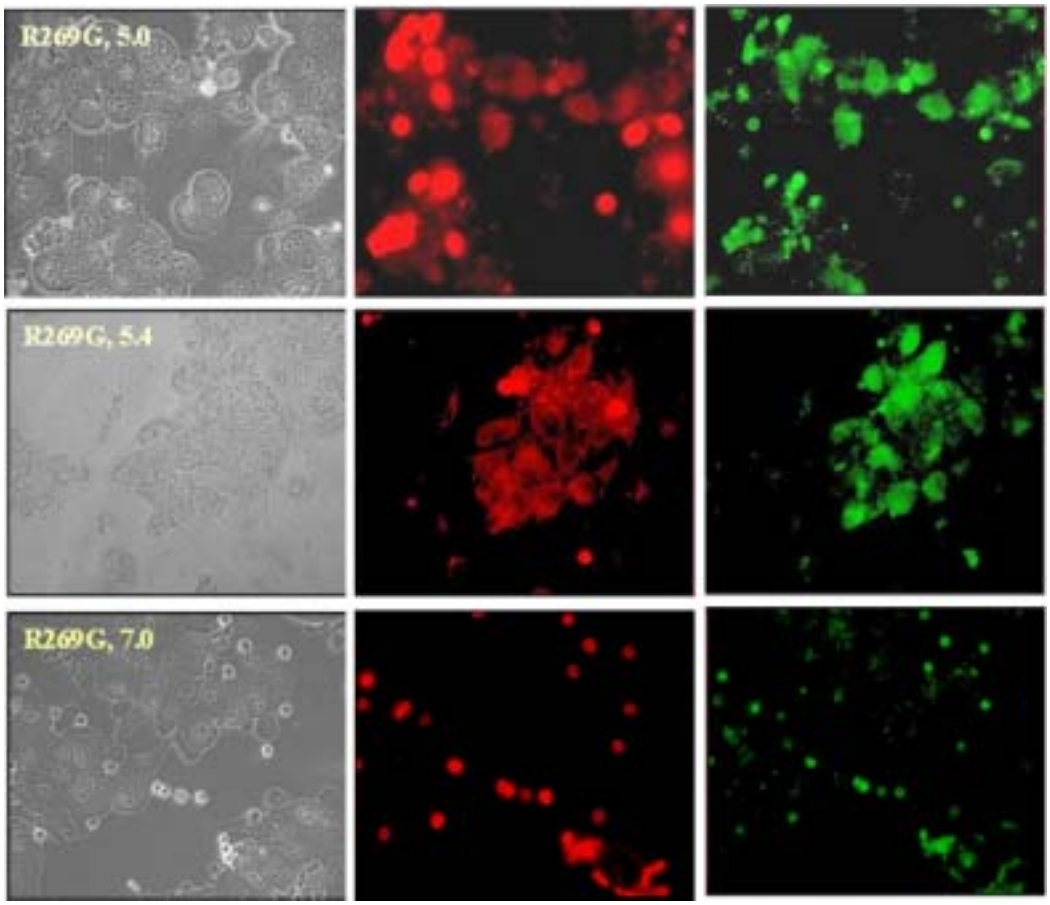

Fig 5.10e: Fusion assay for R269G.
Transfer of R18 and calcein fluorescent lipid dyes was observed at pH 5.0 and 5.4. Fusion activity was not observed at either pre incubated pH 5.6 (not shown) or at pH 7.0. Proteinase K assay showed that R269G was sensitive below 5.6.

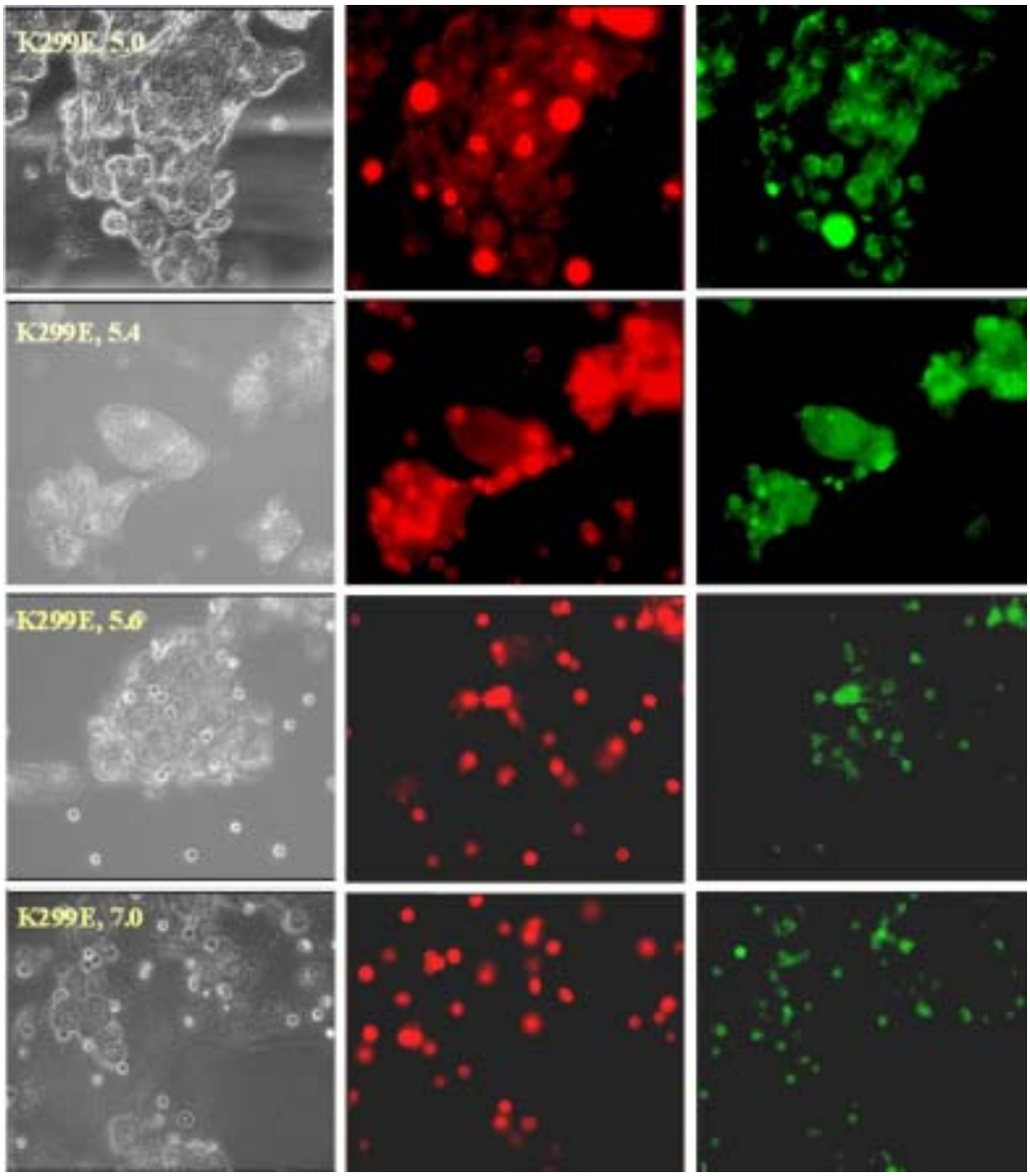

Fig 5.10f: Fusion assay for K299E.
Transfer of fluorescent lipid dyes (R18 and Calcein) was observed at preincubated pH 5.0 and 5.4. No dye transfer was observed at pH values of 5.6 and 7.0. In comparision, proteinase K assay showed that protein was sensitive to conformational change below pH 5.8.

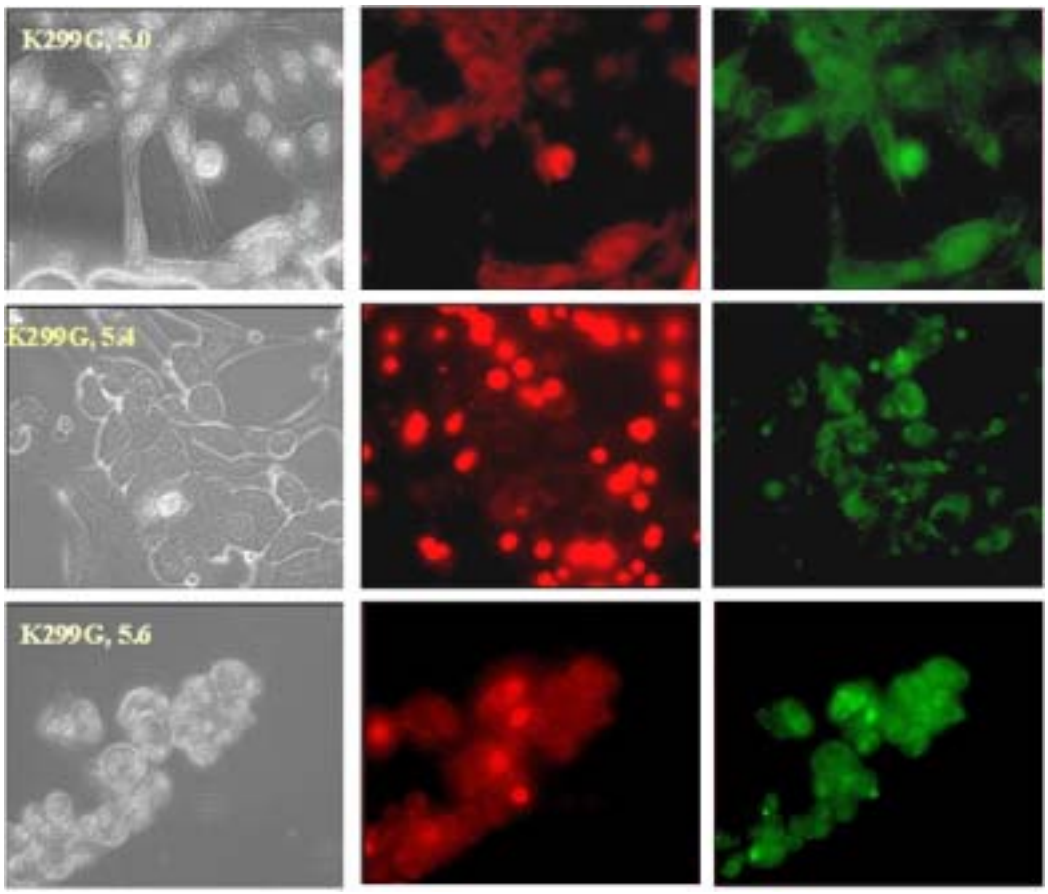

Fig 5.10g: Fusion assay for R299G.
Transfer of fluorescent lipid dyes (R18 and Calcein) was observed at pH 5.0, 5.4, and 5.6. No dye transfer was not observed at pH 7.0 (not shown). Proteinase K assay showed that mutant protein was sensitive to conformational change below preincubated pH 5.6.

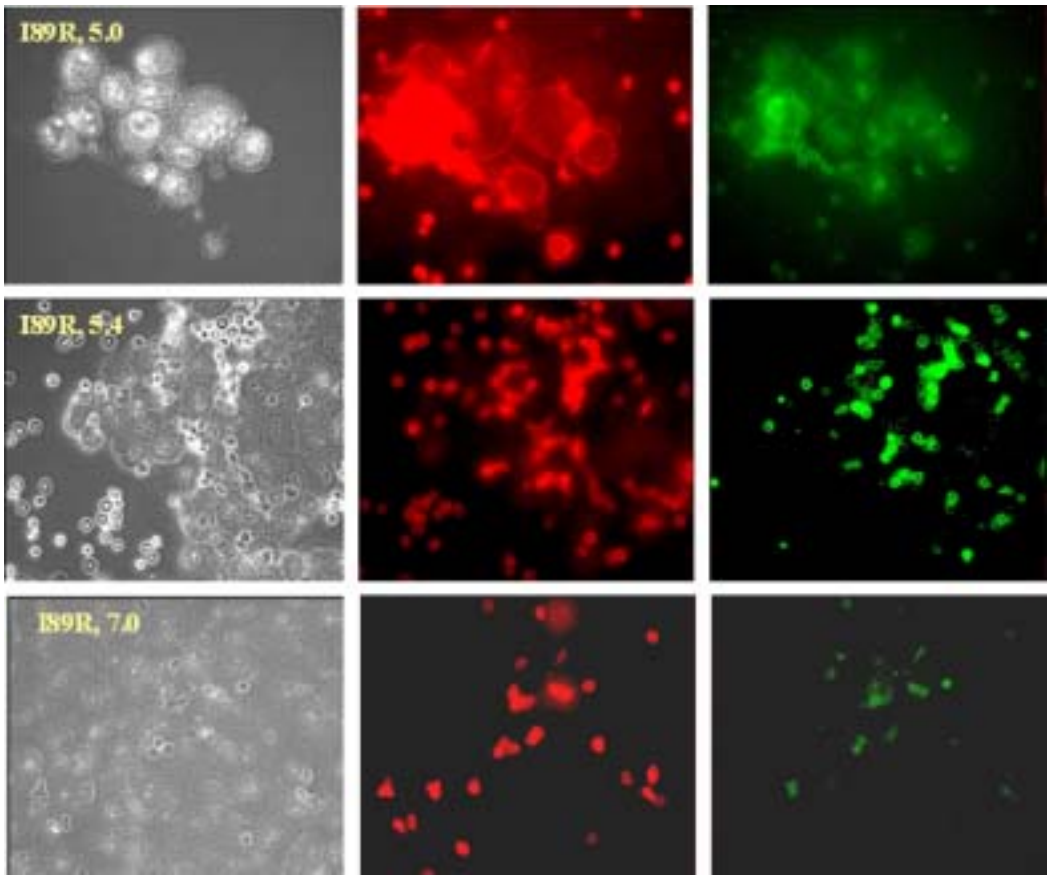

Fig 5.10h: Fusion assay for I89R.
Transfer of fluorescent lipid dyes (R18 and calcien) was observed only at pH 5.0. No fusion activity was seen at either pre-incubated pH of 5.4 and 7.0. Protainase K assay showed that mutant protein was sensitive to conformational change below pH 5.2.

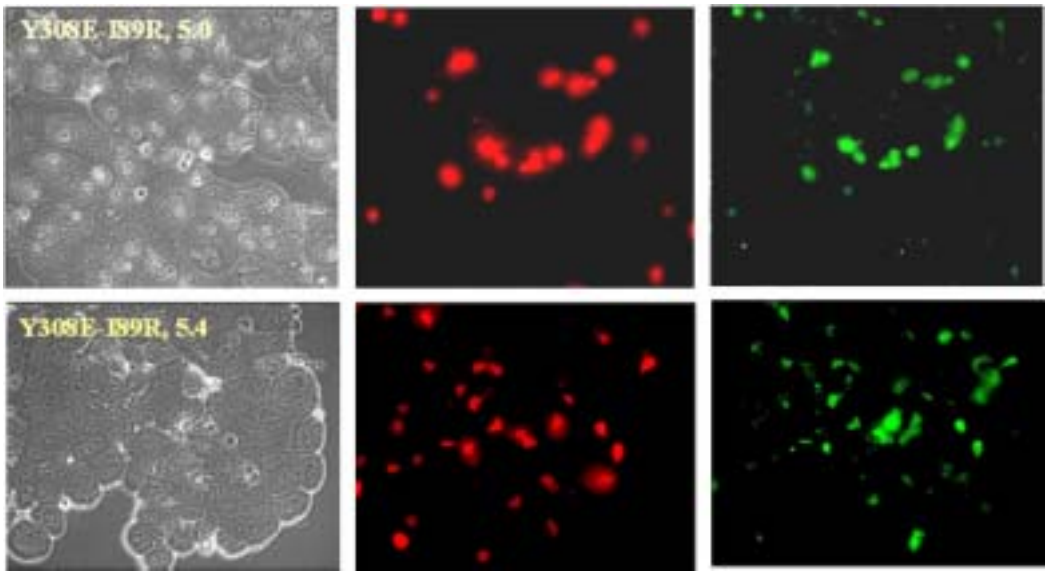

Fig 5.10i: Fusion assay for Y308E-I89R.
Transfer of fluorescent dyes (R18 and Calcein) was not observed at any of pre incubated pH values studied indicating the stability of the mutant protein. Proteinase K assay showed that mutant protein was resistant to conformational change at all pre-incubated pH within a range of pH 5.0 to 7.0.

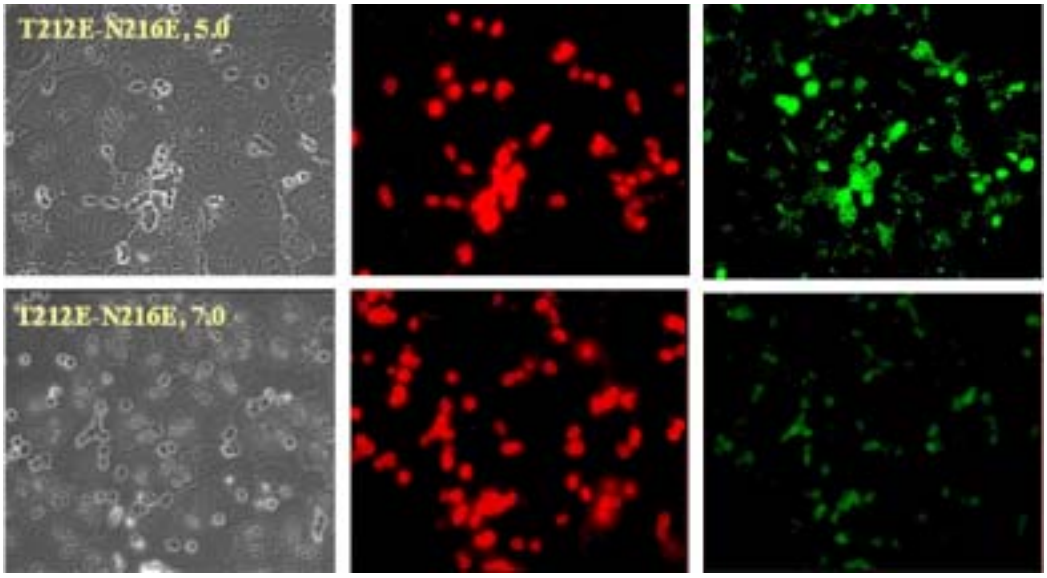

Fig 5.10j: Fusion assay for T212E-N216E.
Transfer of fluorescent dyes (R18 and Calcein) was not observed at any of pre incubated pH values within the pre-incubated pH range of 5.0 till 7.0. On contrary, proteinase K assay showed that the mutant protein was found to be very similar to that of HA-wt in its profile and was sensitive to conformational change below pH 5.4.

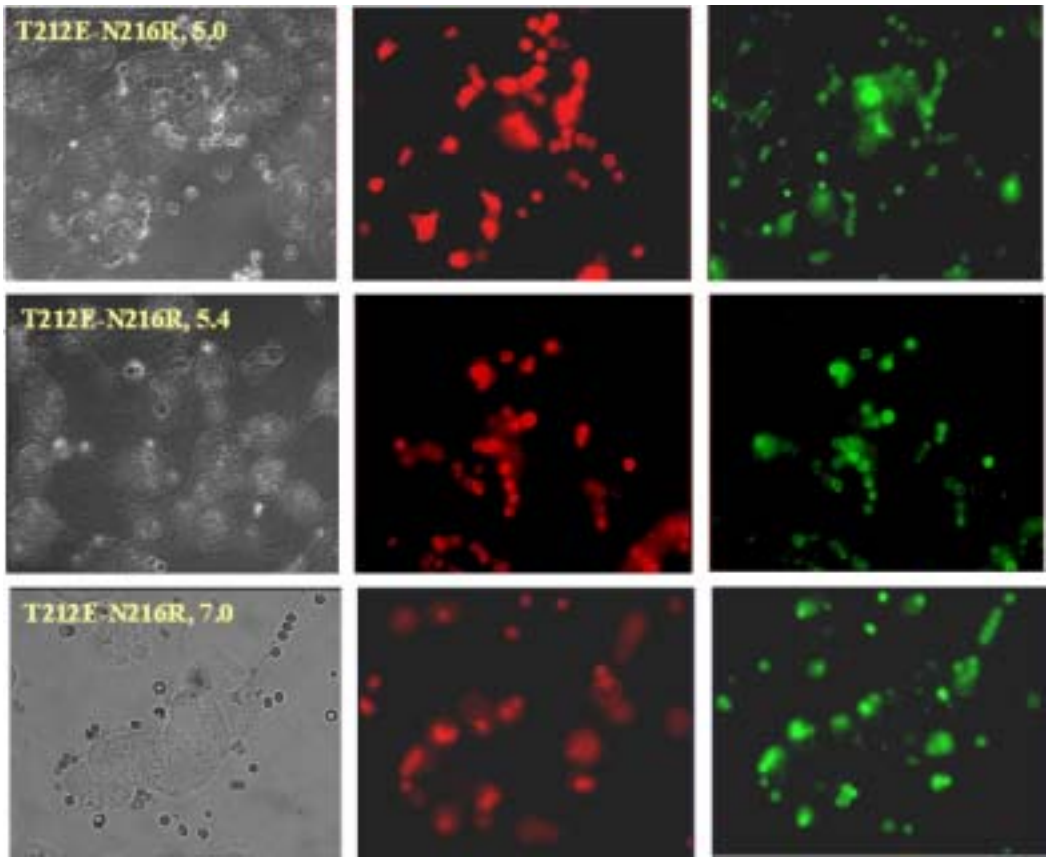

Fig 5.10k: Fusion assay for T212E-N216R.

Transfer of fluorescent dyes (R18 and Calcein) was not observed at any of pre incubated pH values studied indicating the stability of the mutant protein. Proteinase K assay showed that mutant protein was resistant to conformational change at all pre-incubated pH within a range of pH 5.0 to 7.0.

Table. 5.10: The summary of the pH threshold for HA-wt and all the mutants with respect to proteinase K assay and also for fusion assays.

		Fusion assay			
		pH 5.0	**pH 5.4**	**pH 5.6**	**pH 7.0**
HA-wt	5.2, and 5.0	+++	++	NO	NO
De stabilising mutants					
R109E	No surface expression	No fusion			
R109G	5.6, 5.4, 5.2, and 5.0	+++	+++	NO	NO
R269E	5.6, 5.4, 5.2, and 5.0	+++	+++	NO	NO
R269G	5.4, 5.2, and 5.0	++	+	NO	NO
K299E	5.6, 5.4, 5.2, and 5.0	+	+	NO	NO
K299G	5.4, 5.2, and 5.0	++	++	+	NO
T212E-N216E	5.2 and 5.0	NO	NO	NO	NO
Stabilising mutants					
S110D	5.8, 5.6, 5.4, 5.2, 5.0	Not available			
I89R	5.0	+	NO	NO	NO
I89E-Y308R	NO	NO	NO	NO	NO
T212e-N216R	NO	NO	NO	NO	NO
Cysteine mutants					
E74C-R76C	---------	Not available			
I77C	5.4, 5.2, and 5.0	Not available			

The fusion assay was not performed for S110D and for the cysteine mutants. An attempt was made to quantify the fusion activity of the mutants and accordingly the efficiency was shown in the form of "+" symbols. The pH's at which no fusion activity was observed are marked as "NO".

6 DISCUSSION

The present investigation elucidates the significant role of electrostatic interactions in maintaining the stability of the non-fusogenic structure of HA protein of influenza virus (X-31 strain) at neutral pH. The precursor HA protein is cleaved by host proteases which results in the formation of HA1 and HA2 domains. The HA protein at this stage is believed to be metastable. Low pH triggers a conformational change of the metastable HA into a thermodynamically low energy state. This conformational change exposes the otherwise deeply embedded hydrophobic fusion peptide initiating fusion with host target membrane. Exposure of fusion peptide from the HA2 domain is preceded by dissociation of the globular head domains of HA1 region. Site directed mutagenesis of various amino acids in HA2 domain highlights the importance of respective residues in the conformational process and thereby in the fusion (Gething *et al.*, 1986; Qiao *et al.*, 1999; Han *et al.*, 1999; Cross *et al.*, 2001; Gruenke *et al.*, 2002). Though the dissociation of HA1 domains was proved to be essential in the whole process, the destabilising forces are supposed to be due to enhanced protonation of the titratable amino acids on the HA1 domain (Daniels *et al.*, 1985).

Huang *et al.* (2002) pointed out the importance of electrostatic interactions for the stability and destabilisation of HA trimer. The scope of the present research is to determine the contribution of charged residues (ion pairs) to the stability of the cleaved HA protein in its non-fusogenic state. For this purpose, amino acids were selectively mutated, and the effect of mutations on conformational change was analysed. Target of the mutations were those amino acids, which form ion pairs (Fig. 5.1.1-5.1.5). Mutagenesis was aimed, either to destabilise or stabilise the protein (breaking or making salt bridges, respectively). The present work is unique and novel, as it demonstrates the relevance of salt bridges at the interface of HA1 and HA2 for the stability of the HA ectodomain. At the same time it is of relevance to prove that disruption is accompanied with the conformational change of HA. It is for the first time, that the important amino acids (involving salt bridges) which are responsible for the stability of the non-fusogenic HA protein has been identified. The results denote that the conformational transition of the HA ectodomain in different influenza strains could be directly linked to the mentioned salt bridges.

6.1 Choice of mutation sites

All the mutations chosen for the study involved the residues either at the intra-monomer or

at the inter-monomer interface. The interface between HA1 and HA2 regions (intra-monomer) gain importance as the HA2 in this region undergoes "loop to helix" transformation (55-75 residues). The region between the residues 64-72 of HA2 is in direct contact with the globular domain of HA1. This region (64-72) shows more than 70 % conservation among all the influenza A subtypes. The residues 85–90, 104–115, 265–270, and 299-307 form the interface region on the HA1 side. At least 20 out of 33 residues within these regions are conserved to a great extent (color index >7, see Fig.5) among the entire influenza A family. Daniels *et al.* (1985) analysing various naturally occurring mutants surmised that substitutions usually occurred either at interface region of HA1 and HA2 or at the amino-terminus of HA2. Furthermore, the authors quoted that an extensive breakage of intra and inter subunit contacts could possibly lead to conformational change of HA. In accordance with this hypothesis, Huang *et al.* (2002) proposed that protonation of solvent exposed negatively charged amino acids, disrupt electrostatic interactions between residues (i.e. salt bridges). This disruption causes a conformational change leading to a fusion active state of the HA. To prove this model experimentally, the present study lays focus on the interface region between HA1 and HA2, especially salt bridges. A series of mutants (between HA1 and HA2 of a monomer) were constructed either to destabilise or to stabilise the HA protein (section 5.1.1-5.1.4). Similarly, this study also identified inter-monomer interactions contributing to the stability of the HA protein. In particular, inter-monomer interactions between the three HA1 monomers were studied in the distal region, because the initial step in the process of the conformational change is linked to changes in this region. The role of ion pairs for inter-monomer interactions and for the stability of the ectodomain was determined by targeting salt bridges in the distal region of HA2 monomers (section 5.1.5).

All the selected amino acids for mutagenesis were checked for their homology among influenza A virus strains. Figure. 5.2 show that most of the mutated residues were conserved ranging from average to a higher degree. The most conserved residues involving mutants were Arg 109, Ser 110, Lys 299, Tyr 308 of HA1 chain. In addition, the sequence alignment of the HA2 domain showed that Glu 74 and Ile 77 were conserved to a higher degree. Further, the tetrad salt bridge involving Arg 109, Glu 89, Arg 269 of HA1 chain with Glu 67 of HA2 chain has most of the residues conserved to a higher degree. Arg 269 is the only exception with low conservation, while negative charge at position 67 of HA2 is conserved to approximately 70 %. This shows the evolutionary importance of this salt bridge among all the members of influenza A virus.

6.2 Mutants construction and expression in mammalian cells

A prerequisite for assessing the fusion activities of HA expressing cells, is good surface expression of the mutant HA or HA-wt proteins. In connection with this, the surface expression of the HA-wt, and the mutant proteins was adjusted by varying the amount of lipofectin and plasmid DNA. Figs. 5.8.1a-5.8.1f shows that all the mutants were expressed at comparable levels in relation to HA-wt, with the exception of R109E. The failure of surface expression of R109E could be attributed to failure in transport of the mutant protein from Golgi complex to the cell surface (section 5.6, and Fig.5.6). The ability of all the mutants (except R109E) to show cell surface expression and further the formation of HA1 and HA2 by TPCK trypsin treatment showed that mutants formed successful trimers. This is confirmed by chemical crosslinking with DSP (section 5.7 and Fig.5.7). The mutants R109G, R269E, T212E-N216R, and T212E-N216E also showed trimer formation with DSP reagent (results not shown). Even the ability of R109E mutant protein to form trimer underlines the fact that trimerisation is a phenomenon occurring in the ER (Copeland *et al.*, 1988; Boulay *et al.*, 1988). The inability of the surface expression of R109E mutant protein has been discussed in subsequent sections.

6.3 Proteinase K assay revealed difference in conformational changes

The active form of the HA protein undergoes an irreversible conformational change to the fusogenic form depending on the pH milieu. The conformational changes can be probed by the proteinase K assay (section 1.4). The low pH conformational change of the HA is an example of a proton sensitive conformational switch involving Bohr protons (Daniels *et al.*, 1985). The threshold pH for conformation change varies among different strains of influenza A virus. Therefore, this proteinase K assay is very crucial to ascertain whether the desired mutant has a stabilising or destabilising effect on the conformational change.

Figure 5.8 show that HA-wt is sensitive to proteinase K at pH $\leq$ 5.2. On comparison, it was found that all the destabilising mutants showed a higher pH threshold for the conformational change (see fig 5.8.1a-5.8.1f and table 1). It implies that these destabilising mutants lowered the energy barrier requirements for the conformational change. A close look at the Gly and Glu substitutions at the same position, for instance R269G and R269E, respectively, show that Glu substitutions resulted in a conformational change at a higher pH than those with Gly. This confirms that Glu substitutions generated repulsion forces due to Glu-Glu (-ve to –ve) interactions and lowered the energy barrier requirements for

the respective mutants. These results indicate that substitutions lowering the required energy could be due to reduced interaction (or increased repulsion) between the subunit interfaces. In addition, increased repulsion (or lowering the required energy) lowers the concentration of protons required to trigger the conformational change.

Thus the mutations show a decreased pH (proton) requirement for the conformational change in the following order -

Normal ion pair (HA-wt) > no ion pairs (Gly substitutions) > repulsion ion pairs (Glu substitutions).

The stabilising mutations (Fig.5.8.2a-5.8.2c) on the other hand showed no conformational change upon proteinase K treatment till pH 5.0. The only exception being S110D (Fig.5.8.2c), which was intended to be a stabilising mutation but turned out to be destabilising in nature, on proteinase K treatment. Very likely, the reason is that the interacting residue His 64 with its aromatic ring failed to form an ion pair. Another reason could be that the pair Ser 110 – His 64 is in the neighbourhood of the tetrad salt bridge involving Arg 109 and Glu 67. The introduction of S110D would have perturbed the geometry of the tetrad salt bridge. Indeed, the occurrence of a salt bridge involving His residue is not common. Kumar and Nussinov (1999) studying a database of 222 non-equivalent salt bridges from 36 monomeric proteins accounted for only 4 salt bridges involving His residue. The experiments were repeated for three times and the protein concentrations were recorded as percentage taking the sample treated with pH 7.0 fusion buffer as 100 %. Accordingly the concentrations of protein bands seen on the fluorograms (i.e.,quantity or % of the protein resistant to proteinase K at each of pH analysed), were plotted on a graph using standard error as a statistical tool and taking sample size as three.

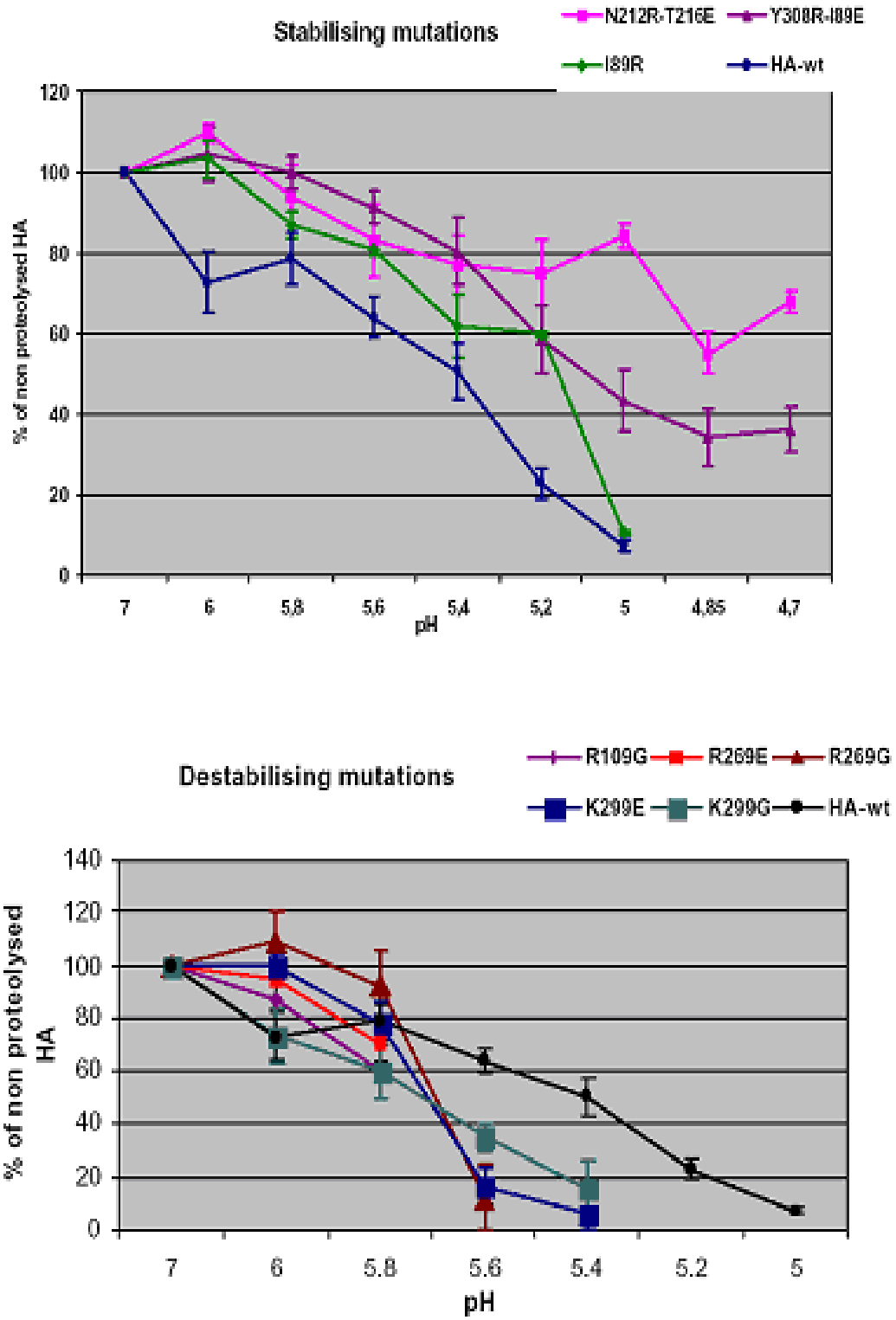

Fig.6.3: Non proteolysed HA content from both the stabilising and de-stabilising mutants after proteinase K assay.
HA-wt is taken as control. The method is described in section 4.10. (mean values ± standard error).

6.4 Relation of destabilising mutants with natural variants

The mutations in the interface region of HA1 and HA2 indicated the significance of charged residues in the conformational transition of HA protein. Inspired by these results, an attempt was made to look for the reports of the natural variants harbouring these mutations and show higher pH requirements for fusion activity. It was observed that natural variants of influenza viruses (X-31 and Weybridge strains) show fusion at higher pH than the HA-wt (Daniels *et al.* 1985). These variants were specifically selected for their resistance to amantadine hydrochloride, which is known to increase the pH of intracellular vesicles. The amino acid sequence analysis revealed that 15 of the 17 mutants from X-31 strain showed substitutions in the HA2 region. On the contrary, 50% of the mutants from Weybridge strain showed substitutions in HA1 region. In both cases, charged residues were substituted to an extent of 75 %. Some of the substitutions were electrostatically destabilising for the salt bridges. Mutations were reported to be either in the interface region (HA1-HA2 or HA2-HA2) or in the amino terminal peptide of HA2.

Similarly Proesch *et al.* (1990), Hoffman *et al.* (1997), and Staschke *et al.* (1998) reported natural variants of various subtypes of influenza virus to be resistant to anti-viral drugs (norakin, tetra-butyl hydroxyquinone, and methyl-*O*-methyl-7-ketopodocarpate respectively). Amino acid sequences of the respective variants revealed substitutions in either amino terminal peptide of HA2 or in the interface region of HA1 and HA2. All the mutants were reported to have elevated pH of fusion.

The reports on natural variants showed several substitutions including those of charged residues, but there is no report on salt bridge destabilisation in the interface region. In other words, the charged amino acids (especially tetrad salt bridge) that were considered for the study were not substituted in any of the natural mutants. This signifies the importance of these amino acids towards the stability of the HA protein. Further, this indicates that the complex salt bridge (in the interface) could have been conserved in all the subtypes of influenza virus. The occurrence of a similar salt bridge in the interface region for H2 subtype will be discussed in the subsequent sections.

6.5 Significance of Arg 109 and tetrad salt bridge in maintaining the stability of the HA ectodomain

The Arg 109 is conserved mostly among all the influenza A viruses and also in influenza B viruses. Only incidence of its mutation was reported in H2 subtype where Arg 109 was substituted with Lys. In other words, a positive charged residue at position 109 (numbering according to X-31 strain) is conserved. As deduced from the 3D structure of X-31 subtype (PDB: 1HGD), the Arg 109 forms a salt bridge network with Glu 89 of HA1 on one side and Glu 67 of HA2 on the other side. In addition, Arg 269 is involved in this network forming a tetrad network. It may be stated that this tetrad salt bridge is especially important in maintaining the stability of the non-fusogenic conformation as it connects different parts of the intact protein. The figure below shows the distance in Å between the residues involved in the salt bridge network.

Musafia *et al.* (1995) studying 1105 salt bridges from 94 proteins concluded that complex salt bridges comprise about 70 % of inter subunit interactions. The significance of this tetrad salt bridge is increased by the presence of Arg, which is an abundantly found residue in inter subunit interactions (Musafia *et al.*, 1995). Further the same authors report that Arg is abundant and constitutes nearly 43.3 % in all the complex salt bridges. Report of Xu *et al.* (1997) suggests that the hydrogen bonds across the interfaces are predominantly oxygen-nitrogen type. Taking into account all these considerations, it is quiet apparent that this complex salt bridge is ideally placed at the interface with perfect geometry.

The failure of the expression of R109E mutant protein could be explained by disturbance caused as a consequence of the repulsion generated by substituted Glu with that of Glu 89 of HA1 and Glu 67 of HA2.

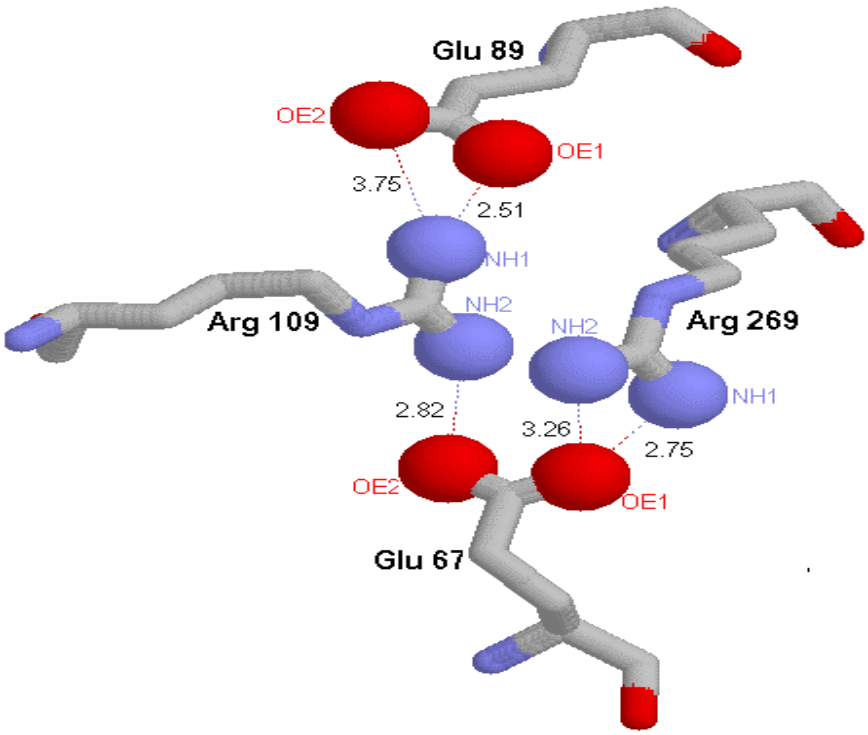

Fig. 6.5: The tetrad salt bridge showing the distance in Å between the residues.

The glycosylation assay (Fig.5.6; lanes10-15; and section 5.6) showed that R109E mutant to be sensitive to EndoH. It may be deduced from the result that R109E could have been retained either in ER or *cis*-Golgi compartments. Since the immunoprecipitation assays showed that N2 antibody detected the protein, it may be said that R109E mutant successfully formed trimer. This gives an indirect hint that R109E passed through ER and possibly held up in *cis*-Golgi compartment. The N2 antibody is specific for neutral pH and trimer HA (Copeland *et al*., 1986). Its inability to recognise monomers (Copeland *et al*., 1986) emphasises that the mutant R109E has formed trimer. In addition, trimerisation is a phenomenon occurring in the ER organelle of the cell (Copeland *et al*., 1988). It is also a prerequisite for efficient transport of the protein from ER (Boulay *et al.*, 1988). The importance of this tetrad salt bridge in stability of HA protein is highlighted by the identification of a second ligand binding site of concave pocket nature at the interface of HA1 and HA2 (Sauter *et al.*, 1992).

6.6 Relation of stabilising mutants with H2N2 (A/JPN/305/57)

The HA protein of A/JPN/305/57 (H2 subtype) was found to be very stable compared to A/PR 8/34 (H1 subtype) and X-31 of H3 subtype. Even at pH 5.0 and 37°C, inactivation is very slow when compared to X-31 and A/PR 8/34 (Korte *et al.*, 1999). In order to gain insight into the stability aspects of this H2 subtype, the amino acid sequence was aligned

with X-31 sequence. The HA2 sequence in both the strains is highly conserved compared to HA1 region. The structure of HA of A/JPN/305/57 strain was determined at neutral and acidic pH by cryo electron microscopy (Böttcher *et al.,* 1999). At neutral pH, the structure of HA was found to be similar to the 3D structure of X-31 strain. At acidic pH (4.9), the structure showed a continuous central cavity retaining the intact trimer structure. Based on the amino acid sequence of A/JPN/305/57 and taking 3D crystal structure as reference, the formation of salt bridges for H2 subtype was probed. Based on the homology of the HA2 amino acid sequence, it was assumed that H2 subtype may have similar HA2 structure like that of X-31 strain. Apparently HA protein would have similar interface region and thereby similar HA1 structure. In addition, Böttcher *et al.* (1999) reported that both the structures of A/JPN/305/57 and X-31 strains are similar, other than for a few minor differences. The first step was to verify whether all the charged residues were conserved in the H2 subtype. Based on the sequence alignment, the interface at the HA1 region of H2 subtype shows additionally 17 charged residues between 74-84, 96-125, 256-274, and 280-295. On the other hand, the number of charged residues on the interface of HA2 region is relatively same. Further, the complex salt bridge in the interface region of X-31 is conserved in the H2 subtype. The amino acids forming this salt bridge are Glu 89, Lys 109, and Lys 269 of HA1 (numbering based on X-31 strain), and Glu 69 of the HA2. In the absence of Glu 67 on the HA2 and Lys 299 on the HA1, it may be assumed that Glu 69 would form similar tetrad salt bridge in the interface region. In X-31 strain, tetrad salt bridge involves Glu 89, Arg 109, and Arg 269.

Table. 6.6a: Tetrad salt bridge formation in A/JPN/305/57 (H2 subtype)

	Residues involved in salt bridge formation	
	HA1	HA2
	Arg 109, Arg 269, Glu 89	Glu 67
	Lys 299	Glu 69
A/JPN/305/57	Lys 101 (109*), Arg 264 (269*), Glu 80 (89*)	Glu 69

*Numbering based on X-31 strain, following sequence homology of A/JPN/305/57 with X-31.

Further, the trimeric shape of the HA of the A/JPN/305/57 (H2 subtype) is very stable even at pH 5.0 (mentioned earlier). The low pH usually affects the charged residues, and further the salt bridges. From on the above results, it is very much evident that salt bridges could destabilise or stabilise the HA structure. The sequence homology and subsequent

alignment of the A/JPN/305/57 sequence onto X-31 3D structure identified potential salt bridges. The focus was more at the interface regions (inter and intra monomers) especially in the distal region of the HA structure. Our intention was to find the potential salt bridges responsible for the stability of the low pH structure (continuous central cavity) of the A/JPN/305/57. At least 7-8 additional possible salt bridges were identified in H2 subtypes, when compared to X-31 strain, and are summarised as shown in the table 6.6a and 6.6b.

Table. 6.6b: The different types of additional salt bridges in A/JPN/305/57 (H2 subtype) when compared to X-31 strain.

		Residues involved in salt bridge formation		
		HA1		***HA2***
	Between HA1 and HA2 (i.e., A-B; C-D; E-F).	His 102 (110*)		Glu 64
	Within HA1 (i.e., A or C or E)	Lys 159 (165*)	Glu 240 (246*)	
	Between HA1 and HA2 (i.e., A-F; C-B; E-D).	Glu 98 (106*) or Glu 99 (107*)		Arg 75
		Arg 206 (212*)	Glu 210 (216*)	
		Asp 181 (187*)	Arg 195 (201*)	
	Between HA2 monomers (i.e., B-D-F)			Arg 83 - Glu 85

*Numbering based on X-31 strain, following sequence homology of A/JPN/305/57 with X-31.

Based on this analysis, it may be surmised that A/JPN/305/57 has three rows of inter-monomer salt bridges connecting all the monomers (either A-C-E or B-D-F) at three different positions (Fig 6.6). In X-31, such an inter-monomer linkage is only found between HA2 monomers (i.e., B-D-F). In addition to these inter-monomer linkages, there is one more salt bridge (Glu 98 or 99 [106* or 107*] with Arg 75 of HA2) involving HA1 and HA2 monomers in the hinge region giving it an extra stability to the HA of A/JPN/305/57 strain. This salt bridge has the potential to form a complex salt bridge in the hinge region with another salt bridge (Glu 74-Arg 76) forming a ring like network between B-D-F chains of HA2 monomers. At least one of these salt bridges i.e., T212E-N216R was generated in X-31 strain (discussed in section 6.7). The mutant was found to be stable till pH 5.0 and showed no fusion activity.

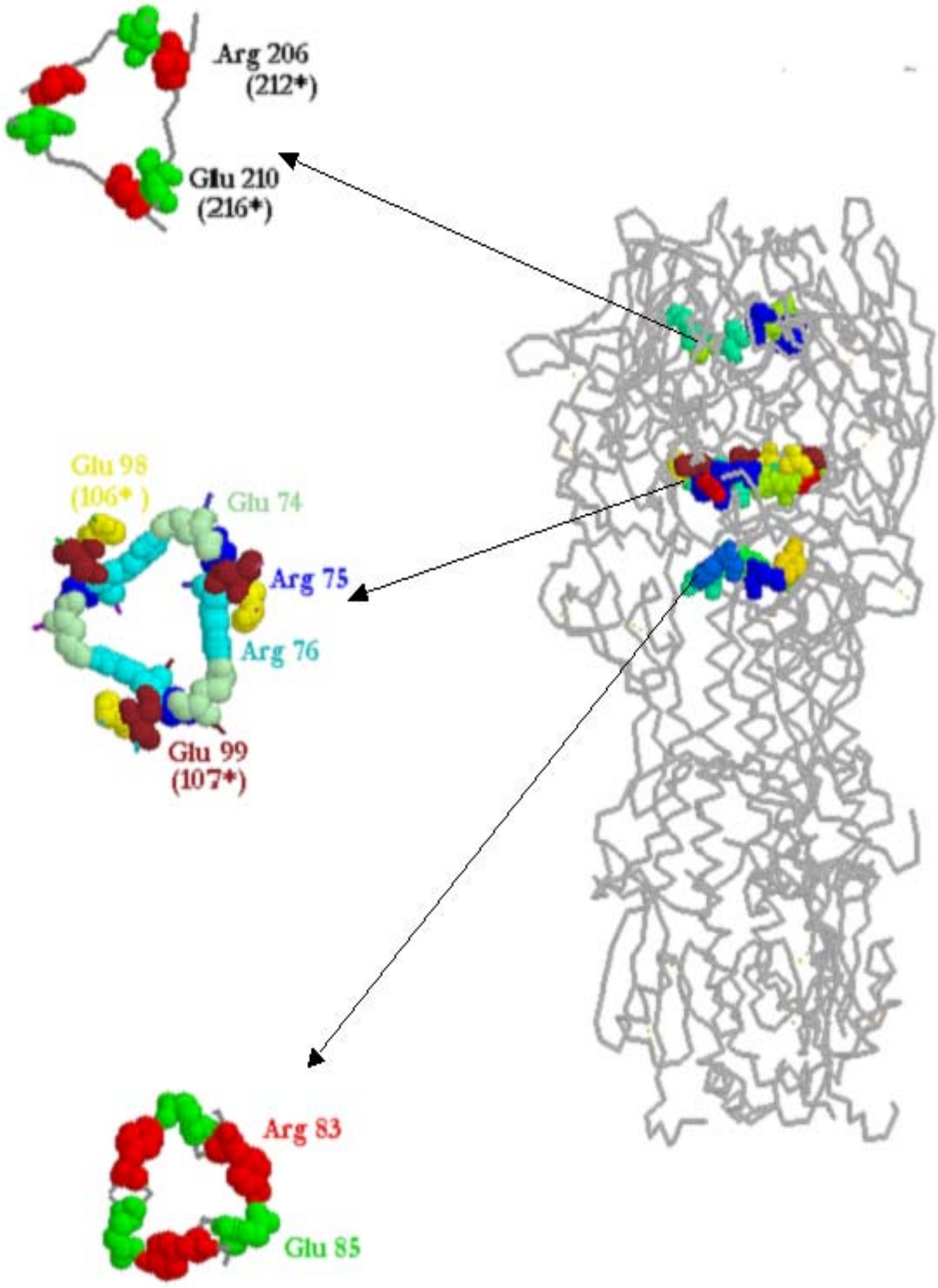

Fig. 6.6: Salt bridge networks in A/JPN/305/57 strain.
The figure shows the amino acid residues of A/JPN/305/57 strain superimposed on 3D structure of X-31 strain implicating a three-layer ring like salt bridge network. HA of A/JPN/305/57 strain has been reported to be very stable and its trimer structure is retained even at pH 5.0.

6.7 Introduction of a salt bridge in the distal region stabilises the HA trimer of X-31 strain

Locking of the distal region of the HA trimer impaired the low pH induced conformational changes and also the fusion activity (Godley *et al.*, 1992; Kemble *et al.*, 1992). Based on this observation, an attempt was made to introduce salt bridges in the same positions viz., T212E and N216R in a HA1 monomer (Fig.5.1.3; section 5.1.3). This double mutation was located at the HA1-HA1 interfaces and was expected to lock the trimer with a ring like complex salt bridge. Probing the conformational change by the proteinase k assay showed that the mutant is resistant to conformational changes till pH 5.0 (Fig.5.8.4). This indicates that the introduction of an ion pair in the distal region enhances the stability of the trimer. On the contrary, introduction of repulsion charges (Fig. 5.8.3) in the same position showed similar activity as that of HA-wt. This result is comparable to that of the disulfide mutation of Godley *et al.* (1992) and Kemble *et al.* (1992), where locking of the HA1 trimers abolished both the conformational change and fusion activity. It was surprising and interesting to note the stability conferred by this salt bridge to the HA trimer. Sequence alignment of A/JPN/305/57 against X-31 showed that this salt bridge exists between Arg 206 and Glu 210 in H2 subtype of A/JPN/305/57.The stability of the distal region conferred by a salt bridge would not be the same as that of disulfide bonding. However, the introduction of an additional salt bridge could have easily raised the stability by 0.4 pH units. This is confirmed by fusion assays (discussed in section 6.8). No fusion activity was observed for pH $\geq$ 5.0 upon incubation for 5 min at 37°C. It may be possible that either longer incubation periods or a pH < 5, could dissociate these stable salt bridges leading eventually to a conformational change. This mutant clearly demonstrates that dissociation of the globular domains is the foremost and most essential step towards a fusogenic conformation of HA. As discussed earlier, this salt bridge seems to be existent in A/JPN/305/57 strain and it may be concluded that this is one of the important factors for the stability and slow inactivation of HA of A/JPN/305/57 at pH 5.0.

6.8 Fusion assays

Membrane fusion i.e., lipid mixing upon acidification is essential to show the functional activity of all the mutants. All the destabilising mutants (except T212E-N216E) showed comparable fusion activities to that of HA-wt, but the extent of activity differed between the mutants. R109E did not show any fusion activity as was expected due to its failure to

show surface expression. The fusion assay was performed at a series of pH 5.0, 5.4, 5.6, and 7.0, respectively, in order to see if there is any correlation between the pH threshold of the conformational change assessed by proteinase k assay (conformational assay) and fusion assay. For all of the destabilising mutants (except T212E-N216E) the pH threshold was 5.4 and 5.6, respectively. Thus a difference of ±0.2 pH units was observed between the proteinase k conformation assay and the fusion assay.

Fusion activity was quantitatively higher for R269E than R269G, as it was evident from conformational assay, while the former requires less energy to gain fusion competent structure and hence more fusion activity. On the contrary, the K299G mutant showed relatively more fusion activity than K299G. Further, the K299G mutant showed fusion activity even at pH 5.6, while the conformational assay shows sensitivity only below pH 5.4. Similarly, T212E-N216E mutant though was sensitive to conformational change below pH 5.2, showed no fusion activity even at pH 5.0. The stabilising mutants did not show any fusion at any of the pH, and was in agreement with proteinase K assay.

In the present state of investigation, no conclusive explanation was possible for this difference. One reason could be that the pH dependence of the exposure of the fusion peptide is different from that of the complete exposure of the hinge region of HA1, which requires a more acidic pH. Another reason could rely in the specific conditions of the assays. While the fusion assay is done in the presence of the target membrane, the proteinase K assay does not involve interaction with the target membrane. It may be that the conformational change is supported by interaction with the target membrane.

Thus to state, the fusion assay confirmed the conformational changes based on proteinase K assay and thereby the fusion abilities of destabilising and stabilising mutants.

6.9 The conformational change also requires interaction of the acidic solvent with the HA2 monomers

There is a notion that acidic pH is required only for the dissociation of globular head domains of HA1. The report of Chen *et al.* (1995) that HA2 domain in the absence of HA1 is capable of attaining fusion competent structure, even at neutral pH gives credence to this notion. To ascertain this, salt bridge network (E74-R76) connecting all the three HA2 domains (Fig.5.1.5) was targeted. This salt bridge is present at the interface of HA2 monomers in the distal region, and moreover in the neighbourhood of the tetrad salt bridge of the hinge region. Hence it was assumed that this salt bridge will have similar effect on the conformational transition of the HA protein like that of tetrad salt network in the hinge

region. To investigate the contribtution of this salt bridge to the stability of HA, Glu 74 and Arg 76 were substituted with E74C-R76C.

If the Cys residues formed disulfide bond connecting all the three HA2 monomers, the proteinase K assay profile of the mutant HA protein would probably resemble HA-wt. Then it may be deduced that conformational changes in HA2 are independent of low pH. In other words, the acid pH resistant covalent linkage should not change the pH threshold of the cys mutant HA protein. On the contrary, E74C-R76C failed to show good surface expression compared to HA-wt. A very little quantity of the expressed HA is cleaved by TPCK trypsin indicating that the majority of the HA remained in the cell (Fig 5.8.5; lane 1). The distance from the Arg 329 (trypsin cleavage site; Fig 1.2.1) rules out the possibility of trypsin cleavage site being affected in this mutant. In addition, Glu 74 and Arg 76 are totally covered by the globular head domains of the HA1 and they unlikely affect the trypsin cleavages site. Based on these assumptions, the mutations of Glu 74 and Arg 76 should not affect the surface expression of the mutant HA protein. The lack of the cell surface expression indicates the role of these charged residues in the surface expression of the protein. However, the formation of a disulfide linkage for E74C-R76C mutant was confirmed from the fig. 5.9, lane 2 (section 5.9). The conformational assay using proteinase K showed that the E74C-R76C mutant protein was relatively resistant to conformational changes (Fig 5.8.5a).

Moreover, the study investigated, if the lack of surface expression of E74C-R76C has been due to the absence of E74-R76 salt bridge or if the presence of Cys has changed the conformation of the HA. It was envisaged that retaining E74-R76 salt bridge, and incorporating a Cys in the neighbourhood (I77C), would determine if Cys has misfolded the HA protein. If the resultant I77C has lacked surface expression then, it would be the presence of Cys in the distal region of HA2 that has affected the structure of HA.

In contrast to the expectations, the I77C mutant has surface expression and proteinase K assay profile very similar to HA-wt. It was evident from Fig.5.1.5a, that a disulfide bond at I77C, if formed would only link any of the two HA2 monomers. Therefore, the purpose of I77C mutant was primarily not to lock the HA trimer. Accordingly, the autoradiogram from fig.5.9 (lane 4) does not seem to show any indication of disulfide linkage.

From these disulfide linkage experiments, it can be concluded that

1. The salt bridge network connecting the HA2 monomers cannot be substituted. The HA gene sequence alignment of all the members of influenza A virus indicate that E74 is highly conserved. On the other hand, R76 is conserved to approximately 75

% and the absence of R76 is compensated in these strains by R75. This only shows that this salt bridge is highly conserved in all the members of influenza A virus.

2. The importance of this salt bridge could be surmised in bringing all the three HA monomers together, to form a trimer. Though other interactions between the monomers are equally important in trimer formation, E74-R76 is the only interaction in some strains (eg., X-31) connecting all the monomers. Therefore it may be proposed that substitution of this salt linkage would weaken the trimer formation.
3. Further, at low pH the E74-R76 salt bridge also breaks facilitating the dissociation of the ectodomain. This facilitates the entry of the solvent into regions of the HA2 trimer shielded from solvent at neutral pH. In the process, the contact of the solvent with the hydrophilic cavity (discussed in 1.2.1) would force the hydrophobic fusion peptide out of the cavity.
4. It may also be concluded (personal communication with Huang and Herrmann) that interaction of solvent with the loop region of HA2 triggers the formation long helix forming the extended trimer coiled coil structure and, by that, the release of the fusion peptide from the hydrophilic cavity.

6.10 Model for the role of salt bridges for HA conformation and its stability

It is very much evident from the present investigation that salt bridges (ion pairs) play a vital role in low pH regulated protein conformational changes of HA protein. Similar views were reported by Wedekind *et al.* (2001) for exotoxin A of *Psuedomonas aeruginosa*. The electrostatic free energy contribution to protein stability does not correlate with the number of ion pairs in a protein, but rather depends on the exact location and geometrical constraints of the ion pairs.

Protein interfaces are generally more hydrophilic than the protein interiors. The residue composition of most protein-protein interfaces appears to be more similar to that of protein surfaces (Xu *et al.,* 1997). In addition, the interfaces tend to form more hydrogen bonds and salt bridges than protein interiors (Sheinerman *et al.*, 2000, Tsai *et al.*, 1997) and thus are the major contributors to the electrostatic interactions. It is rare to observe a single large hydrophobic patch on the interface (Larsen *et al.,* 1998). Rather, the hydrophobic residues are scattered over the entire surface and form small patches interspersed with polar and charged residues. Xu *et al.* (1997) further point out that the polar nature of the protein interfaces allows larger electrostatic stabilisation with reference to the interior of

the proteins. This sort of stability is exemplified in thermophilic proteins (Musafia *et al.,* 1995).

From the present research, it could be inferred that, mainly interfacial salt bridges are responsible for the stability of the non-fusogenic HA protein at neutral pH. At low pH, the negatively charged residues become protonated initiating the dissociation of the trimer. This facilitates the entry of solvent into otherwise tightly packed trimer. Upon expoure to solvent, the salt bridges at the interface of HA1-HA2 (tetrad salt network) and that of HA2-HA2 (E74-R76) become disrupted. The present study showed that the tetrad salt bridge connecting HA1 and HA2 subunits is vital for maintaining the stability of HA trimer in its non-fusogenic structure. More so, the high degree of conservation of ARG at 109 position in the influenza A family shows the importance of this residue for the stability of the HA trimer. In addition, the presence of a conserved negative residue at position 67of HA2 in all influenza A members makes it ideal for the formation of interfacial salt bridge. In the process, the solvent exposure also disrupts the ring salt network connecting the three HA2 monomers exposing the interiors of the stem region. It may be surmised that in the process, the hydrophilic pocket protecting (harbouring) the fusion peptide is destroyed, thus forcing the expulsion of hydrophobic fusion peptide. At the same time the disruption of tetrad salt bridge in the hinge region transforms the loop region of HA2 into helix (Fig.6.10). Thus it may be stated, that the protonation resulting from the exposure of the HA trimer to the solvent, leads to dramatic and irreversible conformational changes in the HA protein.

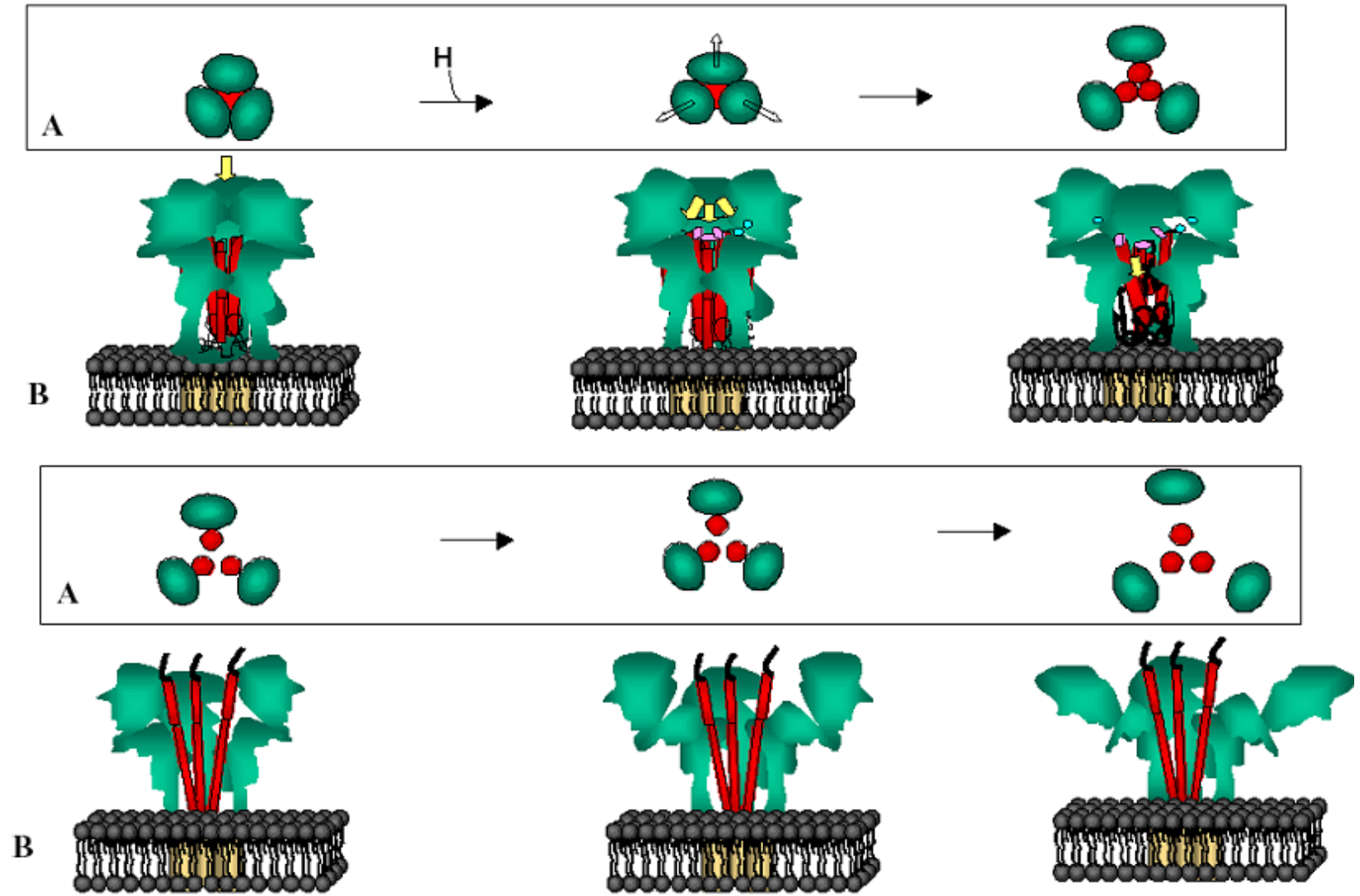

Fig.6.10: Predicted model for the conformational changes at low pH of the ectodomain of the influenza virus HA.
Shown in the picture are two rows A and B. Row A shows the HA protein from the top view and row B shows the HA protein from lateral view.

7 CONCLUSIONS

The present study clearly demonstrated that the pH sensitivity of the HA protein is determined by the charged residues especially those involved in salt bridge formation in and around the hinge region (interface region; therefore the residue easily gets exposed to solvent). The destabilising mutants showed a lower pH dependency for the conformational change in agreement with those of amantadine resistant mutants. On contrary, stability of the protein was increased with introduction of a possible salt bridge in the neighbourhood of hinge region (I89R or I89E-Y308R). Not only in the hinge region, stability to the protein could also be conferred by introduction of an ion-pair (T212E-N216R) in the distal region of the HA trimer.

The present research work provided an explanation for the stability of A/JPN/305/57 strain at pH 5.0. Very likely, the stability of the A/JPN/305/57 strain is enhanced by at least 2 –3 complexes of salt bridges around the hinge region. Indeed, this present study proved that introduction of attractive forces (possibly salt bridges) as for example in the distal region stabilised the HA ectodomain. In addition, the salt bridge network of A/JPN/305/57 strain with additional two ring like salt networks connecting either the HA1 monomers (R206-E210) or HA2 (R83-E85) provides the stability of the HA ectodomain at pH 5.0.

REFERENCES

1. Ali A and Nayak DP.(2000). Assembly of Sendai virus: M protein interacts with F and HN proteins and with the cytoplasmic tail and transmembrane domain of F protein. Virology. 276(2):289-303.
2. Andrewes CH, Bang FB, and Burnet FM (1955) A short description of the myxovirus group (influenza and related viruses). Virology 1: 176-184.
3. Avalos RT, Yu Z, and Nayak DP.(1997). Association of influenza virus NP and M1 proteins with cellular cytoskeletal elements in influenza virus-infected cells. J Virol. 71(4):2947-58.
4. Barbey-Martin C, Gigant B, Bizebard T, Calder LJ, Wharton SA, Skehel JJ, and Knossow M. (2002) An antibody that prevents the hemagglutinin low pH fusogenic transition. Virology. 294(1): 70-4.
5. Bentz J and Mittal A. (2000). Deployment of membrane fusion protein domains during fusion. Cell Biology International 24(11): 819-838.
6. Bentz J. (2000) Minimal aggregate size and minimal fusion unit for the first fusion pore of influenza hemagglutinin-mediated membrane fusion. Biophys J. 78(1):227-45.
7. Beroza P, Fredkin DR, Okamura MY, and Feher G. (1991). Protonation of interacting residues in a protein by a Monte Carlo method: application to lysozyme and the photosynthetic reaction center of Rhodobacter sphaeroides. Proc Natl Acad Sci U S A. 88(13):5804-8.
8. Bizebard T, Gigant B, Rigolet P, Rasmussen B, Diat O, Bosecke P, Wharton SA, Skehel JJ, and Knossow M. (1995) Structure of influenza virus haemagglutinin complexed with a neutralizing antibody. Nature. 376(6535): 92-4.
9. Blumenthal R, Sarkar DP, Durell S, Howard DE, and Morris SJ.(1996). Dilation of the influenza hemagglutinin fusion pore revealed by the kinetics of individual cell-cell fusion events. J Cell Biol. 135(1):63-71.
10. Boettcher C, Ludwig K, Herrmann A, Heel VM, and Stark K.(1999). Structure of in£uenza haemagglutinin at neutral and at fusogenic pH by electron cryo-microscopy. FEBS Lett.463: 255-259.

11. Boulay F, Doms RW, Webster RG, and Helenius A. (1988). Posttranslational oligomerisation and cooperative acid activation of mixed influenza hemagglutinin trimers. The Journal of Cell Biology.*106*: 629-639.

12. Bui M, Whittaker G, and Helenius A. (1996) Effect of M1 protein and low pH on nuclear transport of influenza virus ribonucleoproteins. J Virol. *70(12*):8391-401.

13. Bullough PA, Hughson FM, Skehel JJ, and Wiley DC (1994). Structure of influenza haemagglutinin at the pH of membrane fusion. Nature *371*, 37-43.

14. Carr CM and Kim PS. (1993). A spring-loaded mechanism for the conformational change of influenza hemagglutinin. Cell *73(4*):823-32.

15. Carr CM, Chaudhry C, and Kim PS (1997) Influenza hemagglutinin is spring-loaded by a metastable native conformation. Proc Natl Acad Sci U S A. *94 (26):*14306-13.

16. Chen J, Skehel JJ and Wiley DC (1999). N- and C-terminal residues combine in the fusion-pH influenza hemagglutinin HA(2) subunit to form an N cap that terminates the triple-stranded coiled coil. Proc Natl Acad Sci U S A. *96(16*):8967-72.

17. Chen J, Wharton SA, Weissenhorn W, Calder LJ, Hughson FM, Skehel JJ, and Wiley DC. (1995). A soluble domain of the membrane-anchoring chain of influenza virus hemagglutinin (HA2) folds in Escherichia coli into the low-pH-induced conformation. Proc Natl Acad Sci U S A *92(26*):12205-9.

18. Chen, J, Lee KH, Steinhauer DA, Stevens DJ, Skehel JJ, and Wiley DC. (1998). Structure of the hemagglutinin precursor cleavage site, a determinant of influenza pathogenicity and the origin of the labile conformation. Cell *95*:409–417.

19. Chernomordik LV, Leikina E, Kozlov MM, Frolov VA, and Zimmerberg, (1999) Structural intermediates in influenza haemagglutinin-mediated fusion. J. Mol. Membr. Biol. *16*,33-42.

20. Chernomordik LV, Frolov VA, Leikina E, Bronk P, and Zimmerberg J (1998).The pathway of membrane fusion catalyzed by influenza hemagglutinin: restriction of lipids, hemifusion, and lipidic fusion pore formation. J Cell Biol. *140(6*):1369-82.

21. Clague MJ, Schoch C, and Blumenthal R. (1991). Delay time for influenza virus hemagglutinin-induced membrane fusion depends on hemagglutinin surface density. J Virol. *65(5):*2402-7.

22. Colman PM and Lawrence MC. (2003). The structural biology of type I viral membrane fusion. Nat Rev Mol Cell Biol. *4(4*):309-19.

23. Copeland CS, Doms RW, Bolzau EM, Webster RG, and Helenius A. (1986). Assembly of influenza hemagglutinin trimers and its role in intracellular transport. The Journal of Cell Biology. *103*: 1179-1191.

24. Copeland, C. S., K. P. Zimmer, K. R. Wagner, G. A. Healey, I. Mellman, and A. Helenius. (1988). Folding, trimerization, and transport are sequential events in the biogenesis of influenza virus hemagglutinin. Cell. *53*:197-209.

25. Cross KJ, Wharton SA, Skehel JJ, Wiley DC, and Steinhauer DA. (2001). Studies on influenza haemagglutinin fusion peptide mutants generated by reverse genetics. EMBO J; *20(16)*:4432-42 .

26. Dalit Bechor and Nir Ben-Tal (2001). Implicit solvent model studies of the interactions of the influenza hemagglutinin fusion peptide with lipid bilayers. Biophysical Journal 80: 643–655

27. Danieli T, Pelletier SL, Henis YI, and White JM. (1996). Membrane fusion mediated by the influenza virus hemagglutinin requires the concerted action of at least three hemagglutinin trimers. J Cell Biol *133(3)*:559-69.

28. Daniels RS, Downie JC, Hay AJ, Knossow M, Skehel JJ, Wang ML, and Wiley DC. (1985) Fusion mutants of the influenza virus hemagglutinin glycoprotein. Cell. *40(2)*: 431-9.

29. Epand RM (2003). Fusion peptides and the mechanism of viral fusion. Biochim Biophys Acta.*1614(1)*:116-21.

30. Epand RM and Epand RF. (2002). Thermal denaturation of influenza virus and its relationship to membrane fusion. Biochem J *365*: 841-8.

31. Fodor E, Palese P, Brownlee GG, and Garcia-Sastre A (1998). Attenuation of influenza A virus mRNA levels by promoter mutations. J Virol. *72(8):*6283-90.

32. Geiss GK, Salvatore M, Tumpey TM, Carter VS, Wang X, Basler CF, Taubenberger JK, Bumgarner RE, Palese P, Katze MG, and Garcia-Sastre A. (2002) Cellular transcriptional profiling in influenza A virus-infected lung epithelial cells: the role of the nonstructural NS1 protein in the evasion of the host innate defense and its potential contribution to pandemic influenza. Proc Natl Acad Sci U S A. *99(16)*:10736-41

33. Gething MJ, Doms RW, York D, and White JM. (1986). Studies on the mechanism of membrane fusion: site-specific mutagenesis of the hemagglutinin of influenza virus. J Cell Biol ; *102(1):*11-23.

34. Godley L, Pfeifer J, Steinhauer D, Ely B, Shaw G, Kaufmann R, Suchanek E, Pabo C, Skehel JJ, Wiley DC, and Wharton S. (1992) Introduction of intersubunit disulfide bonds in the membrane-distal region of the influenza hemagglutinin abolishes membrane fusion activity. Cell. 21; *68(4)*: 635-45

35. Gomez-Puertas P, Albo C, Perez-Pastrana E, Vivo A, and Portela A. (2000) Influenza virus matrix protein is the major driving force in virus budding. J Virol. *74(24)*:11538-47.

36. Gray C and Tamm LK (1997). Structural studies on membrane-embedded influenza hemagglutinin and its fragments. Protein Science *6*: 1993-2006.

37. Gray C, Tamm LK (1998) pH-induced conformational changes of membrane-bound influenza hemagglutinin and its effect on target lipid bilayers. Protein Sci. *7(11)*:2359-73.

38. Gruenke JA, Armstrong RT, Newcomb WW, Brown JC, and White JM. (2002).New insights into the spring-loaded conformational change of influenza virus hemagglutinin. Journal of Virology *76(9)*:4456-66.

39. Han X, Steinhauer DA, Wharton SA, and Tamm LK. (1999). Interaction of mutant influenza virus hemagglutinin fusion peptides with lipid bilayers: probing the role of hydrophobic residue size in the central region of the fusion peptide. Biochemistry *38 (45)*:15052-9.

40. Hernandez LD, Hoffman LR, Wolfsberg TG, and White JM (1996).Virus-cell and cell-cell fusion. Annu Rev Cell Dev Biol *12*:627-61.

41. Hoffmann LR, Kuntz ID, and White JM. (1997). Structure based identification of an inducer of the low pH conformational change in the influenza virus hemagglutinin: irreversible inhibition of infectivity. Journal of Virology *71(11)* 8808-8820.

42. Huang Q, Opitz R, Knapp E-W, and Herrmann A. (2002). Protonation and stability of the globular domain of influenza virus hemagglutinin. Biophysical Journal *82*: 1050-1058.

43. Huang Q, Sivaramakrishna RP, Ludwig K, Korte T, Bottcher C, and Herrmann A (2003) Early steps of the conformational change of influenza virus hemagglutinin to a fusion active state: stability and energetics of the hemagglutinin. Biochim Biophys Acta. *1614(1)*: 3-13.

44. Jackson HC, Roberts N,. Wang ZM, and Belshe R. (2000). Management of influenza: use of new antivirals and resistance in perspective. Clin. Drug Investig. *20*:447–454.

45. Jahn R and Sudhof TC. (1999).Membrane fusion and exocytosis. Annu Rev Biochem; *68*:863-911.

46. Jones S and Thorton JM (1996). Principles of protein-protein interactions. Proc. Natl. Acad. Sci. USA *93*, 13-20.

47. Kelly ML, Cook JA, Brown-Augsburger P, Heinz BA, Smith MC, and Pinto LH. (2003). Demonstrating the intrinsic ion channel activity of virally encoded proteins. FEBS Lett. *552(1)*:61-7.

48. Kemble GW, Bodian DL, Rose J, Wilson IA, and White JM. (1992) Intermonomer disulfide bonds impair the fusion activity of influenza virus hemagglutinin. J Virol. *66(8)*: 4940-50.

49. Kemble GW, Danieli T, and White JM. (1994) Lipid-anchored influenza hemagglutinin promotes hemifusion, not complete fusion. Cell. *76(2)*:383-91.

50. Klenk HD and Garten W. 1994. Host cell proteases controlling virus pathogenecity. Trends Microbiol. *2:*39–43.

51. Korte T, Ludwig K, Booy FP, Blumenthal R, and Herrmann A. (1999). Conformational intermediates and fusion activity of influenza virus hemagglutinin. Journal of Virology *73*: 4567-4574.

52. Kozerski C, Ponimaskin E, Schroth-Diez B, Schmidt MF, and Herrmann A. (2000) Modification of the cytoplasmic domain of influenza virus hemagglutinin affects enlargement of the fusion pore. J Virol. *74(16*):7529-37.

53. Kozlov MM and Chernomordik LV. (1998). A mechanism of protein-mediated fusion: coupling between refolding of the influenza hemagglutinin and lipid rearrangements. Biophys J. 1998 Sep;*75(3*):1384-96.

54. Kumar S and Nussinov R. (2002) Close-range electrostatic interactions in proteins. Chembiochem. *3(7*):604-17.

55. Lamb RA and Krug RM. (2001). Orthomyxoviridae: the viruses and their replication. In: Knipe, D.M., Howley, P.M. (Eds.), Fields Virology, *4th ed*. Lippincott Williams and Wilkins, Philadelphia, pp. 1487–1532.

56. Lamb RA, Holsinger L.J, and Pinto LH. (1994). Receptor-Mediated Virus Entry into Cells (*Wimmer,E.,Ed.*),pp.303-321, Cold Spring Harbor Laboratory Press,Cold Spring Harbor,NY.

57. Larsen TA, Olson AJ, Goodsell DS.(1998).Morphology of protein-protein interfaces. Structure. *15;6(4*):421-7.

58. Li Y, Han X, and Tamm LK. (2003).Thermodynamics of fusion peptide-membrane interactions. Biochemistry. Jun 17;*42(23*):7245-51.

59. Lindau M and Almers W. (1995).Structure and function of fusion pores in exocytosis and ectoplasmic membrane fusion. Curr Opin Cell Biol. Aug;7(*4*):509-17.

60. Maley F, Trimble RB, Tarentino AL, and Plummer TH Jr. (1989). Characterization of lycoproteins and their associated oligo- saccharides through the use of endoglycosidases. Anal. Biochem. *180*, 195–204

61. Marqusee S and Sauer RT. (1994) Contributions of a hydrogen bond/salt bridge network to the stability of secondary and tertiary structure in lambda repressor. Protein Sci. *3(12*):2217-25.

62. Monto AS (2003). The role of antivirals in the control of influenza. Vaccine. (2003) May 1;*21(16*):1796-800.

63. Musafia B, Buchner V, and Arad D. (1995) Complex salt bridges in proteins: statistical analysis of structure and function. J Mol Biol. *254(4*):761-70.

64. Neumann G, Hughes MT, and Kawaoka Y. (2000) Influenza A virus NS2 protein mediates vRNP nuclear export through NES-independent interaction with hCRM1. EMBO J. *19(24*):6751-8.

65. Nicholson KG, Wood JM, and Zambon M. (2003) Influenza. Lancet. *362(9397*):1733-45.

66. O'Neill RE and Palese P. (1995). NPI-1, the human homolog of SRP-1, interacts with influenza virus nucleoprotein. Virology.*206(1*):116-25.

67. Oxford JS and Lambkin R. (1998). Targeting influenza virus neuraminidase - a new strategy for antiviral therapy. Drug Discov. Today *3*:448–456.

68. Proesch S, Heider H, Schroeder C, Shilov AA, Sinitzyn BV, Blinov VM, Krueger DH, and Froemmel C (1990). Mapping mutations in influenza A virus resistant to norakin. FEBS *267 (1*): 19-21.

69. Puri A, Booy FP, Doms RW, White JM, and Blumenthal R (1990). Conformational changes and fusion activity of influenza virus hemagglutinin of the H2 and H3 subtypes: effects of acid pretreatment. J.Virol *64:*10108-10113.

70. Qiao H, Armstrong RT, Melikyan GB, Cohen FS, and White JM. (1999). A specific point mutant at position 1 of the influenza hemagglutinin fusion peptide displays a hemifusion phenotype. Mol Biol Cell; *10(8)*:2759-69.

71. Remeta DP, Krumbiegel M, Minetti CA, Puri A, Ginsburg A, and Blumenthal R. (2002). Acid-induced changes in thermal stability and fusion activity of influenza hemagglutinin. Biochemistry. *41(6*): 2044-54.

72. Ruigrok RW, Wrigley NG, Calder LJ, Cusack S, Wharton SA, Brown EB, and Skehel JJ. (1986) Electron microscopy of the low pH structure of influenza virus haemagglutinin. EMBO J *5(1*): 41-9.

73. Sambrook J, Fritsch E, and Maniatis T (1989). Molecular cloning: a laboratory manual, *2 nd edition*, COld Spring harbor, N.Y.

74. Sauter NK, Glick GD, Crowther RL, Park S-J, Eisen MB, Skehel JJ, Knowles JR, and Wiley DC. (1992). Crystallographic detection of a second ligand binding site in the influenza hemagglutinin. Proc.Natl.Acad.Sci.USA. *89*: 324-328.

75. Shangguan T, Siegel DP, Lear JD, Axelsen PH, Alford D, and Bentz J (1998). Morphological changes and fusogenic activity of influenza virus hemagglutinin. Biophys J. 1998 Jan;*74(1*):54-62.

76. Sheinerman FB, Norel R, Honig B.(2000). Electrostatic aspects of protein-protein interactions. Curr Opin Struct Biol. *10(2):*153-9.

77. Skehel JJ and Wiley DC. (2000). Receptor binding and membrane fusion in virus entry: The Influenza Hemagglutinin. Ann. Rev. Biochem. *69*:531-69.

78. Skehel JJ and Wiley DC.(1998). Coiled coils in both intracellular vesicle and viral membrane fusion. Cell. *95(7*):871-4.

79. Skehel JJ, Bayley PM, Brown EB, Martin SR, Waterfield MD, White JM, Wilson IA, and Wiley DC. (1982) Changes in the conformation of influenza virus hemagglutinin at the pH optimum of virus-mediated membrane fusion. Proc Natl Acad Sci U S A. *79(4):* 968-72.

80. Staschke KA, Hatch SD, Tang JC, Hornback WJ, Munroe JE, Colacino JM, and Muesing MA. (1998). Inhibition of influenza virus hemagglutinin-mediated membrane fusion by a compound related to podocarpic acid. Virology. *248*, 264-274.

81. Stegmann T, Booy FP, and Wilschut J. (1987) Effects of low pH on influenza virus. Activation and inactivation of the membrane fusion capacity of the hemagglutinin. J Biol Chem. *262(36*): 17744-9.

82. Stegmann T, Morselt HWM, Booy FP, van Breemen JFL, Scerphof G, and Wilschut J. (1987). Functional reconstitution of influenza virus enveloped. EMBO J. *6*:2651-2659.

83. Stegmann T, White JM, and Helenius A. (1990) Intermediates in influenza induced membrane fusion. EMBO J. *9(13*): 4231-41.

84. Steinhauer DA and Skehel JJ. (2002) Genetics of influenza viruses. Annu Rev Genet. *36*:305-32. Epub 2002 Jun 11.

85. Suomalainen M (2002). Lipid Rafts and Assembly of Enveloped Viruses. Traffic *3(10*): 697-762

86. Tamm LK (2003) Hypothesis: spring-loaded boomerang mechanism of influenza hemagglutinin-mediated membrane fusion. Biochim Biophys Acta. 11;*1614(1*):14-23.

87. Tatu U and Helenius A (1997). Interactions between newly synthesized glycoproteins, calnexin and a network of resident chaperones in the endoplasmic reticulum. J Cell Biol. *136(3*):555-65.

88. Tatulian SA and Tamm LK (2000) Secondary structure, orientation, oligomerization, and lipid interactions of the transmembrane domain of influenza hemagglutinin. Biochemistry.25;*39(3*):496-507.

89. Tatulian SA and Tamm LK. (1996) Reversible pH-dependent conformational change of reconstituted influenza hemagglutinin. J Mol Biol. 1996 Jul 19;*260(3*):312-6.

90. Tse FW, Iwata A, and Almers W. (1993). Membrane flux through the pore formed by a fusogenic viral envelope protein during cell fusion. J Cell Biol. May;*121(3*):543-52.

91. Ullmann GM and Knapp EW. (1999). Electrostatic models for computing protonation and redox equilibria in proteins. Eur Biophys J. *28(7*):533-51.

92. Varghese JN, and. Colman PM. (1991). Three-dimensional structure of the neuraminidase of influenza virus A/Tokyo/3/67 at 2.2 A resolution. J. Mol. Biol. *221*:473–486.

93. Varghese JN, Epa VC, and Colman PM. (1995). Three-dimensional structure of the complex of 4-guanidino-Neu5Ac2en and influenza virus neuraminidase. Protein Sci. *4:*1081–1087.

94. Ward AC, Castelli LA, Lucantoni AC, White JF, Azad AA, and Macreadie IG. (1995) Expression and analysis of the NS2 protein of influenza A virus. Arch Virol. *140(11*):2067-73.

95. Watanabe K, Handa H, Mizumoto K, and Nagata K. (1996). Mechanism for inhibition of infuenza virus RNA polymerase activity by matrix protein. J. Virol. *70,* 241-247.

96. Wedekind JE, Trame CB, Dorywalska M, Koehl P, Raschke TM, McKee M, FitzGerald D, Collier RJ, McKay DB.(2001). Refined crystallographic structure of Pseudomonas aeruginosa exotoxin A and its implications for the molecular mechanism of toxicity. J Mol Biol. *7;314(4*):823-37.

97. White J, Helenius A, and Gething M-J. (1982). Hemagglutinin of influenza virus expressed from a cloned gene promotes membrane fusion. Nature (London) *300*:658-659

98. White JM and Wilson IA (1987) Anti-peptide antibodies detect steps in a protein conformational change: low-pH activation of the influenza virus hemagglutinin. J Cell Biol. *105(6 Pt 2*): 2887-96

99. Whittaker GR. (2001) Intracellular trafficking of influenza virus: clinical implications for molecular medicine. Exp. Rev. Mol. Med. 8 February, http://www-ermm.cbcu.cam.ac.uk/01002447h.htm

100. Wiley DC and Skehel JJ (1987) The structure and function of the hemagglutinin membrane glycoprotein of influenza virus. Ann.Rev.Biochem *56*: 365-394.

101. Wilson IA, Skehel JJ, and Wiley DC. (1981) Structure of the haemagglutinin membrane glycoprotein of influenza virus at 3 A resolution. Nature. *289(5796*): 366-73.

102. Wright PF and Webster RG. (2001). Orthomyxoviruses. In: Knipe, D.M., Howley, P.M. (Eds.), Fields Virology, *4th ed.* Lippincott Williams and Wilkins, Philadelphia, pp. 1533–1579.

103. Xu D, Tsai CJ, and Nussinov R. (1997) Hydrogen bonds and salt bridges across protein-protein interfaces. Protein Eng. *10(9*):999-1012.

104. Zhirnov OP, Ikizler MR, and Wright PF. (2002) Cleavage of influenza a virus hemagglutinin in human respiratory epithelium is cell associated and sensitive to exogenous antiproteases. J Virol. *76(17)*:8682-9.

ACKNOWLEDGEMENTS

This work has been a result of collaboration between Prof. Andreas Herrmann, Institute of Biology/Molecular Biophysics, Humboldt University Berlin and Prof. M. F. G. Schmidt, Institute of Immunology and Molecular Biology (IMB), Department of Veterinary medicine, Free University Berlin. Majority of the work has been done at IMB, FU-Berlin.

At the outset, I wish to express my profound thanks to my employer and supervisor Prof. Andreas Herrmann on whose invitation I arrived in Germany to conduct research work. He has been a great support for me through out my research work. His observations and critical suggestions have invigorated my thinking into finding new ways to deal with the research. I appreciate his keen interest in my scientific career and his attitude of helping by going out of the way in my needy hour. I consider it as a boon to work with him.

I am also thankful to PD. Dr. Michael Veit and Prof. Michael F. G. Schmidt for allocating me working space and for the wonderful milieu at IMB, FU-Berlin. I express my sincere gratitude to Dr. Veit for his helpful discussions in research related problems and also for critically reviewing this thesis work. Discussions with Dr. Veit always used to give good clues thwarting away the crisis periods.

A friend in need is friend indeed. Dr. Lydia Scharek, IMB has been a great friend and a great colleague at IMB. Without Lydia's help, it would have been a great trouble for me to understand the nitty-gritty of life in Germany. I am very thankful for all her help and appreciate her patience in critically proof-reading this thesis.

My thanks are due to Dr. Thomas Korte at Mol. Biophysics for helping me out with fluorescence microscopy. It is because of his help in writing a macro for my fluorescence microscopy; I could handle with ease more than ten mutants.

No work would be complete with out the help of technical staff and I owe my deep sense of gratitude to Mrs. Ingrid Poese for all her help in making my work simple.

I am indebted to all the staff at Institute of Mol.Biophysics and IMB for their whole hearted help and making my stay memorable. My special thanks to Mrs. Angela Piater,

secretary to Prof. Herrmann for helping me to get over all the bureaucracy matters.

Friends have always been my strength and it is a delight to acknowledge all those who have been with me for various periods of time. I take this opportunity to acknowledge one and all.

Finally, my fondest appreciations go to my parents, brothers, and wife. It is their love and encouragement for what I am today.

LEBENSLAUF

Name	P. Sivaramakrishna Rachakonda
Geburstdatum	15. Januar 1969
Geburtsort	Machilipatnam, Indien
Nationalität	Indisch
Familienstand	Verheiratet
STUDIUM	
08 / 1988 – 04 / 1994	B.V.Sc & A.H. Bachelor of veterinary sciences, College of Veterinary Sciences, Hyderabad, India.
08 / 1994 – 12 / 1997	M.V.Sc (Animal Biotechnology) Masters in veterinary sciences (Biotechnology), Indian Veterinary Research Institute, Izatnagar, India.
BERUFSTÄTIGKEIT	
01 / 1996 – 06 / 1997	M.V.Sc. thesis work, Indian Veterinary Research Institute, Bangalore, India. *Thema*: Molecular characterization of a glycoprotein gene g IV of an Indian isolate of BHV-1.
12 / 1998 – 06 / 2001	Research Assistant, Indian Institute of Technology, Biotechnology Center, Mumbai, India. *Thema*: t-RNA mediated SNAAR mutagenesis of bacteriorhodopsin protein.
PROMOTION	
Seit Sept. 2001:	Promotionstudium – am Institute of Biologie / Molekularbiophysik, Humboldt Universität, Lehrstuhl Prof. Dr. Andreas Herrmann

PUBLIKATIONEN

Sivarama KR, Sreekumar E, Rasool TJ.(1999). Cloning and sequencing of truncated gIV glycoprotein gene of an Indian isolate of bovine herpesvirus 1. *Acta Virol*. 43(6):387-9.

Huang Q, **Sivaramakrishna RP**, Ludwig K, Korte T, Bottcher C, Herrmann A. (2003). Early steps of the conformational change of influenza virus hemagglutinin to a fusion active state: stability and energetics of the hemagglutinin. *Biochim Biophys Acta*. 11;1614(1):3-13.

POSTER

Poster at "46th Biophysical Society Annual Meeting in San Francisco, California, February 23-27, 2002"

Title: STUDY ON ELECTROSTATIC INTERACTIONS AND STABILITY OF THE ECTODOMAIN OF INFLUENZA VIRUS HEMAGGLUTININ

Original abstract control number: 870.

SELBSTÄNDIGKEITSERKLÄRUNG

Hiermit erkläre ich, die vorliegende Arbeit selbständig ohne fremde Hilfe verfasst zu haben und nur die angegebene Literatur verwendet zu haben.

Ich besitze keinen entsprechenden Doktorgrad und habe mich anderwärts nicht um einen Doktorgrad beworben.

Die dem Promotionsverfahren zugrunde liegende Promotionsordnung vom 28.03.2001 ist mir bekannt.

Sivaramakrishna Rachakonda
15. Oct. 2004.